Molecular Equilibria Determined by van der Waals' Attraction

by

Peter Alexander Kirsch

A thesis presented to the University of London in partial fulfilment of the requirements for the degree of Doctor of Philosophy.

Department of Chemistry

University College London

June 1991

Abstract

This thesis is primarily concerned with a nuclear magnetic resonance study on the effect of intramolecular van der Waals' attractive forces between alkyl groups. This phenomenon is investigated by devising certain two-fold conformational equilibria, such that one side of the equilibrium has two alkyl groups positioned relatively close to one another and attracting one another, the other side has the alkyl groups further apart and experiencing a greatly reduced interaction.

The valence bond isomerisation between 1,4 and 1,6-dialkylcyclooctatetraenes **7**(R=Me), **8**(R=Et), **9**(R=ipr), **10**(R=^{t}Bu) is observed to favour the more compact 1,6-isomers in solution. This preference is attributed to van der Waals' attraction between the pendant alkyl groups. Molecular mechanics agree as to the preferred valence isomer and confirm it has greater attractive steric interactions.

The two-fold 1-(3-alkylphenyl)-group rotational equilibrium in 1(e)-(3-alkylphenyl)-2(e),6(e)-dimethylcyclohexan-1-ols **23**(R=Me), **24**(R=^{t}Bu) and 1(e)(3-alkylphenyl)-2(e),6(e)-dimethylcyclohexanes **25**(R=Me), **26**(R=^{t}Bu) is observed to favour the more compact conformer for **23**, **24** but the less compact conformer for **26**, while no preference is seen for **25**. A combination of buttressing and attractive steric effects are postulated to explain these preferences, the results being supplemented with molecular mechanics calculations.

The 1-(1-methylneopentyl) rotational equlibrium in 1-(1-methylneopentyl)-3-alkylbenzenes **33**(R=Me), **34**(R=^{t}Bu) and 3-(1-methylneopentyl)phenanthrene **35** favours the less compact conformers

for **34** and **35**, while no preference is seen for **33**. Buttressing is invoked to explain the observed conformational preferences, the results being supplemented with molecular mechanics calculations.

The rotational conformations of a 2-methylalkyl-group in 2-methylalkyl-4,4-dimethyl-1,3-dioxanes **39**(R=ipr), **40**(R=1-Ad), **41**(R=Ph) are investigated via analysis of the three bond methyl ^{1}H-NMR coupling constants. For **41**, two unequally populated gauche conformations are indicated while for **39**,**40** no population difference is observed about the indicated bond. However, spin decoupling at the 2-H ring hydrogen in **39** suggests a preferred conformation about the ipr-CH_2 bond in this compound. These results are interpreted in terms of buttressing and attractive steric effects.

An assignment of NMR signals to rotamers for **23**, **24**, **25**, **26** is performed *via* an NOE difference experiment on 1(a)-(3-^{t}Buphenyl)-2(e),6(e)-dimethylcyclohexane, **30**. Signal assignment for meta-alkylbenzenes **33**, **34**, **35** is *via* an NOE difference experiment on **35**.

Acknowledgements

I would like to express my sincere appreciation to my supervisor Dr Anderson, for his help and guidance during the course of this work.

I am indebted to Smith Kline and French (now Smith Kline and Beecham) for the award of a Case Studentship.

Steven Corker gave some invaluable practical advice on the GLC separations of my products.

Finally, I would like to thank all my colleagues at U.C.L. for the many interesting discussions that arose concerning this work during the past few years.

Table of Contents

Note: A paper detailing the results of the present work on 1,4 and 1,6-dimethyl-cyclooctatetraene is appended at the end of this thesis.

Chapter 1:

Introduction

(a) Alkyl/alkyl van der Waals' Interactions

(b) Molecular Mechanics Calculations and its Treatment of van der Waals' Interactions

(c) Literature Survey of alkyl/alkyl van der Waals' Attraction in the Conformational Analysis of Organic Molecules

(d) Rate Processes, Free Energy and NMR Spectra

(e) Aims of the Present Work

(a) **Alkyl/alkyl van der Waals' Interactions**

Non-bonded intramolecular interactions play a principal role in determining the conformations taken up by organic molecules. For neutral, relatively non-polar species such as hydrocarbons, these non-bonded interactions are the van der Waals' repulsive and attractive forces between the atoms of adjacent alkyl groups. The repulsive forces (also known as steric repulsion) are dominant at short interatomic distances and have their origin in the destabilisation arising from the interpenetration of electron shells. The attractive forces (also known as dispersion forces or electron correlation forces) result from a weak induced dipole/induced dipole interaction between electron clouds and dominate when any two atoms are further apart than approximately 3-4 Å. The general shape of any van der Waals' potential function describing non-bonded intramolecular interactions between alkyl groups arises therefore from two forces: a repulsive short range force and a longer range attractive force. This situation is frequently described by a Lennard-Jones (12,6)- potential function (see Fig.1) of the form

$$V = 4\,\varepsilon \left\{ \left(\frac{\sigma}{R}\right)^{12} - \left(\frac{\sigma}{R}\right)^{6} \right\}$$

which has its origins in studies aimed at the determination of the second virial coefficients of gases.[1]

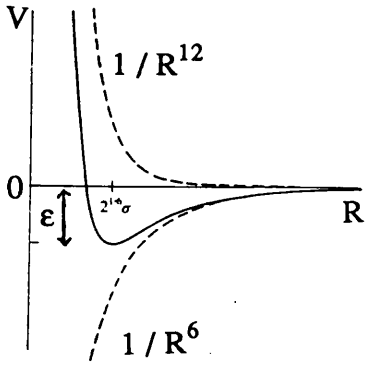

V = potential energy
ε = depth of well
σ = separation at which V = 0
R = separation of atoms

Fig. 1: Lennard-Jones (12,6)- potential for two interacting molecules.[2] The dotted lines are the attractive and repulsive contributions to the curve.

All atoms within a molecule, with a separation greater than σ, will experience mutual attraction. The number of these attractive interactions, in all but the smallest molecules, normally far exceeds the number of repulsive interactions. However, the attractive interactions are much weaker and hence the contribution to the total enthalpy of a molecule from the few atoms acting repulsively usually far exceeds the stabilisation from any attractive interactions. As a consequence of this, examples of conformational equilibria determined by van der Waals' attraction are quite rare in the literature.

(b) **Molecular Mechanics Calculations and its Treatment of van der Waals' Interactions**

Over the past twenty years or so, molecular mechanics has developed into a powerful standard computational method for the prediction of conformational preferences among the rotational isomers of a molecule.[3] The steric energy of a molecule is calculated using a series of classical potential energy functions (*the force field*) to be the sum of stretching (E_s), bending (E_b), torsional (E_w), van der Waals' (E_{vdw}), dipole-dipole (E_d) and several cross terms. Each term consists of the sum of atomic contributions and these terms are evaluated independently, so the local contribution to the total energy can be estimated by examining the detailed data from a computer.

There are a number different force fields in current use and hence the derived partitioning of the steric energy into its various component forms is likely to reflect the chosen force field. Therefore any attempt to try to attach physical significance to the detailed breakdown of the steric energy should be viewed with caution. However, with this stipulation in mind, molecular mechanics may nonetheless be used to attempt to gain a deeper

understanding of the conformational energetics of a molecule.

For non-polar,saturated hydrocarbons, the only non-bonded interactions considered by molecular mechanics are the van der Waals' interactions between carbon and hydrogen atoms. These van der Waals' interactions are calculated practically by summing up the interatomic terms of the attractive and repulsive van der Waals' energies. Thus the approximate contribution to the total steric energy by the dipersive (attractive van der Waals') energy can be easily estimated by examining the results of molecular mechanics calculations.

Various sets of van der Waals' potential functions have been used in molecular mechanics by different workers and are based on the potential functions originally used to describe the interaction potentials of rare gases. MM2 calculations[4] use a potential function based on that of Hill,[5] which is dependent on two parameters for each atomic interaction: The combined van der Waals' radius of the two interacting atoms, D, and an energy scale factor, ε, which measures the depth of the van der Waals' energy well.

$$E_{vdw} = \varepsilon\left\{ 2.90 \times 10^5 \exp\left(-12.5\, d / D \right) - 2.25 \left(D / d \right)^6 \right\}$$

Interaction	D	ε
C/C	3.80	0.044
C/H	3.34	0.046
H/H	3.00	0.047

D = sum of van der Waals' radii of atom pair / (Å)

d = separation of atom pair / (Å)

ε = energy scale factor / ($kcalmol^{-1}$)

Figure 2: Hill potential for van der Waals' interactions. Data taken from reference (4).

The attraction term in the Hill expression includes a d^{-6} factor arising from the fact that the dispersion force originates from the interaction between

two dipole-induced dipoles.

The non-bonded potential parameters in MM2 for saturated hydrocarbons are derived[6] from the crystal structure data of parafin hydrocarbons, which have been determined rather accurately by X-ray crystallography.

Recently an MM3 force field has been published utilizing improved van der Waals' parameters and a slightly modified Hill potential.[7]

(c) **Literature Survey of alkyl/alkyl van der Waals' Attraction in the Conformational Analysis of Organic Molecules**

Organic chemistry is dominated by examples where conformational equilibria are determined by intramolecular van der Waals' repulsive forces.[8] A classic example is found in substituted cyclohexanes where alkyl substituents on the ring prefer to be equatorial rather than axial to reduce steric repulsion between the substituent and the ring.[9] A case in point in tert-butyl-cyclohexane, which is calculated to exist as virtually 100% the equatorial conformer at room temperature.[10] Much more uncommon in the chemical literature are cases of conformational equilibria determined by attractive van der Waals' forces. One of the earliest examples appears to occur in the 2.4,6-tribromo-1,3,5-trineopentylbenzene molecule. Carter, Nilsson and Olsson found that at -20°C in deutereochloroform solution, the rotamer **2** with all three tert-butyl groups on the same side of the benzene ring is more heavily populated than the 2-proximal, 1-distal rotamer **1** by a 3:1 ratio[11] (see Fig. 3).

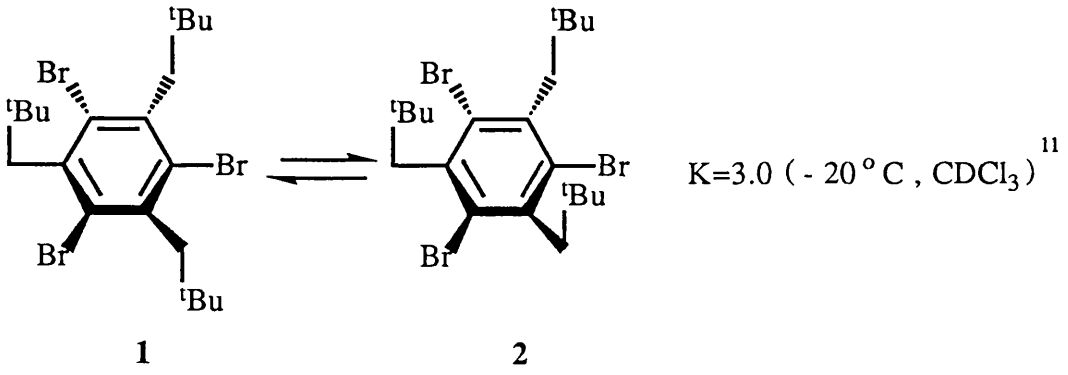

Fig. 3: 1,3,5-trineopentylbenzene equilibrium in $CDCl_3$ (-20°C).

A casual inspection of molecular models reveals that the tert-butyl groups are too far apart to repel one another, and the greater stabilisation of rotamer **2**, with all three tert-butyl groups on the same side of the benzene ring, was interpreted in terms of attractive steric effects among the tert-butyl groups.[11] Molecular mechanics calculations provide theoretical support for this interpretation.[12]

The most comprehensive study of van der Waals' attraction in organic molecules has been carried out by Berg and Pettersson.[13] They made a systematic study of the *syn/anti* equilibrium present in dialkyl-substituted thiobarbiturates, **3**, and imidazoline-2-thiones **4** (Fig.4) using a variety of alkyl

groups of diverse sizes and symmetries.

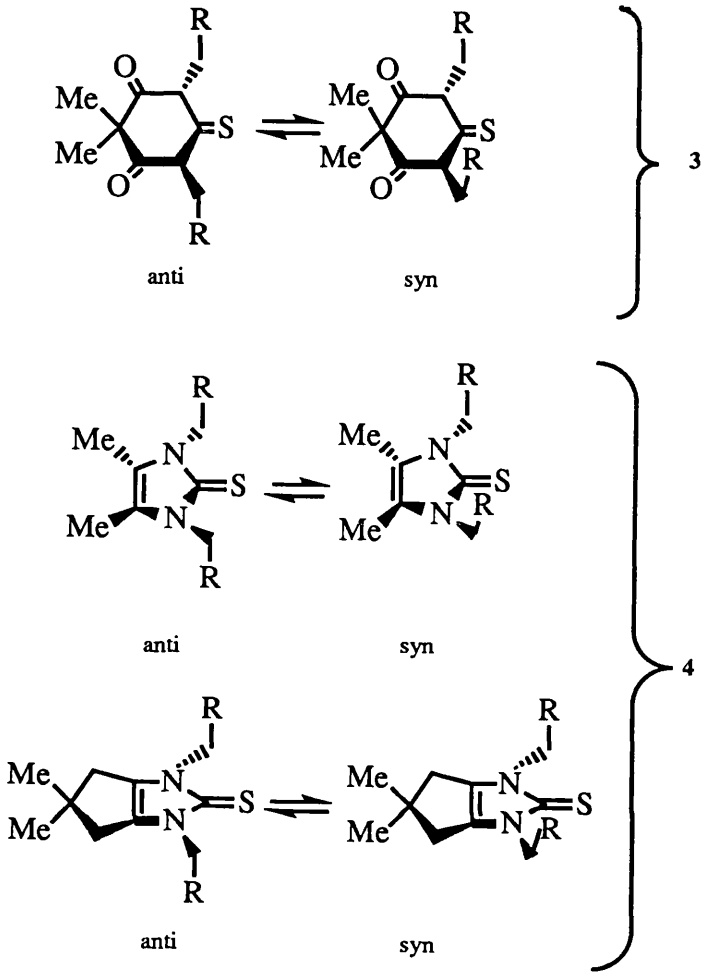

Fig. 4: *Syn/anti* isomerism is dialkyl-substituted thiobarbiturates, **3**, and imidazoline-2-thiones, **4**.[13]

They concluded that in general, the more crowded *syn* conformer predominates in solution. Molecular mechanics calculations are in agreement with this and provide support for the operation of van der Waals' attraction as the most important factor determining the conformational equilibrium.[13]

Van der Waals' attraction has also been implicated in the unusual equilibrium associated with the valence bond isomers of di-tert-butyl cyclooctatetraene (Fig. 5):

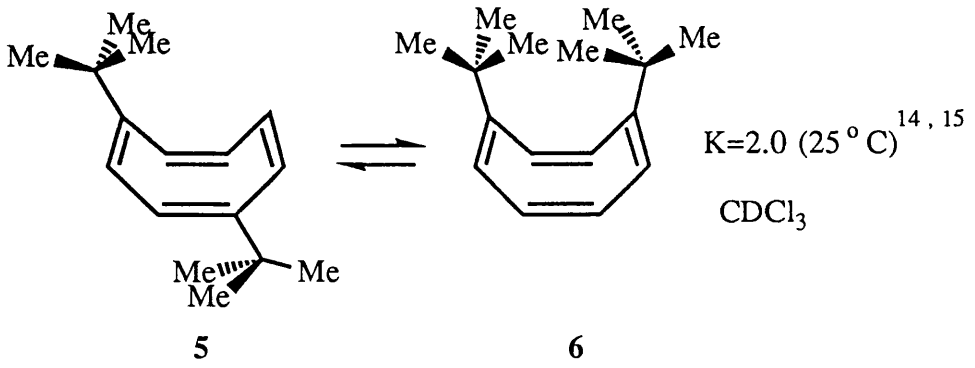

5 6

1,4-di-tert-butylcyclooctatetraene 1,6-di-tert-butylcyclooctatetraene

Fig. 5: Valence bond isomers of di-tert-butylcyclooctatetraene.

Streitwieser and his co-workers found[14] that the 1,6-isomer **6** is more populated than the 1,4-isomer **5** by a 2:1 ratio ($CDCl_3$, + 25°C). This result was also confirmed by Paquette *et al.*[15] The conclusion reached was that the nearest atoms of the two tert-butyl groups in **6** are positioned just at the edge of steric repulsion, and, overall, van der Waals' attraction dominates the equilibrium. Molecular mechanics calculations on the bond-shift isomers correctly predict the 1,6-isomer to be the more stable, the calculations showing that the position of the equilibrium is governed by the magnitude of the van der Waals' attraction between the tert-butyl groups.[16] It is interesting to note that *ab initio* calculations performed on the **5** ⇌ **6** equilibrium only model the experimental results if they are undertaken without approximations precluding electron correlation between atoms pairs *i.e.* attractive steric interactions.[17]

Nishio and Hirota have recently produced an extensive report[18] on the

preferred folded conformations adopted by certain compounds containing both alkyl groups and electron rich π-systems, such as a phenyl group. In these compounds, the most stable conformation appears to be the one that brings the alkyl group and π-system into close proximity. Particular attention in this report was focussed on compounds with the common structure $C_6H_5CHMeX^tBu$ (X = CH_2,CHOH,CO,S,SO,SO_2). Using a variety of experimental techniques including LIS (Lanthanide-Induced NMR Chemical Shift) measurements, X-ray crystallographic analyses, dipole moment measurements and molecular mechanics calculations, it was concluded that in general the preferred conformation has the ^{t}Bu-group orientated synclinal to the phenyl and antiperiplanar to the methyl, irrespective of the nature of the group X for both solution and crystal structures.

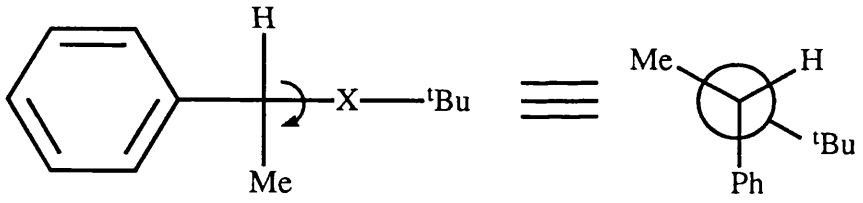

X = CH_2 , CHOH , CO , S , SO , SO_2

Synclinal alkyl/phenyl conformations were also found to be common for compounds bearing smaller alkyl groups in place of ^{t}Bu.

A *CH/π interaction* between the ^{t}Bu-group and the phenyl group was invoked by Nishio and Hirota as contributing to the stabilisation of the preferred synclinal conformation. The stabilisation arising from this interaction was considered to result from two contributory factors: firstly, a dispersion contribution (namely van der Waals' attraction) between the phenyl and ^{t}Bu-groups, and, secondly, a somewhat weaker hydrogen-bond-like interaction

between the electron rich π-system of the phenyl ring and the ^{t}Bu-group.

Dispersion forces are also implicated in many biological macromolecular structures. The tertiary structure of proteins for example often involves folded conformations. Van der Waals' attractive forces between hydrocarbon side chains in the protein are mooted as one of the causitive factors contributing to the stability of the folded structure.[19]

Intrinsic to the structure of biological cell membranes are lipid molecules which contain polar head groups attached to non-polar hydrocarbon tails. In aqueous media these lipids form bimolecular sheets called lipid bilayers in which the hydrocarbon tails of the lipids are sequestered inside a sheet-like structure, with the polar head groups lying on the surface. Van der Waals' attractive forces between the hydrocarbon tails of the lipids contribute to the stability of the bimolecular sheets.[19] Bimolecular sheet formation in biological cell membranes is analogous to micelle formation[20] in aqueous solution by salts of fatty acids such as sodium palmitate ($CH_3(CH_2)_{14}CO_2Na$). The micelles are globular structures containing polar head groups on the surface and hydrocarbon tails within the interior of the structure. Again van der Waals' attractive forces between the hydrocarbon tails in the interior of micelle are thought to stabilise these structures.

Van der Waals' attractive forces are also acknowledged as playing a major role in the high degree of specificity encountered in enzyme/substrate and drug/receptor interactions.[21] The specificity of the interaction is thought to be due in part to the substrate or drug occupying a precise orientation in a cleft of the enzyme of receptor, the orientation being stabilised by van der Waals' attractive interactions.

(d) **Rate Processes, Free Energy and NMR Spectra**

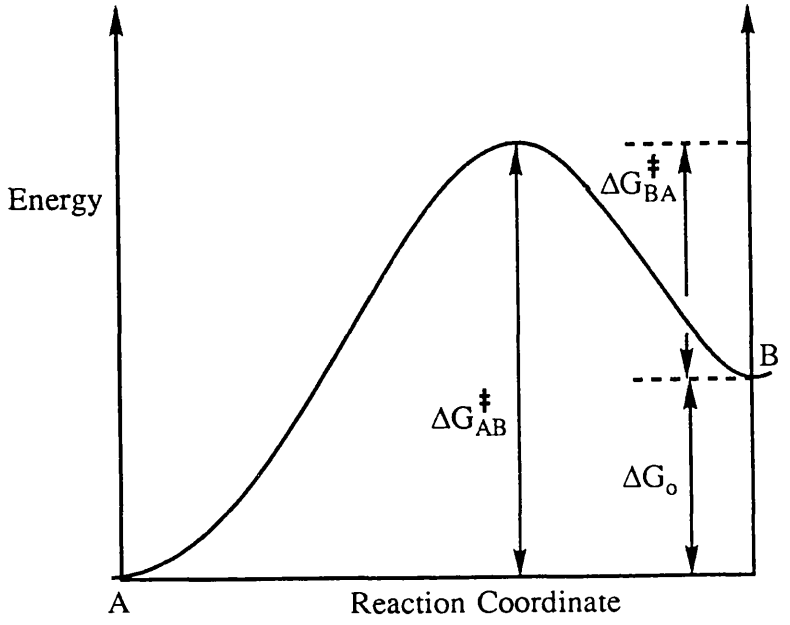

The above figure depicts the energy profile to be expected for a molecule interconverting between two states **A** and **B** (of unequal energy), via a single transition state.

The position of the equilibrium at a particular temperature is determined by ΔG_o, the free energy for the process:

$$\Delta G_o = -RT \ln\left\{\frac{[B]}{[A]}\right\}$$

and is obtainable directly from an NMR spectrum under conditions of slow exchange on the NMR timescale[22] by NMR integration of the peaks corresponding to **A** and **B**.

To convert state **A** to state **B** it is necessary to supply the free energy of activation, $\Delta G^{\ddagger}_{AB}$, and it is the magnitude of $\Delta G^{\ddagger}$ which determines the rate of interconversion, k_T.

The rate constant for interconversion, k_T, is related to $\Delta G^{\ddagger}$ in accordance with the Eyring equation[23]:

$$k_T = \frac{k_B T f}{h} \exp\left(-\frac{\Delta G^{\ddagger}}{RT}\right)$$

k_B = Boltzmann's constant
h = Planck's constant
f = transmission coefficient
R = Gas constant
T = absolute temperature

$$\text{or} \quad \Delta G^{\ddagger} = RT\left\{23.76 + \ln T_c - \ln k_T\right\}$$

The rate constant k_c of a chemical exchange process at the coalescence temperature[22] T_c for two exchanging NMR signals ν_A and ν_B is given by[24]

$$k_c = \frac{\pi \Delta \upsilon}{\sqrt{2}}$$

enabling $\Delta G^{\ddagger}$ to be readily determined by observation of the lineshape of two coalescing signals.

(e) Aims of the present work

All the literature examples of non-macromolecular alkyl/alkyl van der Waals' attraction cited previously possess the common feature of a two-fold conformational equilibrium, one side of the equilibrium has two or more alkyl groups close to one another and attracting one another, the other has the alkyl groups further apart and not interacting. Both sides of the equilibrium have putatively the same repulsive steric interactions and hence these repulsive interactions may be considered to cancel and can be neglected in

the analysis, resulting in a conformational equilibrium, the position of which is determined solely by van der Waals' attraction.

Once the conformational process interconverting the two sides of the equilibrium becomes slow on the NMR timescale, it is possible to measure directly the populations of the two states by NMR integration of the appropriate signals.

The literature relating to conformational analysis contains many examples of the effects of steric repulsion in molecules, but very few on the consequences of van der Waals' attraction. It was therefore felt that this neglected topic merits more detailed research. The present work sets out to devise more examples of such two-fold equilibria as described above, various alkyl groups for a given system being employed to study the effect on the equilibrium of changing the nature of the attracting alkyl groups. It was also hoped to supplement the experimental results with the results from molecular mechanics calculations. The following four chapters, (**2**)-(**5**), detail the results of the present research on four such conformational equilibria.

Chapter 2:

Unusual Equilibrium Between the Valence Bond Isomers of 1,4- and 1,6-Dialkylcyclooctatetraenes

(a) Introduction

(b) Molecular Mechanics Calculations

(c) NMR Results

(d) Solvent Dependence of the Cyclooctatetraene Bond-Shift Equilibrium

(e) Enthalpy (ΔH_o) and Entropy (ΔS_o) Changes for the Cyclooctatetraene Bond-Shift Equilibrium

(f) Conclusions

(g) Synthesis

(h) Experimental

(a) **Introduction**

It has recently been shown that 1,4-disubstituted cyclooctatetraenes **A** equilibrate with the 1,6-isomers **B** by a bond-shift process slow enough on the NMR timescale to allow direct measurement of the populations of the two states.[14,15,25]

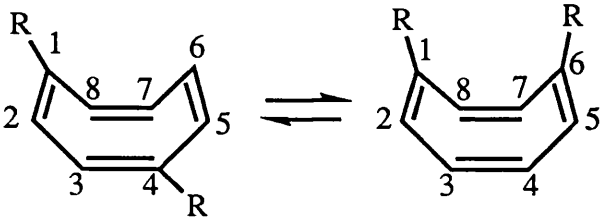

R	Cmpd
Me	**7**
Et	**8**
ipr	**9**
^{t}Bu	**10**

A 1,4-isomer

B 1,6-isomer

The ground state cyclooctatetraene conformation is tub-shaped and the immediate environment of group R in both forms is the same, the only difference appearing to be whether the groups R are near to each other as in the 1,6-isomer **B** or further away as in the 1,4-isomer **A**. Bond-shift isomer **B**, where both R groups are close together might be expected to have greater van der Waals' attractive forces between the pendant R groups and therefore be more stable than isomer A. Indeed, this has been confirmed by NMR studies and molecular mechanics calculations for the di-^{t}bu-cyclooctatetraene equilibrium.[14,15,16,17]

For the purposes of the present work, four such 1,4-dialkyl substituted cyclooctatetraenes, **7**,**8**,**9** and **10** were synthesised and studied by NMR and molecular mechanics calculations.

(b) Molecular Mechanics Calculations

(i) 1,4 and 1,6-dimethylcyclooctatetraenes **7A** and **7B**

	anti/anti		*anti/syn*		*syn/syn*	
	1,6-isomer **7B**	1,4-isomer **7A**	1,6-isomer **7B**	1,4-isomer **7A**	1,6-isomer **7B**	1,4-isomer **7A**
Methyl-1 dihedral angle[a]	-172.1	-179.6	-172.7	-179.7	-2.0	-4.1
Methyl-4(6) dihedral angle	171.8	-179.6	1.5	-3.5	3.2	-4.1
Total steric energy	10.3742	10.4253	10.6420	10.6798	10.8946	10.9322
Compression[b]	0.1784	0.1800	0.1860	0.1927	0.1950	0.2053
Bond angle bending	2.1514	2.2018	2.2365	2.2584	2.3059	2.3140
Stretch-bend	0.0366	0.0345	0.0388	0.0375	0.0411	0.0403
van der Waals' 1,4-energy	4.4016	4.3988	4.2986	4.3067	4.2050	4.2186
van der Waals' longer-range energy[c]	-1.7460	-1.7615	-1.5406	-1.5026	-1.3233	-1.2418
Torsional strain	5.3332	5.3561	5.4035	5.3716	5.4518	5.3802
Dipolar	0.0191	0.0155	0.0192	0.0155	0.0192	0.0155
Sum of 16 pairwise methyl atom interactions	-0.0898	-0.0223	-0.0967	-0.0223	-0.1059	-0.0222

Table 1: Molecular mechanics calculation of the three conformations *anti/anti, anti/syn, and syn/syn* of **7A** and **7B** in kcalmol^{-1}

Notes:

a Angle in degrees. For *Syn* and *anti* methyl groups dihedral angles reported are for the hydrogen nearly eclipsing the double bond and nearly antiperiplanar to the double bond, respectively. Values are never exactly 0 and 180°, and in every case the sign indicates that rotation has taken the hydrogen to a position outside perfectly periplanar rather than inside.

b Strain energy from lengthening or shortening of bonds.

c The negative sign indicates stabilisation rather than strain.

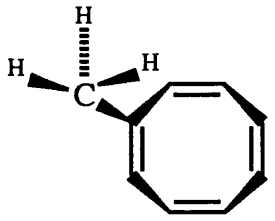

11

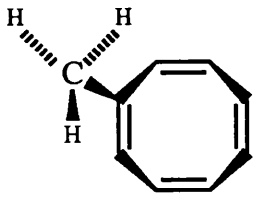

12

Calculations for bond shift isomers **7A** and **7B** have been reported elsewhere.[16,17] For the purposes of the present work these calculations were repeated in rather more detail with respect to the methyl groups' rotational conformations which are undoubtedly significant but which were not considered in that earlier report.

There are two stable conformations for a methyl group separated by approximately 60°, depending on whether a proton is antiperiplanar **11** or synperiplanar **12** with respect to the contiguous double bond, and the former is calculated to be more stable by about 0.26 kcalmol^{-1}. For both dimethylcyclooctatetraenes there are thus three different conformations, *anti/anti, anti/syn, and syn/syn*. The calculated enthalpies of these are shown in Table 1, and in each case the 1,6-dimethyl compound **7B** is more stable than the 1,4-dimethyl compound **7A** by 38-51 calmol^{-1}. The Table shows the various contributions to the total enthalpy of the two isomers and the sum of the sixteen pairwise atomic interactions of the two methyl groups for each conformation.

The difference between bond-shift isomers is thus smaller than the difference between methyl group conformations within each isomer. Each bond-shift isomer may therefore be calculated (*via* $\Delta G_o = -RT \ln K$) to be similarly composed of 37% *anti/anti*, 24% each of *anti/syn* and *syn/anti* and 15% of *syn/syn* at +20°C. The conformationally weighted equilibrium constant for the **7A** $\rightleftharpoons$ **7B** equilibrium is thus calculated to be 1.076.

(ii) 1,4 and 1,6-diethylcyclooctatetraenes, **8A** and **8B**

	in/in [b]		*in/out* [c]		*out/out* [d]	
	1,6-isomer **8B**	1,4-isomer **8A**	1,6-isomer **8B**	1,4-isomer **8A**	1,6-isomer **8B**	1,4-isomer **8A**
Methyl-1 dihedral angle[a]	87.8	79.9	79.0	80.7	-78.9	-78.8
Methyl-4(6) dihedral angle	-70.8	77.7	80.5	-77.5	77.4	77.5
Total steric energy	12.0023	12.4367	12.2132	12.3989	12.3062	12.3413
Compression	0.3381	0.3381	0.3169	0.3300	0.3127	0.3220
Bond angle bending	2.5023	2.1434	2.2576	2.2764	2.4341	2.4561
Stretch-bend	0.0729	0.0651	0.0676	0.0667	0.0707	0.0693
van der Waals' 1,4-energy	6.3066	6.3458	6.2566	6.2670	6.1702	6.1854
van der Waals' longer-range energy	-3.1188	-2.8985	-3.0593	-2.8454	-2.8267	-2.7645
Torsional strain	5.8823	6.4273	6.3546	6.2886	6.1261	6.0576
Dipolar	0.0189	0.0155	0.0193	0.0155	0.0191	0.0155
Sum of 49 pairwise Et-Et atom interactions	-0.5242	-0.0523	-0.3042	-0.0519	-0.1220	-0.0461

Table 2: Molecular mechanics calculation of the three conformations *in/in*; *in/out*; and *out/cut* of **8A** and **8B** in kcalmol^{-1}

Notes:

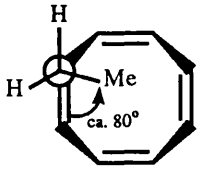

13 *in* conformation of an ethyl group

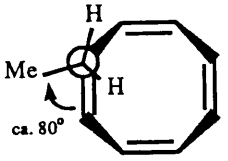

14 *out* conformation of ethyl group

a Angle in degrees. The angle referred to is the dihedral angle between the CH_2-CH_3 bond of the ethyl group and the contiguous olefinic double bond.

b *in/in* refers to the conformation where both ethyls point in towards the COT ring, the CH_2-CH_3 bond of the ethyl group lying approximately orthogonal to the contiguous double bond.

c *in/out* refers to the conformation where one ethyl points in towards the ring, one ethyl out from the ring.

d *out/out*: both ethyls point out from the COT ring.

Initial calculations were performed on mono-ethyl COT to determine the preferred conformation of an ethyl group substituted on a COT ring. Two

ground states were found, the *in* conformation **13** where the CH_2-CH_3 bond of the ethyl group points in towards the ring at approximately 80° to the contiguous double bond and the *out* conformation **14** where the CH_2-CH_3 bond lies *out* from the COT ring at approximately 80°. The *in* conformation was calculated to be 61 cal mol^{-1} less stable than the *out* one.

On moving to 1,4 and 1,6-diethylCOT, it was thus possible to calculate three conformations for each bond-shift isomer, namely *in/in*, 2 x *in/out* and *out/out*. The calculated enthalpies for these are shown in Table 2. In each case the 1,6-isomer **8B** is calculated to be more stable than the 1,4-isomer **8A** by between 35 and 435 $calmol^{-1}$, the greatest stabilisation arising in the *in/in* conformation. The 1,6-bondshift isomer **8B** may thus be calculated to be composed of 34% *in/in*, 23% each of *in/out* and *out/in* and 20% of *out/out*. Likewise the 1,4-isomer **8A** is calculated to be composed of 27% *out/out*, 25% each of *in/out* and *out/in* and 23% of *in/in*. The conformationally weighted equilibrium constant for the **8A** $\rightleftharpoons$ **8B** equilibrium is thus calculated to be 1.458 at +20°C (assuming $\Delta G_o = \Delta H_o$).

It is interesting to note that molecular mechanics calculates the *out* conformer to be the more stable for mono-ethylcyclooctatetraene and the *out/out* conformer to be the most stable for 1,4-diethylCOT. This is to be contrasted to the 1,6-diethylcyclooctatetraene bond-shift isomer, where the *in/in* conformation is calculated to be the most stable of the three possible conformations *in/in*, *in/out* and *out/out*, the *in/in* conformation maximising van der Waals' attraction between the two ethyl groups of the 1,6-isomer. It would thus appear that molecular mechanisms calculations predict a change in the preferred conformation of the alkyl groups in 1,4 and 1,6-diethylcyclooctatetraene, although it was not possible to obtain any spectral evidence from the ^{1}H-NMR spectrum of the **8A** $\rightleftharpoons$ **8B** equilibrium to confirm this.

(iii) 1,4 and 1,6-di-isopropylcyclooctatetraenes 9A and 9B

	in/in [b]		*in / anti* [c]		*anti / anti* [d]	
	1,6-isomer **9B**	1,4-isomer **9A**	1,6-isomer **9B**	1,4-isomer **9A**	1,6-isomer **9B**	1,4-isomer **9A**
Methyl-1 dihedral angle[a]	24.7	32.8	33.6	33.3	179.1	177.3
Methyl-4(6) dihedral angle	-37.5	32.9	-178.6	177.9	-175.4	178.4
Total steric energy	13.9107	14.4171	14.1967	14.6472	14.4294	14.8356
Compression	0.6825	0.6724	0.6205	0.6519	0.6161	0.6373
Bond angle bending	2.8594	2.2872	2.3479	2.4391	2.7079	2.6546
Stretch-bend	0.1337	0.1269	0.1356	0.1329	0.1429	0.1402
van der Waals' 1,4-energy	8.0506	8.1232	8.0369	8.0406	7.9295	7.9439
van der Waals' longer-range energy	-3.8699	-3.6415	-4.1884	-3.6295	-3.9633	-3.5904
Torsional strain	6.0356	6.8334	7.2246	6.9967	6.9770	7.0345
Dipolar	0.0187	0.0155	0.0197	0.0155	0.0193	0.0154
Sum of 100 pairwise ipr-ipr atom interactions	-0.5732	-0.0743	-0.6578	-0.0842	-0.5112	-0.0928

Table 3: Molecular mechanics calculation of the three conformations *in/in*; *in/anti*; and anti/anti for **9A** and **9B**.

Notes:

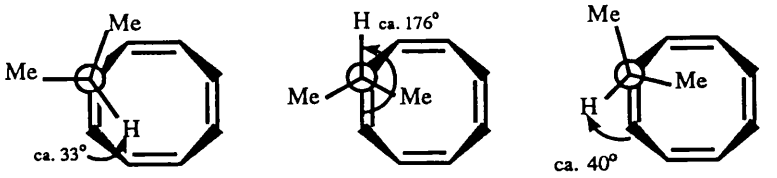

15 : *in* **16** : *anti* **17** : *out*

[a] Angle in degrees. The angle referred to is the dihedral angle between the ipr-methine hydrogen and the contiguous double bond of the COT ring.

[b] *in/in* refers to the conformation where both ipr-methine hydrogens point in towards the ring.

[c] *in/anti* refers to the conformation where one ipr-methine hydrogen points in towards the ring, the other is antiperiplanar to the contiguous double bond of the COT ring.

[d] *anti/anti* refers to the conformation where both ipr-methine hydrogens lie antiperiplanar to the contiguous double bond.

Calculations performed on mono-isopropylCOT indicate three preferred conformations **15**, **16**, **17** of an isopropyl group on a COT ring with calculated energies of 11.5309, 11.7463 and 12.3171 kcalmol^{-1} respectively. A dihedral drive of mono-iprCOT showed conformation **17**, where the methine hydrogen lies at 40° to the double bond, to occupy a relatively shallow potential energy minimum which was separated by only a small energy barrier of about 0.1 kcalmol^{-1} from conformer **15**. It was therefore decided to neglect conformation **17** and treat **15** and **17** as a single energy minimum. On this basis it was possible to calculate three preferred conformations each for 1,4 and 1,6-di-isopropyl cyclooctatetraenes **9A** and **9B**, namely *in/in*, *in/anti* and *anti/anti*. The calculated enthalpies for these are shown in Table 3. In each case the 1,6-isomer **9B** is calculated to be more stable than the 1,4-isomer **9A** by between 406 and 506 calmol^{-1}. The 1,6-isomer **9B** can thus be calculated to be composed of 38% *in/in*, 23% each of *in/anti* and *anti/in* and 16% of *anti/anti*. Likewise the 1,4-isomer is calculated to be composed of 35% *in/in*, 24% each of *in/anti* and *anti/in* and 17% of *anti/anti*. The conformationally weighted equilibrium constant for the **9A** $\rightleftharpoons$ **9B** equilibrium is thus calculated to be 2.215 at +20°C.

(iv) 1,4 and 1,6-di-^{t}Bu-cyclooctatetraenes **10A** and **10B**

	1,6-isomer, **10B**	1,4-isomer, **10A**
^{t}Bu-1 dihedral angle [a]	169.5	169.8
^{t}Bu-6-(4) dihedral angle	-178.9	169.7
Total steric energy	17.6924	18.7077
Compression	1.4951	1.5550
Bond angle bending	2.8016	2.4512
Stretch bend	0.2036	0.1916
van der Waals' 1,4 energy	9.6602	9.7183
van der Waals' longer range energy	-4.0894	-3.2418
Torsional strain	7.6020	8.0180
Dipolar	0.0194	0.0153
Sum of 169 pairwise ^{t}Bu-^{t}Bu atom interactions	1.0756	0.1318

Table 4: Molecular mechanics calculations on 1,4 and 1,6-di-^{t}BuCOT. Energies in kcal/mol.

Notes:

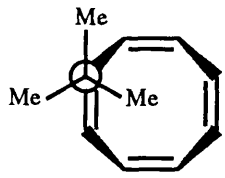

18

[a] Angle in degrees. The angle referred to is the dihedral angle between a CH_3-C_{qual} bond of the ^{t}Bu-group and the contiguous double bond of the COT ring (see structure **18**). In both the 1,4 and the 1,6-isomers **10A** and **10B**, the methyl group lies slightly in towards the COT ring.

Calculations for bond-shift isomers **10A** and **10B** show only one preferred conformation for a ^{t}Bu-group on a COT ring with a methyl group of the ^{t}Bu-group lying more or less antiperiplanar to the contiguous double bond (**18**).

The 1,6-isomer **10B** was calculated to be approximately 1.0 kcalmol^{-1} more stable than the 1,4-isomer **10A**. The equilibrium constant for the **10A** $\rightleftharpoons$ **10B** equilibrium is thus calculated to be 5.545 at + 25°C. These molecular mechanics results for the (^{t}Bu)$_2$COT equilibrium are in good general agreement to those reported by Allinger[16] *et al* for this compound.

Final note on Molecular mechanics calculations

The calculations predict differences in several terms as contributing to the overall stability of the 1,6-isomer in cyclooctatetraenes **7-10**, which suggests caution in assigning the greater stability of the 1,6-isomer to attractive steric interactions alone. However the 1,6-isomer is calculated to have greater *vdw* attraction for each bond-shift isomer pair in the series of compounds **7-10**, and certainly for the di-^{t}Bu-COT equilibrium, the van der Waals' attraction component of the steric energy is seen to be a major factor in determining the 1,6-isomers' greater stability.

(c) **NMR results for dialkylcyclooctatetraenes 7 - 10**

(i) 1,4 and 1,6-dimethylcyclooctatetraenes **7A** and **7B**

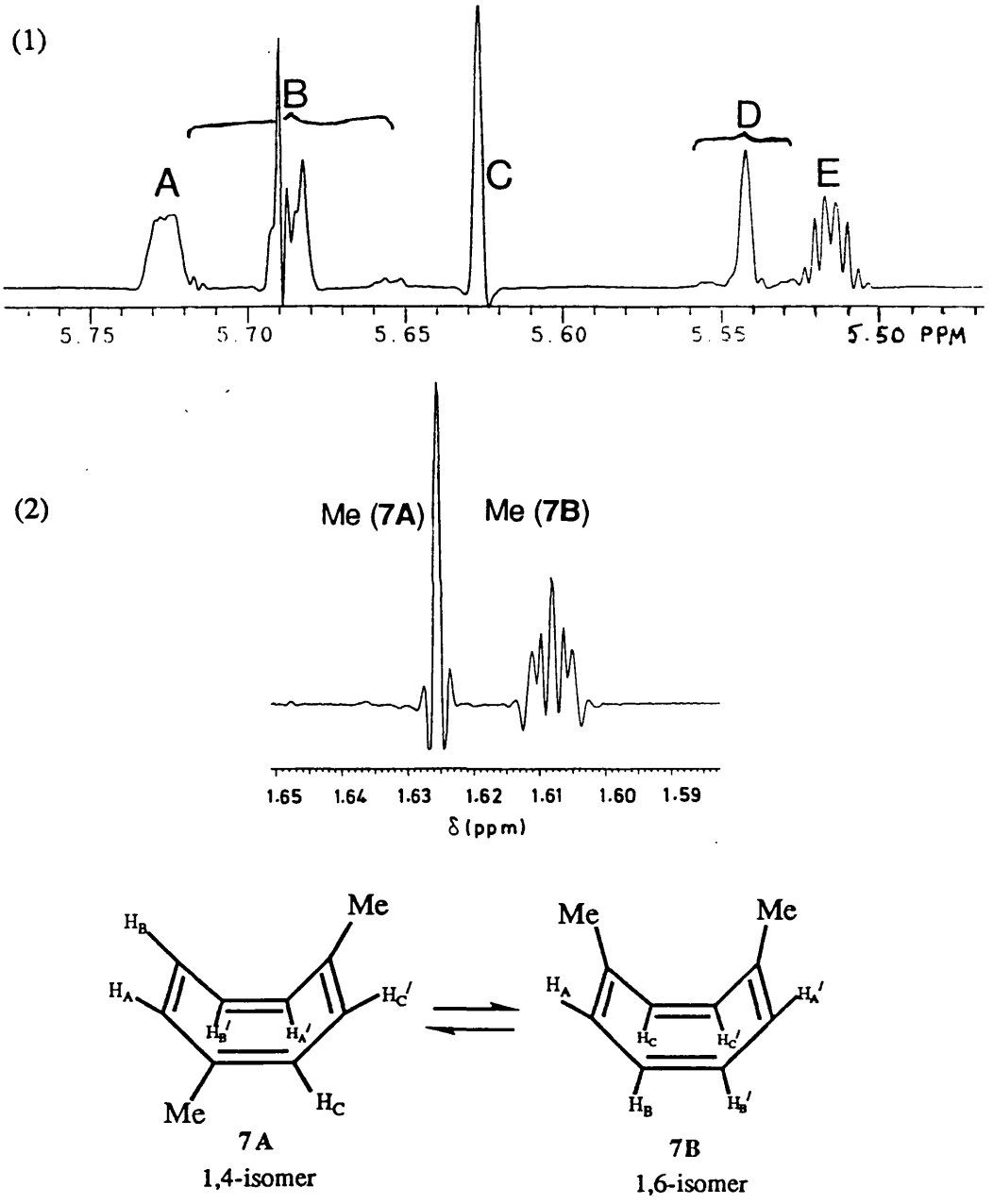

Figure 6 ^{1}H-NMR, resolution enhanced spectrum of 1,4 and 1,6-dimethylcyclooctatetraenes in C_6D_6 at +20°C (400 MHz), with assignments. Spectrum (1) Shows the olefinic region; Spectrum (2) the methyl region.

Notes:

A: half-multiplet of AA'BB' for 1,6-isomer
E: half-multiplet of AA'BB' for 1,6-isomer
B: AA'BB' of 1,4-isomer
C: CC' of 1,6-isomer
D: CC' of 1,4-isomer

The ^{1}H-NMR spectrum of the **7A** ⇌ **7B** equilibrium at 200 and 400 MHz showed slow bond-shift on the NMR timescale for most signals. In $CDCl_3$, some of the olefinic signals were seen to overlap; the most simple spectrum was obtained in C_6D_6 due to this solvent's well known high magnetic anisotropy (Fig.6). On warming a $CDCl_3$ soln. of **7** at 200 MHz, the methyl signals ($\Delta\nu$ = 3.9 Hz) were seen to broaden, coalesce (+52°C) and sharpen up to a single peak, whence a free energy of activation for bond-shift of 17.70 kcalmol^{-1} may be calculated via the Eyring equation.

Conformational assignment of ^{1}H-NMR signals in 7

It was possible to group together signals from a single bond-shift isomer by spin decoupling at a signal and observing which other signals in the spectrum sharpened up. Clearly, signals that are coupled together must arise from the same bond-shift isomer, as opposed to signals which are undergoing mutual exchange via the bond-shift process, which should show no sharpening up on spin decoupling. In this manner, it was possible to group together two sets of signals in Fig. 6, one set belonging the 1,4-isomer **7A** and the other set to the 1,6-isomer **7B**.

For the 1,6-isomer **7B**, where the dihedral angle between H_A and H_B is approximately 47° according to molecular mechanics calculations, $^3J_{AB}$ is expected to be ≈ 3Hz. The coupling constant $^3J_{BB'}$ is a vicinal coupling *cis* on a double bond and is therefore expected to be about 11Hz.

For the 1,4-isomer **7A**, $^3J_{AB}$ = 11Hz and $^3J_{BB'}$ = 3Hz. Hence the AA'BB'CC' spin systems for the two bond-shift isomers are expected to have quite different appearances.

Spin simulation of an AA'BB'CC' spin system for the 1,6-isomer using $^3J_{AB}$ = 3Hz, $^3J_{BB}$ = 11Hz and other reasonable J-values for the 1,6-isomer resulted in a simulated spectrum that resembled closely the experimental spectrum obtained by spin decoupling at the most upfield of the two methyls.

Spin simulation of an AA'BB'CC' spin system using $^3J_{AB}$ = 11.0 Hz, ^{3}JBB' = 3Hz and other reasonable J values to be expected for the 1,4-isomer resulted in a simulated spectrum that resembled closely the experimental spectrum obtained by spin decoupling at the most downfield of the two methyls.

Integration of the methyl resonances yielded an equilibrium constant, K, of 1.290 ($CDCl_3$, +20°C).

It was possible to obtain a saturation transfer[26] measure of the valence isomerisation rate for the **7A** ⇌ **7B** equilibrium. Pre-irradiation of the CC' (**7B**) signal (Fig. 6) at + 20°C results in saturation transfer to CC' (**7A**), whence a rate constant of 0.36 S^{-1} and hence a $\Delta G_A^{\ddagger}$ of 17.76 $kcalmol^{-1}$ is calculated for interconversion of **7B** to **7A**. Likewise, pre-irradiation of CC' (**7A**) results in saturation transfer to CC' (**7B**), whence a rate constant of 0.50 S^{-1} ($\Delta G_A^{\ddagger}$ = 17.57 $kcalmol^{-1}$) is calculated for interconversion of **7A** to **7B**. Both $\Delta G_A^{\ddagger}$ values are in good agreement to that determined by the coalescence of methyl signals (17.70 $kcalmol^{-1}$, + 52°C).

(ii) 1,4 and 1,6-diethylcyclooctatetraenes **8A** and **8B**

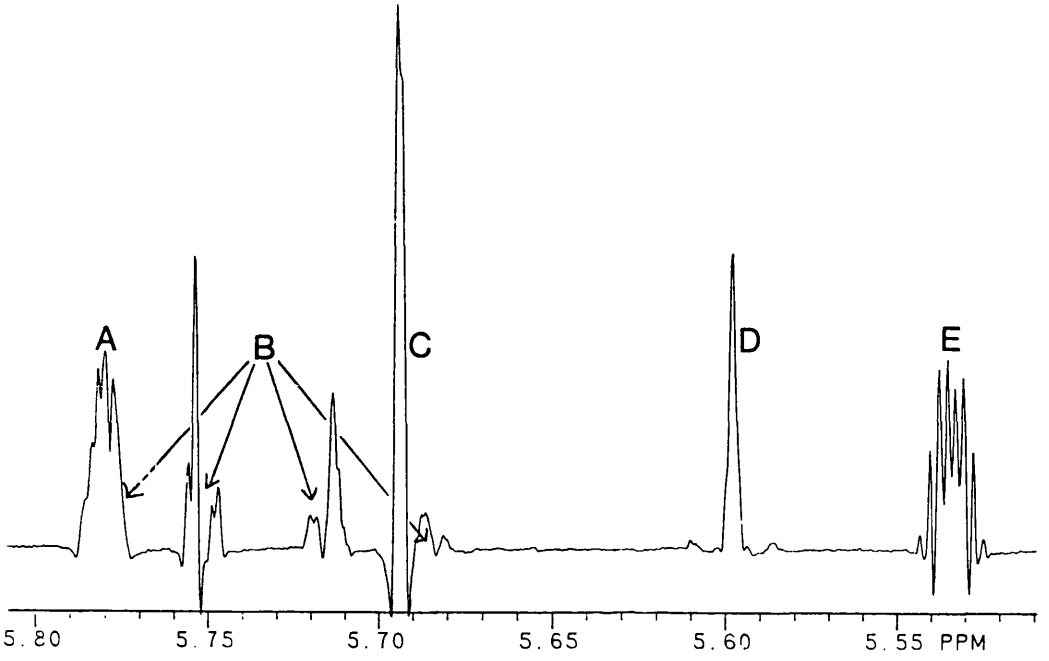

Fig. 7: ^{1}H-NMR resolution enhanced spectrum of 1,4 and 1,6-diethylcyclooctatetraenes **8A** and **8B** in C_6D_6(+20°C) at 400 MHz, with assignments. For signal assignments A-E, refer to Fig. 6 (notes), p.32.

A barrier to bond-shift was determined by observing methyl signal coalescence as the temperature was raised. At +49°C ($CDCl_3$) the two methyl triplets ($\Delta\nu$=2.5Hz) had coalesced to a single triplet, whence a free energy of activation of 17.82 kcalmol^{-1} is calculated *via* the Eyring equation.

The methylene ^{1}H-NMR signals showed changes consistent with *ring inversion*[27] becoming slow on the NMR timescale at temperatures between + 40°C and -40°C, although these results are not reported here.

Integration of signals D and E (Fig.7) yielded an equilibrium constant,

K, of 1.505 (C_6D_6, +20°C) for the **8A** $\rightleftharpoons$ **8B** equilibrium.

(iii) <u>1,4 and 1,6-di-isopropylcyclooctatetraenes **9A** and **9B**</u>

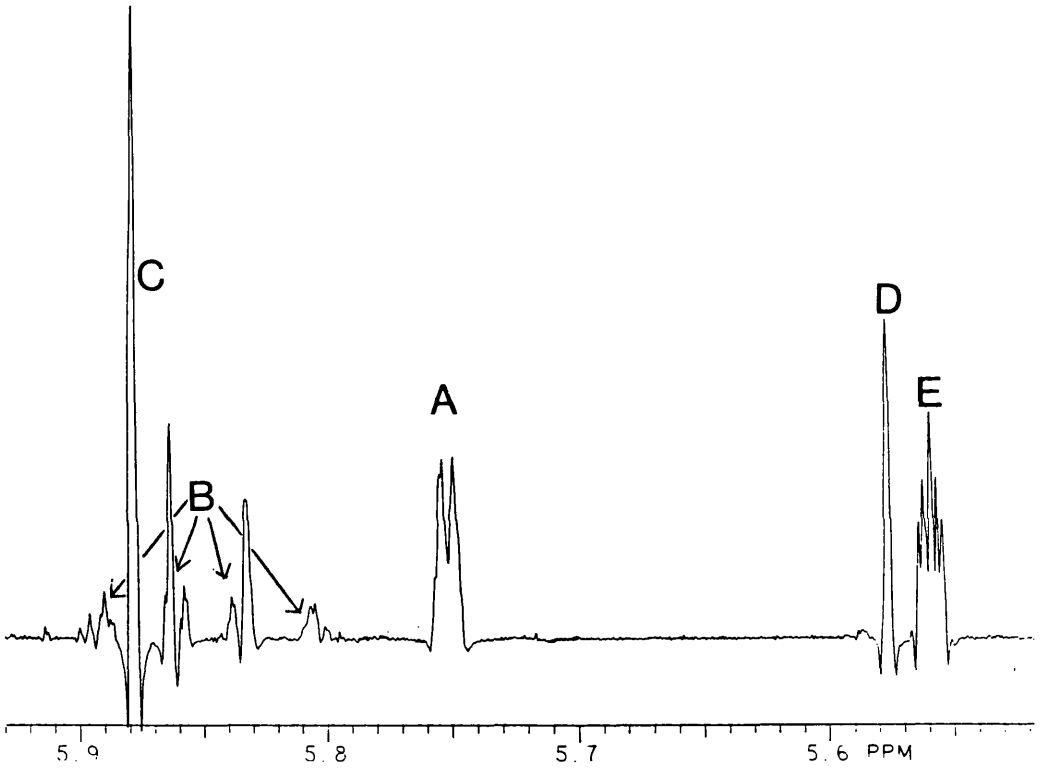

<u>Fig.8</u>: ^{1}H-NMR resolution enhanced spectrum of 1,4 and 1,6-di-isopropylcyclooctatetraenes **9A** and **9B** in $CDCl_3$(+20°C) at 400 MHz. For signal assignments A-E, refer to Fig.6(notes).

A barrier to bond-shift was determined by observing methyl signal coalescence as the temperature was raised. At +86°C the two methyl doublets ($\Delta\nu$=9.3Hz) had coalesced to a single doublet, whence a free energy of activation of 19.00 kcalmol^{-1} is calculated *via* the Eyring equation.

The isopropyl methyl signals (^{1}H and ^{13}C-NMR) showed changes consistent with ring inversion becoming slow on the NMR timescale at temperatures between +20°C and -40°C, although these results are not reported here

Integration of signals D and E yielded an equilibrium constant, K, of 1.859 ($CDCl_3$, +20°C) for the **9A** ⇌ **9B** equilibrium.

(iv) 1,4 and 1,6-di-^{t}Bu-cyclooctatetraenes **10A** and **10B**

Integration of the ^{t}Bu-resonances at 1.08 and 1.06 ppm yielded an equilibrium constant, K, of 1.896 ($CDCl_3$, +25°C) for the **10A** ⇌ **10B** equlilibrium (see Fig. 9).

Fig.9: ^{1}H-NMR resolution enhanced spectrum of 1,4 and 1,6-di-tert-butyl-cyclooctatetraene in $CDCl_3$(+20°C). Signal assignments A-E refer to Fig.6 (notes).

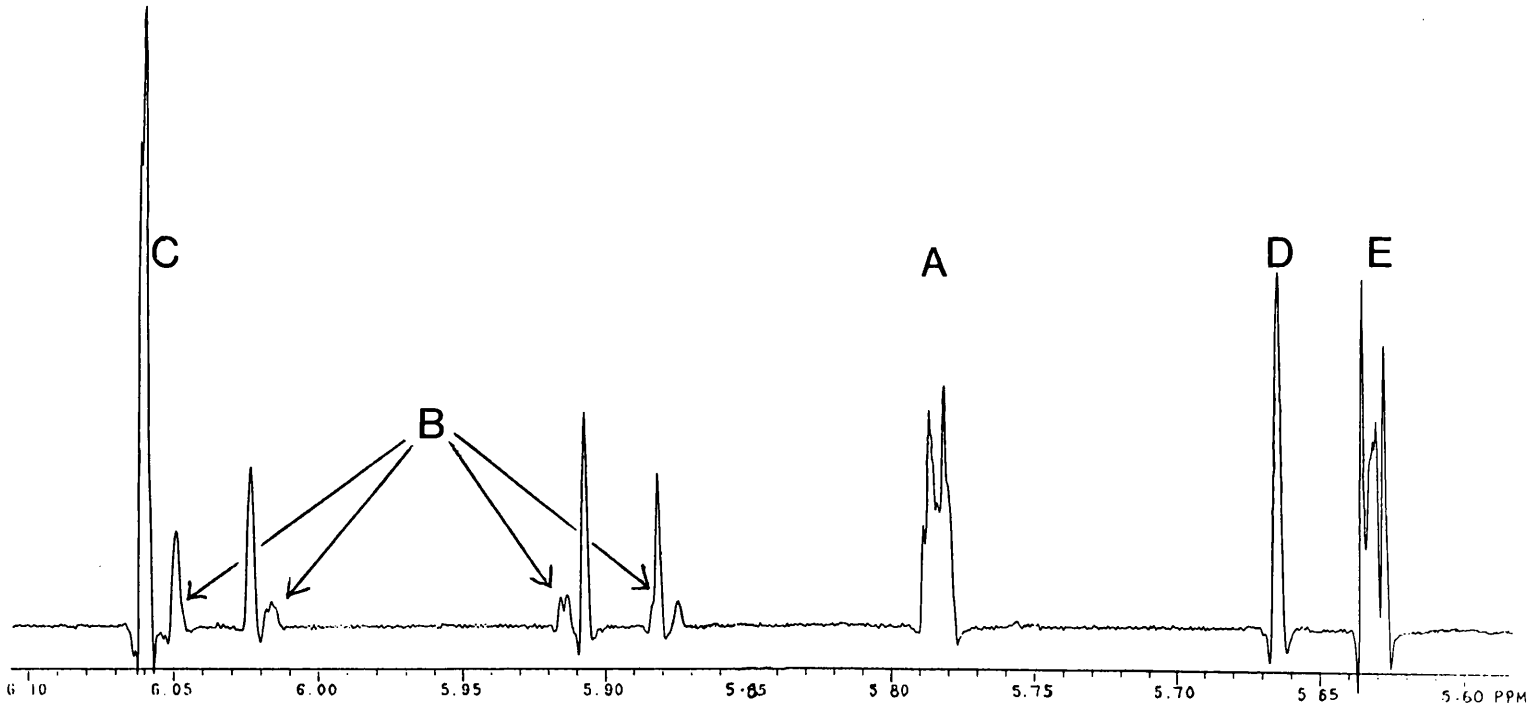

(d) **Solvent Dependence of the Cyclooctatetraene Bond-Shift Equilibrium**

To determine whether the position of the cyclooctatetraene bond-shift equilibrium is solvent dependent, a sample of diethylcyclooctatetraene, **8**, was dissolved in THF-d_8 and increasing amounts of D_2O were added, the equilibrium constant being measured after each addition of D_2O. In this manner it was possible to measure the equilibrium constant in varying amounts of D_2O solvent, up to, and including a solvent mixture comprised of 50%THF-d_8 / 50%D_2O (by volume). The equilibrium constants thus measured did not vary appreciably from the value of 1.505 determined for the **8A** $\rightleftharpoons$ **8B** equilibrium in (C_6D_6, +20°C). It would therefore appear that the cyclooctatetraene equilibrium is solvent independent and is determined principally by intramolecular factors. This conclusion has also been reached by other workers in this field.[25,28]

(e) **Enthalpy (ΔH_o) and Entropy (ΔS_o) Changes for the Cyclooctatetraene Bond-Shift Equilibrium**

Graphs of experimentally determined lnK as ordinate versus 1/T as abscissa were plotted for the cyclooctatetraenes **7-10** (gradient = $-\Delta H_o/R$, y-axis intercept = $\Delta S_o/R$) to determine ΔH_o and ΔS_o. Particular care was taken to ensure that the samples had equilibrated at a particular NMR probe temperature by allowing at least five times the half-life for valence isomerisation to pass before recording a spectrum at a given temperature. For cyclooctatetraenes **7-10**, the proportion of the 1,4-isomer was found to increase as the temperature was raised. For compound **7**, small variations in the equilibrium constant were measured, none of them systematic enough

to indicate a significant temperature dependence over the range that could be measured (-20°C to +40°C).

None of the graphs for compounds **7** - **10** were of sufficient quality to allow determination of ΔH_o and ΔS_o and hence are not shown in this work. This was due to the very small magnitude of the changes in the equilibrium constants as the temperature was varied, and, the limited temperature range over which the equilibrium constants could be measured. At high temperatures, as bond-shift becomes fast on the NMR-timescale, ^{1}H-NMR signals begin to coalesce and hence could not be integrated. At lower temperatures, the rate of bond-shift becomes so slow that it is not feasible to wait the inordinately long times required for equilibrium to be reached before signals can be integrated. In general however, all the graphs showed the 1,6-isomer to have the lower enthalpy and indicated that 1,4 $\rightleftharpoons$ 1,6 equilibrium has a small negative ΔS_o.

That the 1,6-isomer is enthalpically favoured can be interpreted in terms of greater van der Waals' attractive stabilisation between its proximate 1,6-alkyl groups, as compared to the corresponding 1,4-isomer.

The lower entropy value of the 1,6-isomer can be explained as follows. In the 1,6-isomer, where the alkyl groups experience mutual attraction, the internal degrees of rotational freedom associated with the alkyl groups might be expected to be reduced somewhat as compared to the 1,4-isomer, where the alkyl groups are more distant and hence not interacting. Hence the 1,6-isomer is entropically disfavoured.

The exception to the above trend in ΔH_o and ΔS_o was for dimethyl-cyclooctatetraene, **7**, where both ΔH_o and ΔS_o were found to be close to zero. The quality of this graph prevented further investigation of this point,

although there was nothing in the graph to suggest that both ΔH_o and ΔS_o could not have small negative values.

It is interesting to note that Streitwieser[14] claims to have determined ΔH_o and ΔS_o for the **10A** ⇌ **10B** equilibrium *via* a plot of lnK versus 1/T, although Paquette[15] was unable to repeat these results.

However, inspection of Streitwieser's data[14] suggests that he has inadvertently plotted ln (lnK) vs 1/T rather than lnK versus 1/T and hence his reported values of ΔH_o and ΔS_o would appear to be incorrect. Even if this mistake is allowed for and ΔH_o and ΔS_o recalculated from his data, the values of ΔH_o and ΔS_o thus obtained are found to both be *positive* for the 1,4 ⇌ 1,6 equilibrium which implies the 1,6-isomer has the greater enthalpy and entropy, a result which is clearly in disagreement with the results of the present work.

(f) Conclusions

Compound	K(exptl)[a]	K(MMP2)[b]	nxn[c]
7	1.290($CDCl_3$,+20°C)	1.076 (+20°C)	16
8	1.505(C_6D_6, +20°C)	1.458 (+20°C)	49
9	1.859($CDCl_3$, +20°C)	2.215 (+20°C)	100
10	1.896($CDCl_3$, +25°C)	5.545 (+25°C)	169

Table 5: Summary of pertinent NMR and MMP2 results for cyclooctatetraenes **7-10.**

[a] experimentally determined equilibrium constant

[b] MMP2 predicted equilibrium constant

[c] number of pairwise atomic alkyl-alkyl interactions.

The experimentally determined equilibrium constants are seen to increase as the size of the alkyl group increases, a trend which is expected if the equilibrium is determined by van der Waals' attractive forces between the pendant alkyl groups. However, the increase in the equilibrium constant is not in proportion to the number of alkyl-alkyl interactions (nxn), as might be anticipated. Berg and Petterson[13] have pointed out though that the various alkyl groups in a series of compounds like **7** - **10** are situated at different positions on a van der Waals' potential energy curve, and the experimentally determined equilibrium constants may well reflect this, rather than just reflecting the size (n x n) of the two attracting alkyl groups.

Turning to the MMP2 results, it may be seen that in general, the MMP2 predicted K-values do not match very well the experimentally determined K-values. This may well be a reflection of the fact that molecular mechanics calculates the *enthalpy* of a molecule, whereas the experimentally determined K-values represent *free energy differences*. In addition to this, the attractive region of the van der Waals' potential energy function in molecular mechanics is not well defined, nor is the parametisation by any means certain.[3] Nevertheless, the calculations do succeed in correctly predicting the general trend of increasing stability of the 1,6-isomer with increase in alkyl group size, although this result is to be expected if the molecular mechanics parametisation does not overestimate the van der Waals' radii of the two attracting alkyl groups.

In conclusion, it has been determined that the more compact 1,6-isomer is favoured in solution for cyclooctatetraenes **7** - **10**. The greater the size of the alkyl group, the greater the equilibrium constant in favour of the 1,6-isomer. This effect may be attributed to attractive steric interactions

between the pendant alkyl groups. Molecular mechanics calculations on the bond-shift isomers correctly predict the general trend of increasing stability of the 1,6-isomer with increase in size of the alkyl group, and confirm that the 1,6-isomer has greater alkyl-alkyl attractive steric interactions.

(g) **Synthesis**

A survey of the literature shows that direct attack of alkyl lithium reagents on COT has in general only led to the mono-alkylated COT. For example, Miller et al reacted MeLi, n-BuLi, Sec-BuLi, PhLi and $PhCH_2Li$ with COT, only mono-alkylated COTs being returned as products.[29] The exception to this trend appears to be the reaction of ^tBuLi with COT, in addition to mono-^{t}BuCOT as product, di-^{t}Bu-cyclooctatriene **22** is produced which can be oxidised to the 1,4 and 1,6-$(^tBu)_2$COT bond-shift isomers with potassium amide (scheme 2).[30] Attempts to further alkylate the mono-alkylated COT thus produced have proven to be non-regiospecific; for example Cope and Moore prepared a complex mixture of 1,2, 1,3, 1,4 and 1,5 diphenylCOT by reaction of PhLi with PhCOT, the resulting isomeric mixture being separated in very low yield by tedious counter-current distribution techniques.[31]

It was therefore decided to use Paquette's elegant synthesis of 1,4-dialkylCOTs involving sulphonation of cyclooctatetraene, dialkylation and photoinduced sulphur dioxide extrusion.[32] (Scheme 1). This method has the advantage that it yields isomerically pure dialkylCOTs since alkylation is directed to the 1,4-positions only.

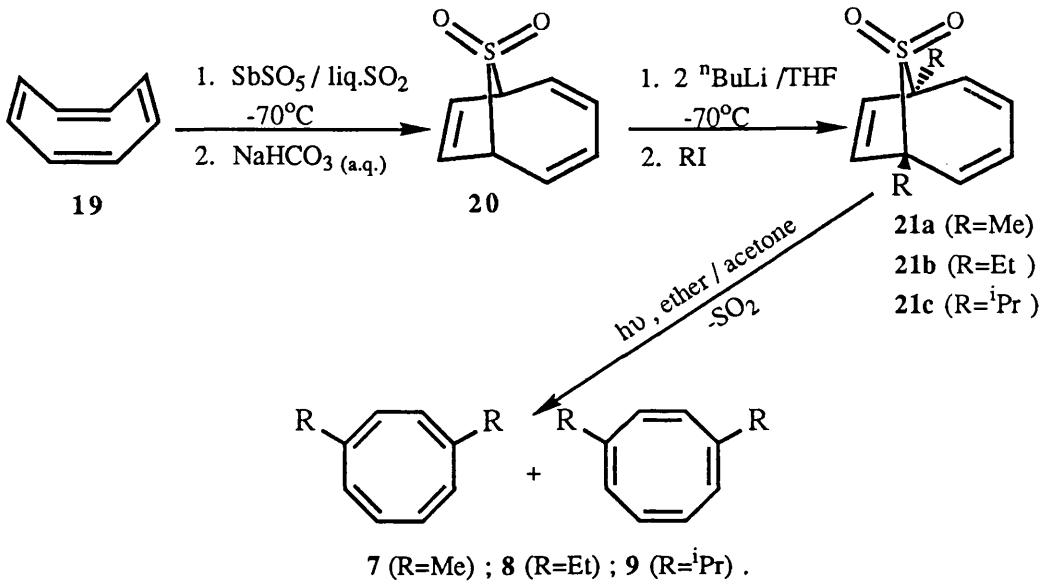

Scheme 1: Synthesis of 1,4-dialkylCOTS **7-9**.

During the course of this work it was found that Paquette's method works well for inserting primary alkyl groups but the yields are poor for 2°-alkyl groups. The "bottle-neck" in the reaction sequence is the quenching of the n-BuLi generated cyclooctatetraene dianion with alkyl halide. Thus, it was possible to produce 1,6-$(Me)_2COTSO_2$, **21a**, *via* quenching with MeI in approximately 81% yield. This is to be compared to a 5% yield of 1,6-$(ipr)_2COTSO_2$ **21c**, for the same step.

The more sterically hindered 1,4-(^{t}Bu)$_2$COT, **10**, was produced *via* Streitwieser's method[30] which involves direct attact of ^{t}BuLi on COT to yield 1,4-di-^{t}Bu-cyclooctatriene **22**, which is then deprotonated with potassium amide to yield the desired 1,4-di-^{t}Bu COT, **10** (scheme 2).

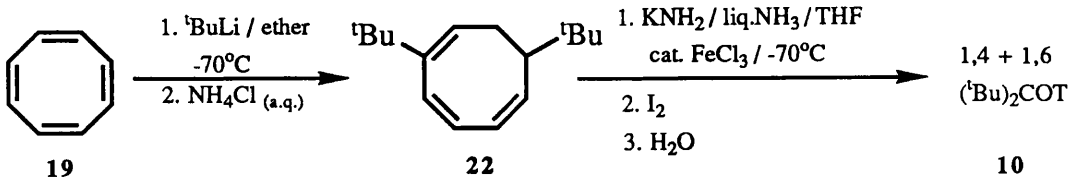

Scheme 2: Synthesis of di-tert-butylcyclooctatetraene, **10**.

(h) **Experimental**

Cyclooctatetraene sulphone **20**[33], 1,4-dimethylcyclooctatetraene **21a**[32] and 1,4-di-^{t}Bu-cyclooctatetraene **10**[30] were prepared according to literature methods. The synthesis of 1,4-dialkylcyclooctatetraenes **8** and **9** *via* Paquette's method (scheme 1) is described below.

(i) Preparation of 1,6-diethyl-9-thiabicyclo[4.2.1]nona-2,4,7-triene-9,9-dioxide, **21b**

To a stirred suspension of **20** (0.191g; 0.001 mol) in 11 cm^3 of THF cooled to -70°C and maintained under dry nitrogen was added dropwise n-BuLi in hexane (1.33cm^3, 2.64 equivs). The resulting black solution was stirred for five minutes at this temperature and was then quenched with EtI (2.84g, 16 equivs.) in 2cm^3 of THF. The reaction mixture was stirred for 20 minutes at this temperature and then allowed to warm to room temperature. The solvent was rotary evaporated, and the residue taken up in 50 ml of CH_2Cl_2 and washed with water. The solvent was dried ($MgSO_4$) and rotary evaporated to yield 190mg of a yellow solid, whose NMR was consistent with that of **21b** in fairly high purity. This material was used unpurified for the next step of the reaction sequence. Contaminating the sulphone **21b** was a small amount (approximately 10%) of

1-ethyl,6-(1-n-Bu)-9-thiabicyclo[4.2.1]nona-2,4,7-triene-9,9-dioxide identified by its ^{1}H and ^{13}C-NMR spectra. This material was not separated from the desired sulphone **21b** at this stage of the reaction sequence, but was photolysed with **21b** and then separated by GLC. A small amount of **21b** was purified by HPLC for the purposes of characterisation, yielding a yellow solid, mp=154°C (column = 50x4.6mm + 250 x 10mm partisil 5 silica; mobile phase = 15% ethylacetate / 85% hexane; flow rate = 4.0cm^3/min; t_{ret} = 14 minutes).

^{1}H-NMR: ($CDCl_3$, ppm, 200MHz): NMR **21b**: 1.19 (CH_3, triplet, 6H, J=7.4Hz); 1.8-2.3 (CH_ACH_B, multiplet, 4H); 5.55 (olefinic, singlet, 2H); 5.71-6.23 (olefinic, AA'BB', 4H).

^{13}C-NMR: ($CDCl_3$, ppm, 100MHz): 8.37 (CH_3); 24.72 (CH_2); 69.90 (C_{quat}); 123.79, 127.50, 132.08 (olefinic).

Analysis: Calculated for $C_{12}H_{16}SO_2$: C,64.25; H,7.19; S,14.29.

Found : C, 63.90; H, 7.40; S, 13.88.

(ii) Preparation of 1,4 and 1,6-diethylcyclooctatetraene, **8**, by photoinduced sulphur dioxide extrusion from **21b**

A solution of **21b**, (0.22g; 0.00098mol) in 58cm^3 of ether and 19cm^3 of acetone contained in a pyrex boiling tube with magnetic stirrer was deaerated with dry nitrogen for 30 minutes. The solution was then externally irradiated at room temperature with a 100 W medium pressure Hanovia lamp, whilst stirring. After 12.5 hours, intermittent TLC-analysis showed the reaction to be complete ($KMnO_{4(aq)}$ development). The solvent was rotary evaporated until a small amount of liquid remained. Isolation of (**8**) was achieved by preparative glc techniques (10ft x 3/8", 10% w/w silicone oil,

+200°C, t_{ret} 10 min). The desired product, **8**, was obtained as a pungent, clear, yellow liquid. Reinjection of **8** onto an analytical glc column showed the product to be homogeneous.

NMR data,**8**

^{1}H-NMR (400 MHz, ppm, C_6D_6) : 0.96 (t, CH_3 , 1,6-isomer, 6H) ; 0.98 (t, CH_3, 1,4-isomer, 6H); 1.83-2.06 (m, CH_2, 8H); 5.54-5.78 (m, olefinic, 12H).

^{13}C-NMR (100MHz, ppm, C_6D_6): 1,6-isomer: 13.57(Me); 30.91(CH_2); 125.57, 131.54, 133.69, 145.87 (olefinic)
1,4-isomer: 13.70(Me); 30.85(CH_2); 126.12, 131.08, 134.46, 144.89 (olefinic)

Mass Spectrum 8 m/e: 160, 145, 131, 117, 105, 91, 77, 65, 51, 39, 27
Calculated: 160.1252
Found : 160.1270

(iii) Preparation of 1,6-di-isopropyl-9-thiabicyclo[4.2.1]nona-2,4,7-triene-9,9-dioxide, **21c**

A suspension of 600mg of cyclooctatetraene sulphone, **19**, (0.00357mol) in THF (36cm^3)was stirred under argon at -65°C. n-BuLi (4cm^3, 0.0094mol, 2.64 equivs.) was then added slowly to the reaction vessel over a 30 second period via a syringe and the deep black solution stirred for five minutes at this temperature. Isopropyl iodide (5.46g, 0.032mol, 9 equivalents) was then injected into the reaction mixture and the mixture

stirred for 22 hours at -65°C. At the end of this time a further 3.8cm^3(0.0091mol) of n-BuLi was injected into the flask followed by 1g of neat isopropyl iodide. The mixture was stirred for a further 6 hours at -65°C, allowed to warm to room temperature, and then rotary evaporated. The residue was taken up in 200cm^3 of dichloromethane and washed with 3x40cm^3 of brine. The volume was then made up to 400cm^3 with dichloromethane, the solution dried over $MgSO_4$ and rotary evaporated to leave a brown tar, mass 587mg, which was subjected to preparative HPLC (2x250x10mm lichnoprep. 5-20 micron silica; 10% EtOAc/90% pet. spirit 30-40°C; 5.0cm^3/min). The desired sulphone **21c** (t_{ret} 19 mins) was isolated as a yellow solid (41mg, yield 5% mp 158°C). Reinjection of **21c** onto an analytical HPLC column showed the material to be slightly impure (<1%).

NMR data, **21c**

^{1}H-NMR ($CDCl_3$, ppm, 400MHz):1.16 (d, Me, 6H); 1.19(d, Me, 6H); 2.45-2.55 (septet, CH, 2H); 5.71 (s, olefinic, 2H); 5.75-6.23 (AA'BB', olefinic, 4H).

^{13}C-NMR ($CDCl_3$, ppm, 100MHz): 17.45, 17.48(Me); 29.00 ($\underline{C}H(Me)_2$); 72.84 (C_{quat}); 122.67, 127.89, 129.58 (olefinic).

Mass Spectrum, **21c**

An electron impact mass spectrum resulted in SO_2 extrusion occuring and hence no M^+ could be detected for **21c**. An M^+ at 220, corresponding to that of the tetraene **9**, was observed instead.

A fast atom bombardment mass spectrum detected an $(M+1)^+$ molecular ion at 253, as required.

(iv) Preparation of 1,4 and 1,6-di-isopropylcyclooctatetraene **9**

A solution of **21c**(41mg, 0.00016mol) in $10cm^3$ of ether and $3cm^3$ of acetone contained in a glass specimen bottle with magnetic stirrer was deaerated with dry N_2 for 30 minutes. The solution was then externally irradiated with a 100W medium pressure Hanovia lamp, whilst stirring. After 31 hours, intermittent TLC analysis showed the reaction to be complete ($KMnO_{4(aq)}$ development). The solvent was carefully rotary evaporated until a small amount of a fragrant yellow oil remained which was 1,4 and 1,6-di-isopropylcyclooctatetraene, **9**, in high purity. Injection of a sample of **9** onto an analytical GLC column showed a small amount of impurity, as did ^{1}H-NMR. The product was not purified further.

NMR data, **9**

^{1}H-NMR ($CDCl_3$, ppm, 400MHz): 1.01 (CH_3 of 1,4-isomer , d(J = 7.0Hz), 12H) ; 1.03 (CH_3 of 1,6-isomer , d, J=7.0 Hz, 6H); 1.04 (CH_3 of 1,6-isomer, d, J=6.9 Hz, 6H); 2.10-2.32 ($C\underline{H}(CH_3)_2$, m, 4H); 5.55-5.90 (olefinic, m, 12H)

Note that the 1,6-isomer shows *slow* ring inversion on the ^{1}H-NMR-timescale at +20°C for the methyl protons while the 1,4-isomer shows *fast* ring inversion at +20°C. Hence *two* methyl doublets are observed for the 1,6-isomer and only *one* methyl doublet for the 1,4-isomer of **9** at +20°C.

^{13}C-NMR ($CDCl_3$, ppm, 100 MHz, +20°C):

1,6-isomer:21.77, 22.24(Me); 35.53 ($\underline{C}H(CH_3)_2$); 123.62, 131.05, 132.56, 150.32 (olefinic).

1,4-isomer: 21.82, 22.17 (Me); 35.35 ($\underline{C}H(CH_3)_2$); 123.96,131.47, 132.37, 149.16 (olefinic).

Accurate mass spectrum, **9**

Calculated = 188.1565

Found = 188.1578

Chapter 3:

Attractive Steric Interactions in 1(e)-(3-alkylphenyl)-2(e),6(e)-dimethylcyclohexan-1-ols and 1(e)-(3-alkylphenyl)-2(e),6(e)-dimethylcyclohexanes

(a) Introduction

(b) Synthesis

(c) Low Temperature NMR

  (i) Conformational Assignment of NMR Signals

  (ii) Low Temperature NMR on 1(a)-(3-^{t}Buphenyl)-2(e),6(e)-dimethylcyclohexane

  (iii) Preferred Conformation of the 1-(3-^{t}Buphenyl)- group in 1(a)-(3-^{t}Buphenyl)-2(e),6(e)-dimethylcyclohexane

(iv) Conformational Assignment of NMR Signals in 1(a)-(3-^{t}Buphenyl)-2(e),6(e)-dimethylcyclohexane via NOE Difference Spectroscopy

(v) Low Temperature NMR on 1(e)-(3-methylphenyl)-2(e),6(e)-dimethylcyclohexan-1-ol

(vi) Low Temperature NMR on 1(e)-(3-^{t}Buphenyl)-2(e),6(e)-dimethylcyclohexan-1-ol

(vii) Low Temperature NMR on 1(e)-(3-methylphenyl)-2(e),6(e)-dimethylcyclohexane

(viii) Low Temperature NMR on 1(e)-(3-^{t}Buphenyl)-2(e),6(e)-dimethylcyclohexane

(d) Discussion of Results

(e) Experimental

(a) **Introduction**

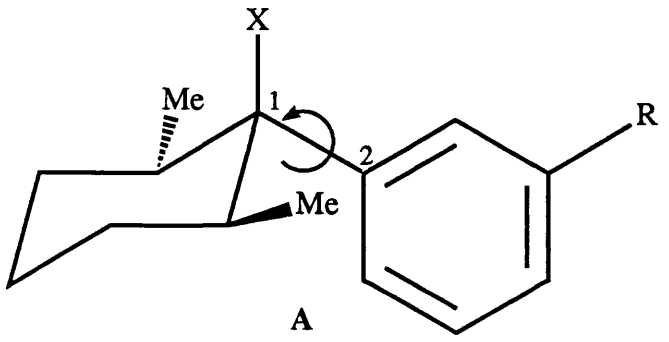

A

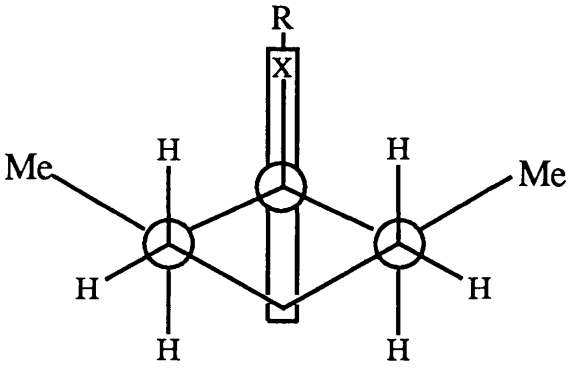

B

Compound	R	X
23	Me	OH
24	^{t}Bu	OH
25	Me	H
26	^{t}Bu	H

Fig. 10: 1e-(3-alkylphenyl)-2e,6e-dimethylcyclohexanols **23** and **24** and 1e-(3-alkylphenyl)-2e,6e-dimethylcyclohexanes **25** and **26**. Structure **B** is an alternative view of structure **A** looking down the C_1-C_2 bond.

For the purposes of the present work, compounds **23-26** were chosen for study. MMP2 calculations carried out during the course of this work indicate that the ground state for these compounds has the plane of the phenyl ring parallel to the plane of symmetry passing through the cyclohexyl ring (structure **B** in fig. 10). Phenyl group rotation gives rise to the equilibrium outlined in fig. 11, where the phenyl group has rotated through 180°, conformers **C** and **D** differing only in the proximity of the meta alkyl group R to the cyclohexyl ring.

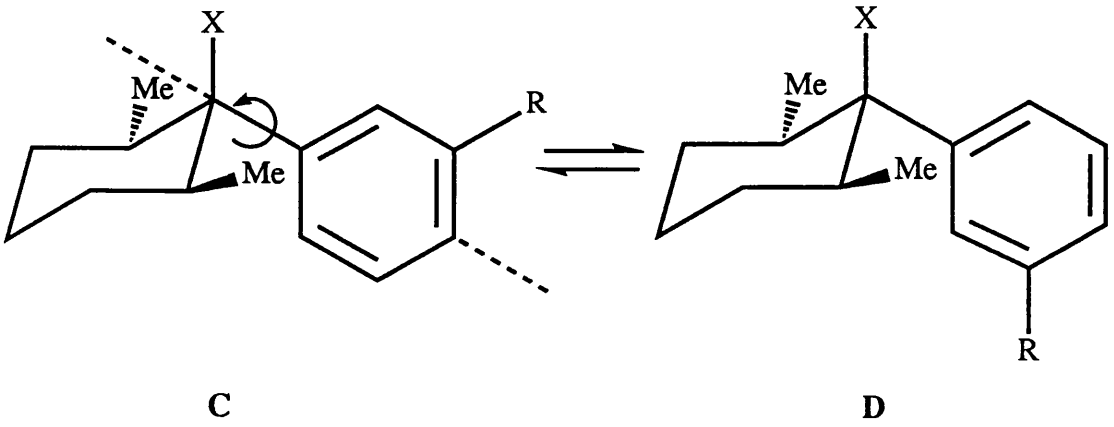

C D

Fig. 11: Rotational equilibrium in compounds **23-26**.
..... = axis of rotation of phenyl group.

In conformer **D**, the remote alkyl group R (remote in the sense that for both conformers **C** and **D**, R is too distant from the cyclohexyl ring for them to interact repulsively) is positioned somewhat closer to the bulk of the cyclohexane ring than in conformer **C**. This is perhaps more clearly seen in the Newman projection-type representation of conformers **C** and **D** depicted in fig. 12.

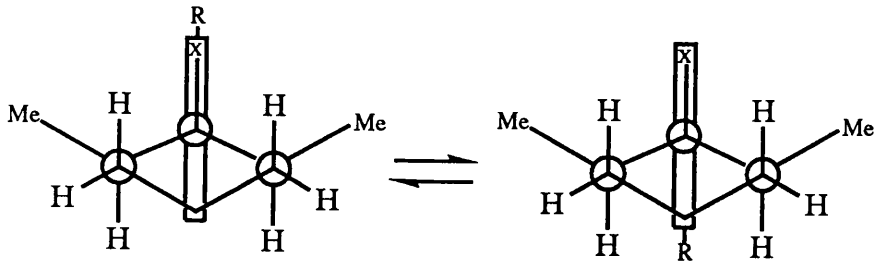

C D

Fig 12: Rotational equilibrium in compounds **23-26**.

MMP2 calculations

Compound	23C	23D	25C	25D	26C	26D
Total Steric energy	9.6512	9.6175	5.3813	5.3530	10.0268	9.8889
Compression[a]	1.3040	1.3473	1.0092	1.0133	1.7784	1.7669
Bond angle bending	1.5470	1.5870	1.0538	1.0374	2.0324	2.0220
Stretch-bend	0.2855	0.2940	0.2031	0.2026	0.3116	0.3107
van der Waals' 1,4-energy	11.0088	10.9799	10.6342	10.6343	13.1771	13.1870
van der Waals' longer-range energy[b]	-2.5946	-2.6838	-3.7831	-3.7933	-3.8906	-4.0144
Torsional strain	-1.6712	-1.6736	-3.7645	-3.7698	-3.4103	-3.4114
Dipolar	-0.2283	-0.2333	0.0286	0.0286	0.0281	0.0281
		ΔE^c=34		ΔE=28		ΔE=138

Notes:

[a] Strain energy from lengthening or shortening of bonds

[b] The negative sign indicates stabilisation rather than strain

[c] Energy difference between conformers C and D. Conformer D is the more stable in each case.

Table 6: MMP2 calculations for conformations C and D in compounds **23, 25** and **26**. Enthalpies in $kcalmol^{-1}$.

MMP2 calculations were performed on compounds **23, 25** and **26** (Table 6) and in each case show the apparently more compact conformer D to be the more stable. For compounds **23** and **25**, the steric energy differences between conformers C and D are calculated to be quite small and the calculations show differences in many terms as contributing to the overall stability of conformer D. However, for compond **26**, where the steric energy difference is calculated to be somewhat larger, the calculations clearly attribute the greater stabilisation of conformer D to the attractive van der Waals' energy component of the steric energy.

It might therfore be expected that for compounds **23-26**, the equilibrium outlined in figures **11** and **12** should favour the more compact conformer D. Certainly, for compound **26**, the calculations attribute the greater stabilisation of the more compact conformer **26D** to the attractive van der Waals' energy component of the steric energy.

Final introductory note

The two methyl groups on the cyclohexyl ring serve two purposes. Firstly they lock the cyclohexyl ring into a single chair conformation, preventing ring inversion from occurring. Secondly they are known to hinder phenyl group rotation to the extent that the conformational populations of **C** and **D** can be measured by NMR at readily accessible temperatures. For example, Leete and Riddle observed slow phenyl group rotation on the NMR timescale at room temperature and below for 1(e)-phenyl-2(e),6(e)-dimethylcyclohexan-1-ol, a barrier to rotation of 15.2 kcal/mol being determined by line shape analysis.[34]

On the basis of the above points it was therefore felt that the series of compounds **23-26** is suitable for a study of van der Waals' attractive interactions.

(b) **Synthesis**

Compounds **23-26** were synthesised via the reaction sequence outlined in scheme 3:

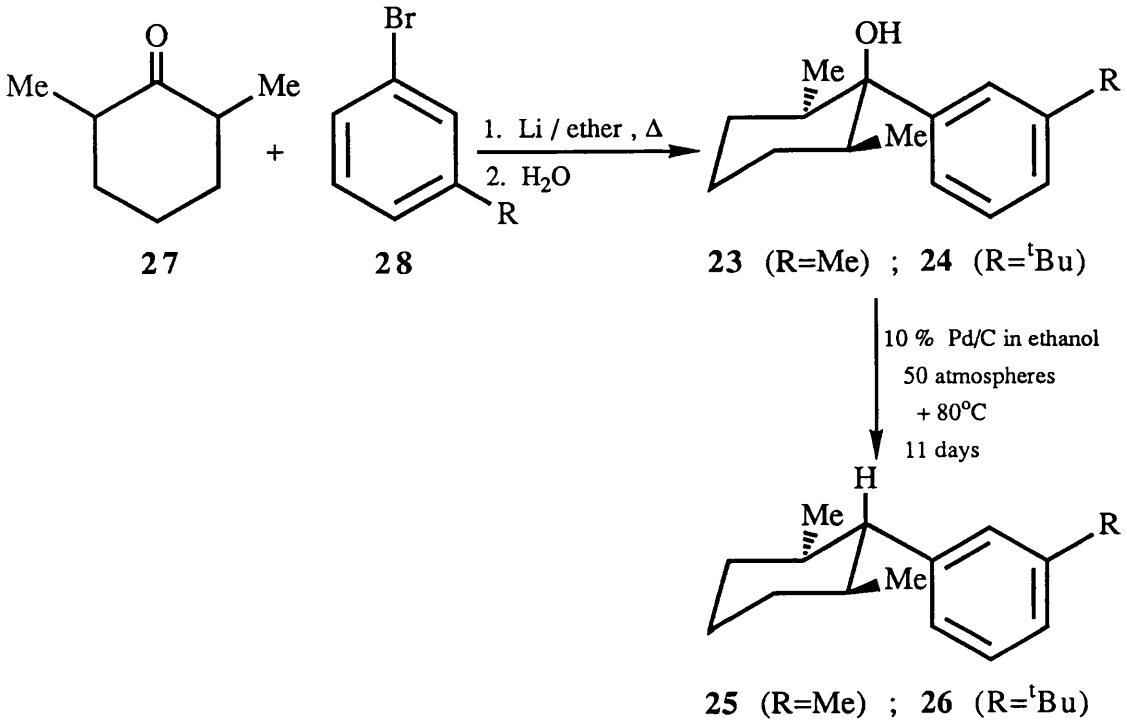

Scheme 3: Reaction sequence for synthesis of compounds **23-26**.

Commercially available 2,6-dimethylcyclohexane **27**, (Aldrich), comes as a mixture of stereoisomers. ^{1}H-NMR shows the major isomer (90%) to possess two equatiorial methyl groups while the minor isomer (10%) possesses one axial and one equatorial methyl group.

Alkylation of the 2,6-dimethylcyclohexanone stereoisomer mixture with 3-methylphenyllithium produces predominantly one alcohol, **23**, with equivalent methyl groups, as is evidenced from ^{1}H-NMR of the crude reaction mixture. It is assumed that in this major alcohol, **23**, the 2,6-dimethyl groups and the 1-(3-methylphenyl)-group are all equatorial substituents on the cyclohexyl ring.

This assumption is based on the reasonable premise that the 3-methylphenyllithium attacks the 2(e),6(e)-dimethylcyclohexanone **27** from the least hindered side of the cyclohexyl ring. It was possible to isolate a sample of this major alcohol *via* preparative TLC.

The possibility of a second minor alcohol with non-equivalent 2,6-dimethyl groups was also seen in the spectrum, suggesting that in this alcohol, one methyl is axial, one equatorial.

The second step of the reaction sequence, the hydrogenolysis of the benzyl alcohols **23** and **24** required extremely forcing conditions for the reaction to go. Attempts using lithium aluminium hydride or hydrogen with palladium on charcoal at 55 psi and +80°C in ethanol gave no reaction, unreacted alcohol being returned.

The reaction was found to proceed very slowly using hydrogen and palladium on charcoal in ethanol at 50 bar and +80°C, a period of several days being required for a satisfactory amount of **25** and **26** to be produced. Under these conditions, a complex mixture of products resulted, preparative GLC techniques being necessary to isolate the required products. In addition to the desired 1(e)-(3-alkylphenyl)-2(e),6(e)-dimethylcyclohexanes **25** and **26**, were produced the corresponding stereoisomers **29** and **30** (fig.13) where the 1-(3-alkylphenyl) group now occupies an axial, rather than an equatorial position, on the cyclohexyl ring. Inversion of configuration during hydrogenolysis reactions is quite common in the literature.[35]

Isomers **25**, **26**, **29** and **30**, differing only as to whether the 1-(3-alkylphenyl) group is axial or equatorial on the cyclohexyl ring, are distinguishable *via* the magnitude of the coupling constant $^3J_{AB}$ (fig. 13).

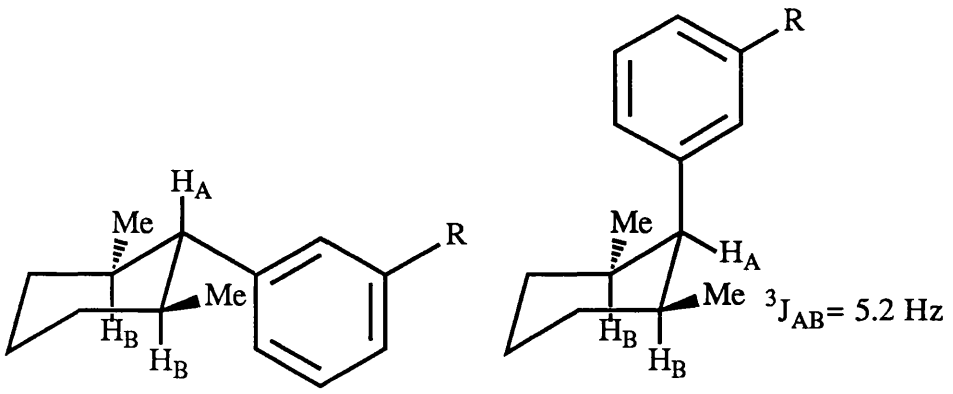

25 (R=Me) ; **26** (R=^{t}Bu) **29** (R=Me) ; **30** (R=^{t}Bu)

Fig. 13: 1(e)-(3-alkylphenyl)-2(e),6(e)-dimethylcyclohexanes **25** and **26** and1(a)-(3-alkylphenyl)-2(e),6(e)-dimethylcyclohexanes **29** and **30** produced *via* the hydrogenolysis of alcohols **23** and **24.**

In **29** and **30**, H_A appears as a triplet ($^3J_{AB}$=5.2Hz) at 2.7ppm. The magnitude of this coupling constant is consonant with H_A being equatorial on the cyclohexyl ring.

The corresponding triplet from **25** and **26**, where H_A is now axial, is not visible in the ^{1}H-NMR spectrum due to complete overlapping with the cyclohexyl resonances.

Also isolated from the hydrogenolysis reaction mixture by GLC were a number of compounds, where, in addition to hydrogenolysis having occurred, hydrogenation of the phenyl ring had also taken place. However, these results are not reported here.

(c) **Low Temperature NMR**

(i) Conformational Assignment of NMR Signals

Compounds **23** - **26** all displayed low temperature NMR behaviour consistent with 1-(3-alkylphenyl) group rotation becoming slow on the NMR timescale. In general, for both rings, NMR signals split to give unsymmetrical doublets on cooling, which is consistent with a two-fold rotational barrier of the unsymmetrical phenyl group, the plane of the phenyl ring lying parallel to the symmetry plane of the cyclohexane ring in the two ground states. Integration of the appropriate low temperature limit NMR signals yields the desired equilibrium constants. However, assignment of the major and minor sets of NMR signals to the two rotational isomers is often, as in this case, not trivial. For example, the *incorrect* assignment was initially suggested for the trineopentyl benzene equilibrium, using intuitive expectations based upon steric repulsion arguments.[36]

For the purposes of this project, the conformational assignment of NMR signals in compounds **23** - **26** was based on an NOE difference experiment performed on compound **30**. A description of compound **30**'s low temperature NMR and NOE difference experiment is now presented.

(ii) Low Temperature NMR on 1(a)-(3-^{t}Buphenyl)-2(e),6(e)-dimethylcyclohexane, **30**

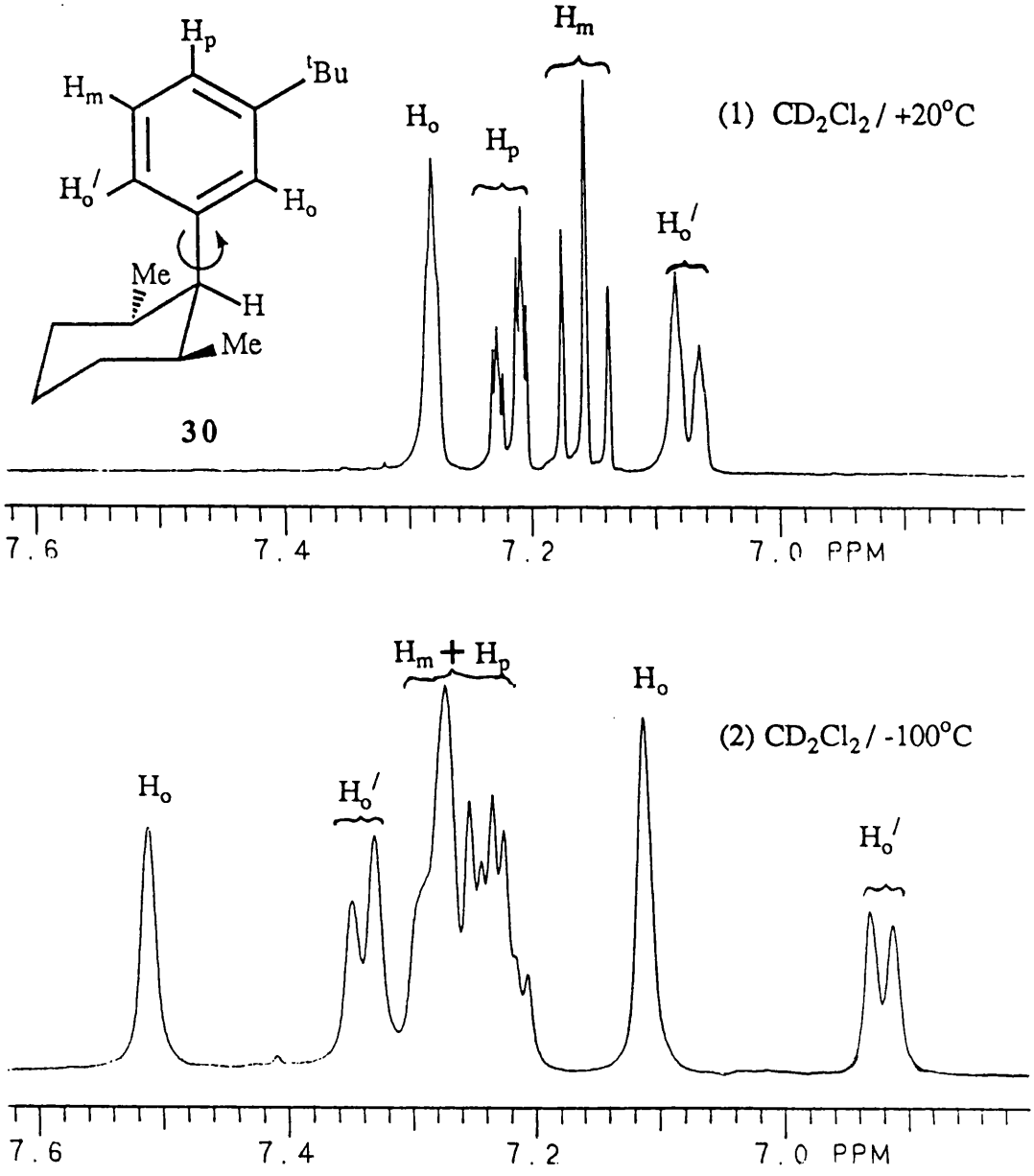

Fig. 14: Aromatic region of **30** at +20°C (spectrum 1) and -100°C (spectrum 2).

The room temperature ^{1}H-NMR spectrum of **30** is consistent with there being fast 1-(3-^{t}Buphenyl) group rotation on the NMR timescale (spectrum 1, fig. 14). On cooling, signals broaden, decoalesce and sharpen up.

At -100°C, spectrum 2, fig. 14 is obtained which shows a doubling of signals. In particular it may be seen that the H_o singlet at -100° has split to an upfield singlet at 7.11 ppm and downfield singlet at 7.52 ppm. Likewise the H_o' doublet has decoalesced to two doublets: an upfield one centred at 6.92 ppm and a downfield one centred at 7.33 ppm. The upfield H_o signal is more intense then the downfield, while for the H_o' the opposite is observed.

(iii) Preferred Conformation of the 1-(3-^{t}Buphenyl) group in 1(a)-(3-^{t}Buphenyl)-2(e),6(e)-dimethylcyclohexane, **30**

The question arises as to the orientation of the phenyl ring with respect to the cyclohexane ring in **30**. Force field calculations have shown[37] that the ground state for an axial phenyl group on an otherwise unsubstituted cyclohexyl ring is, as in I (fig. 15), with the plane of the phenyl ring perpendicular to the symmetry plane of the cyclohexyl ring. This was confirmed experimentally by Squillacote and Neth for axial phenylcyclohexane in solution.[38] The parallel axial phenyl conformation II (fig. 15) is thought to involve substantial steric interaction between the ortho hydrogens (H_o) and the syn-axial hydogens (H_3, H_5).[37]

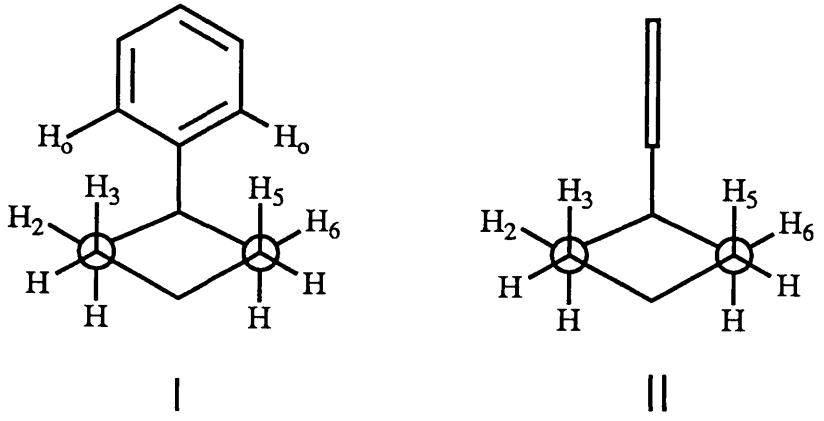

Fig. 15: Perpendicular (I) and parallel (II) orientations of an axial phenyl group on a cyclohexane ring.

If the 2,6-positions on the cyclohexane ring contain bulky substituents as in 1(e), 2(e), 3(e), 4(e), 5(e), 6(e)-hexachloro-1(a)-phenylcyclohexane, then the parallel axial phenyl conformation II is adopted.[39] Though the parallel axial phenyl conformation II introduces a steric interaction between the ortho hydrogens (H_o) and the *syn*-axial hydrogens (H_3, H_5), the strain induced must be less than that produced by the interaction of the ortho hydrogens and the large equatorial chlorine substituents at C_2 and C_6 which would occur in the perpendicular geometry I.

For compound **30**, there is a doubling of NMR signals from both rings on cooling. This implies that the axial 1-(3-^{t}Buphenyl) group adopts the parallel ground state II. If the 1-(3-^{t}Buphenyl) group possessed the perpendicular ground state I, then low temperature NMR should show no decoalescence of the phenyl group signals since rotation of this group exhanges protons between equivalent magnetic sites. Additional evidence for the preferred conformation of the 1-(3-^{t}Buphenyl)- group in **30** comes from the ^{1}H-NMR - highfield chemical shift (0.64 ppm) of the 2(e),6(e)-dimethyl groups. Only in the parallel conformation II do the 2(e),6(e)-dimethyl groups lie in the cone of shielding of the benzene ring. That the 1-(3-^{t}Buphenyl) group in **30** adopts the parallel conformation II is undoubtedly due to the destabilising steric interaction between the ortho hydrogens (H_o) and the bulky 2,6-methyl groups.

(iv) Conformational Assignment of NMR Signals in 1(a)-(3-^{t}Buphenyl)-2(e),6(e)-dimethylcyclohexane **30** *via* NOE Difference Spectroscopy

It is apparent from the preceeding discussion that the rotational potential for the parallel axial 1-(3^{t}Buphenyl) group in **30** is two-fold, giving

rise to the equilibrium outlined in fig. 16.

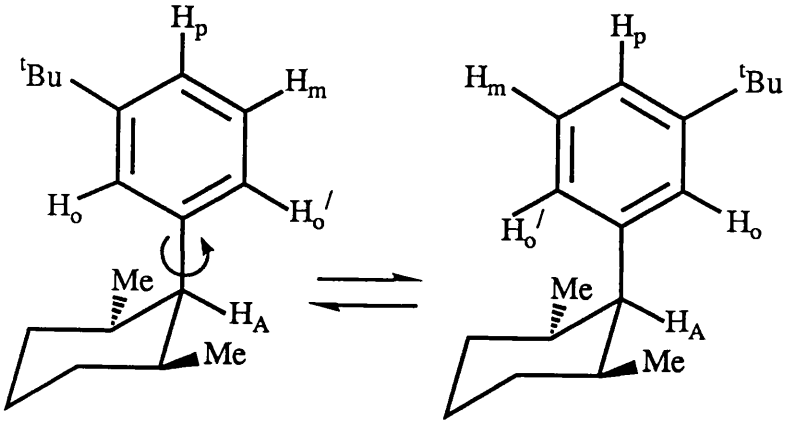

Fig 16: Rotational equilibrium in 1(a)-(3-^{t}Buphenyl)-2(e),6(e)-dimethylcyclohexane **30**.

Pre-irradiation of H_A at +20°C when 1-(3-^{t}Buphenyl) group rotation is fast on the NMR timescale results in NOEs to H_o and H_o', as expected (fig. 17).

Pre-irradiation of H_A at -100°C when 1-(3-^{t}Buphenyl) group rotation is slow on the NMR timescale (fig. 18) results in NOEs to only the upfield H_o singlet at 7.11 ppm and the upfield H_o' doublet at 6.92 ppm. Inspection of structures **30A** and **30B** (fig. 16) reveals that the H_o singlet showing an NOE must arise from **30B** and the H_o' doublet showing an NOE must arise from conformer **30A**. Hence the upfield H_o singlet at 7.11 ppm is assigned to conformer **30B** and the upfield H_o' doublet at 6.92 ppm is assigned to conformer **30A**.

It may thus be concluded that proximity of an ortho phenyl proton to the cyclohexyl ring (*e.g.* H_o in **30A**) shifts the proton downfield relative to its chemical shift when the proton is remote from the cyclohexyl ring (*e.g.* H_o in **30B**).

It is this chemical shift argument which is used for conformational assignment in compounds **23** - **26**.

It is interesting to note that a negative NOE is obtained for the H_o singlet of conformer **30B** at -100°C. Large, slowly tumbling molecules show negative NOEs even at ambient temperature, so it is reasonable to postulate that a molecule of intermediate size such as **30** may show a negative NOE in a viscous solution at -100°C. That the NOEs to H_o and H_o' at -100°C are of opposite sign may reflect different correlation times for the two diastereomeric conformers **30A** and **30B**.

A similar NOE different experiment was performed on 1(a)-(3-methylphenyl)-2(e),6(e)-dimethylcyclohexane **29**, comparable results being obtained to those for **30**, namely, an NOE effect at the upfield of either pair of ortho proton signals.

It was not possible to perform the analogous NOE difference experiment on compounds **25** and **26** because the axial cyclohexyl proton H_A in these compounds is obscured by the cyclohexyl resonances.

A free energy of activation for 1-(3-methylphenyl) group rotation in **29** was obtained by observing benzylic meta-methyl singlet decoalescence. At -68°C, the methyl singlet decoalesces to two singlets ($\Delta\nu$=10.8Hz) whence a free energy of activation of 10.57 kcalmol^{-1} is calculated *via* the Eyring equation.

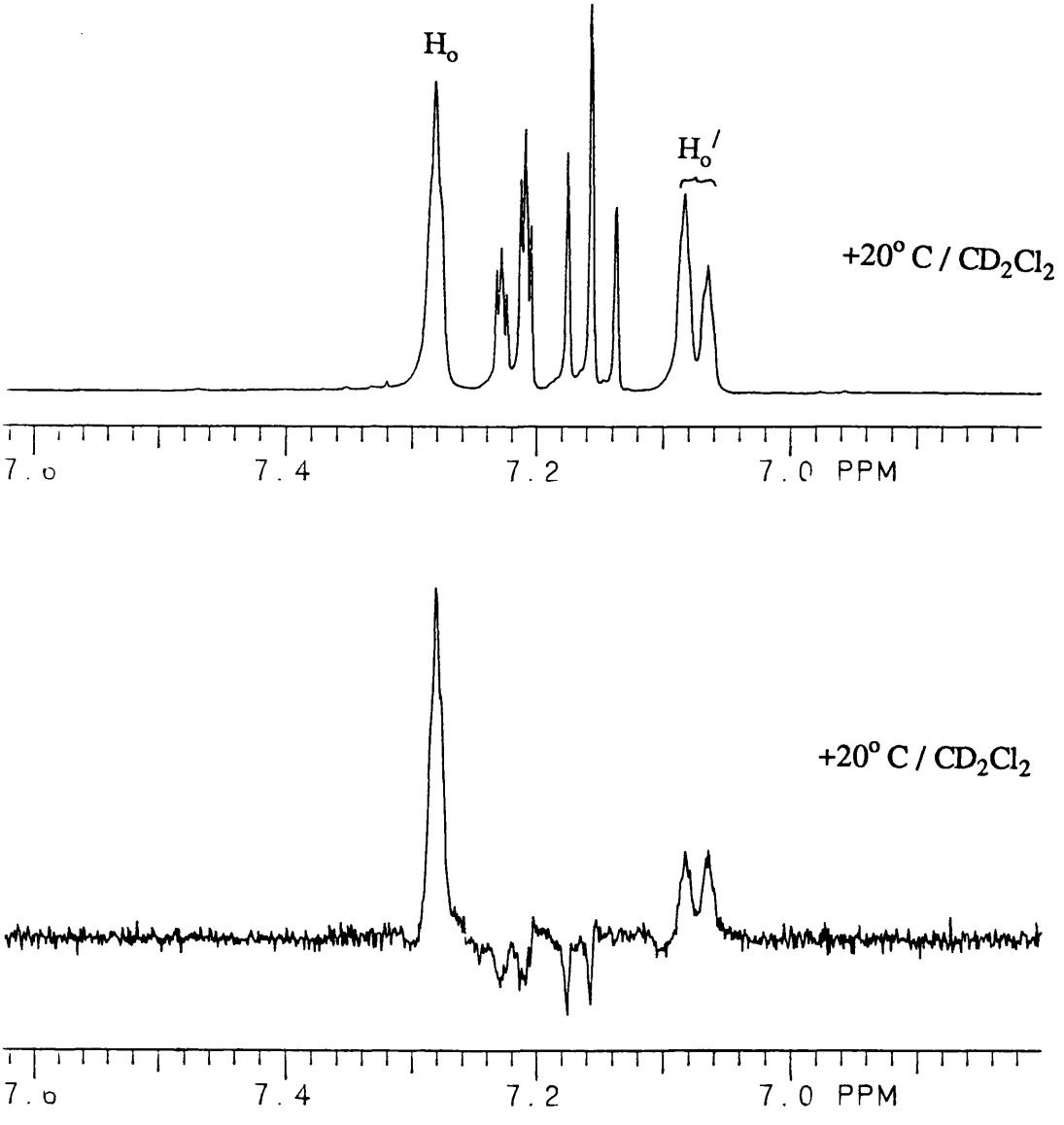

Fig. 17 Spectrum 1: aromatic region of **30** at +20°C in CD_2Cl_2.
Spectrum 2: NOE difference spectrum on pre-irradiation of H_A at +20°C.
Assignments H_o and H_o' refer to structures **30A** and **30B**

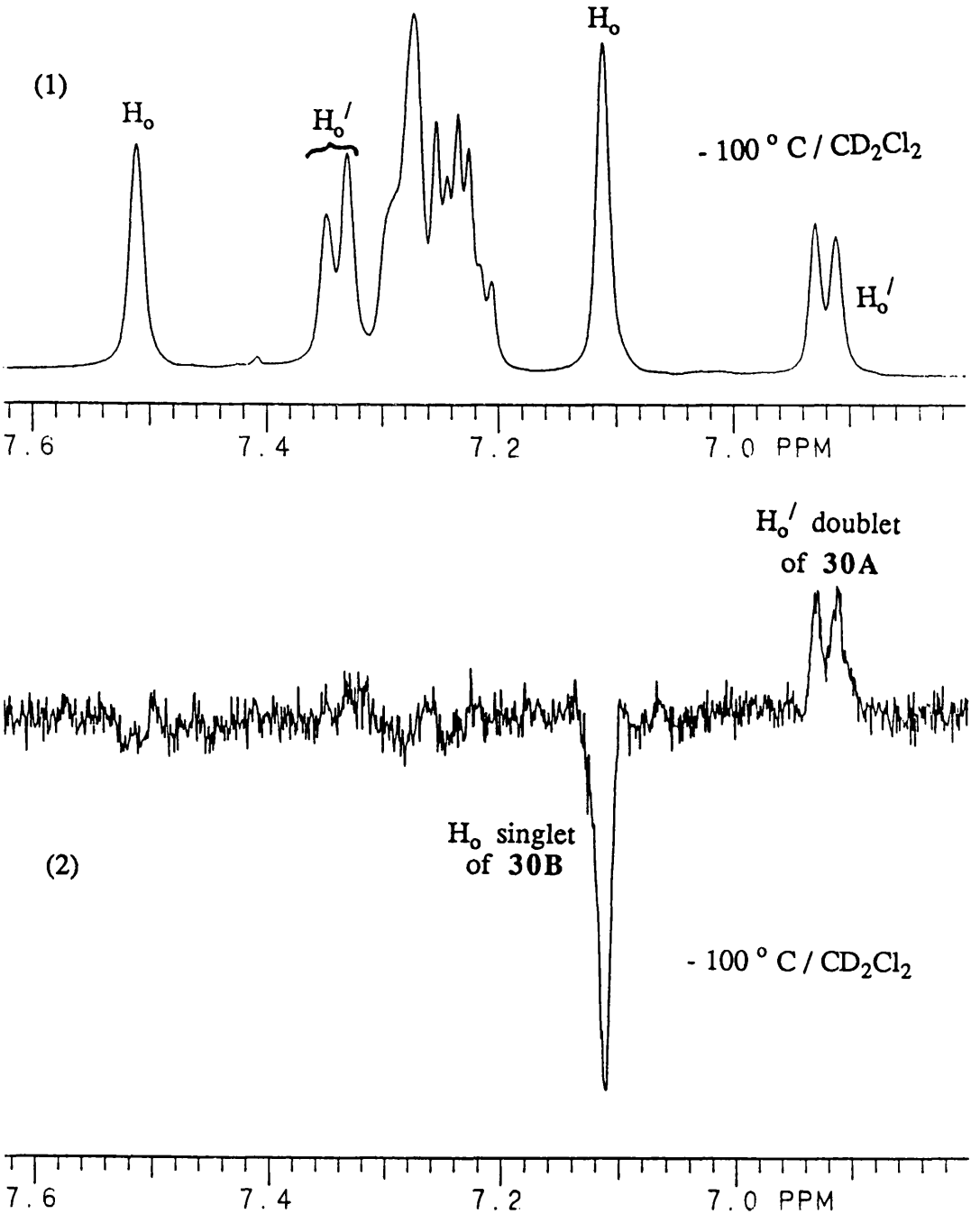

Fig. 18 Spectrum 1: aromatic region of **30** at -100°C in CD_2Cl_2.
Spectrum 2: NOE difference spectrum on pre-irradiation of H_A at -100°C.
Assignments H_o and H_o' refer to structures **30A** and **30B**.

(v) Low Temperature NMR on 1(e)-(3-methylphenyl)-2(e),6(e)-dimethylcyclohexan-1-ol, **23**

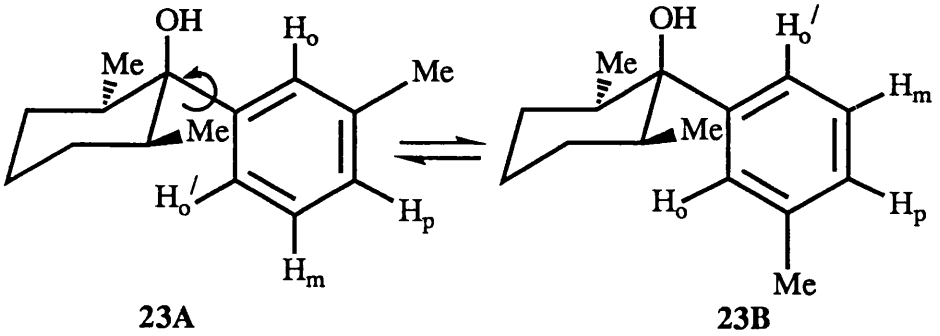

23A **23B**

Fig. 19: Rotational equilibrium in 1(e)-(3-methylphenyl)-2(e),6(e)-dimethylcyclohexan-1-ol, **23**.

The ^{1}H-NMR spectrum of **23** at +25°C shows exchange broadened signals for H_o and H_o' (spectrum 1, fig. 20). H_m (a triplet at 7.20 ppm) and H_p (a doublet at 7.01 ppm) are not yet decoalesced. On cooling to -30°C, spectrum 2 (fig. 20) is obtained, which shows a doubling of all aromatic signals. The cyclohexyl ^{1}H-signals did not appear to show any observable splitting at -30°C.

As regards ^{13}C-NMR, nearly all aromatic signals were doubled at -30°C. In addition to this, several of the cyclohexyl ^{13}C-resonances were also doubled at -30°C, however the splitting was of very small magnitute (≈3Hz).

These changes are consistent with 1-(3-methylphenyl) group rotation becoming slow on the NMR timescale, the ground states for rotamers **23A** and **23B** (fig. 19) having the plane of the phenyl ring parallel to the symmetry plane of the cyclohexane ring.

A barrier to 1-(3-methylphenyl) group rotation was obtained by observing the decoalescence of the benzylic meta-methyl signal at 2.36 ppm. At +8°C, this signal decoalesced to two singlets ($\Delta\nu$=7.0Hz), whence a free energy of activation of 14.90 k calmol^{-1} is calculated *via* the Eyring equation.

This barrier is in good agreement to that calculated for the similar compound 1 (e)-phenyl-2(e),6(e)-dimethylcyclohexan-1-ol[34].

Integration of the two benzylic meta-methyl singlets at -30°C yields an equilibrium constant for **23A** ⇌ **23B** of 1.09. The more downfield of these singlets was assigned to conformer **23B**, by comparison to the low temperature limit spectrum of **24**.

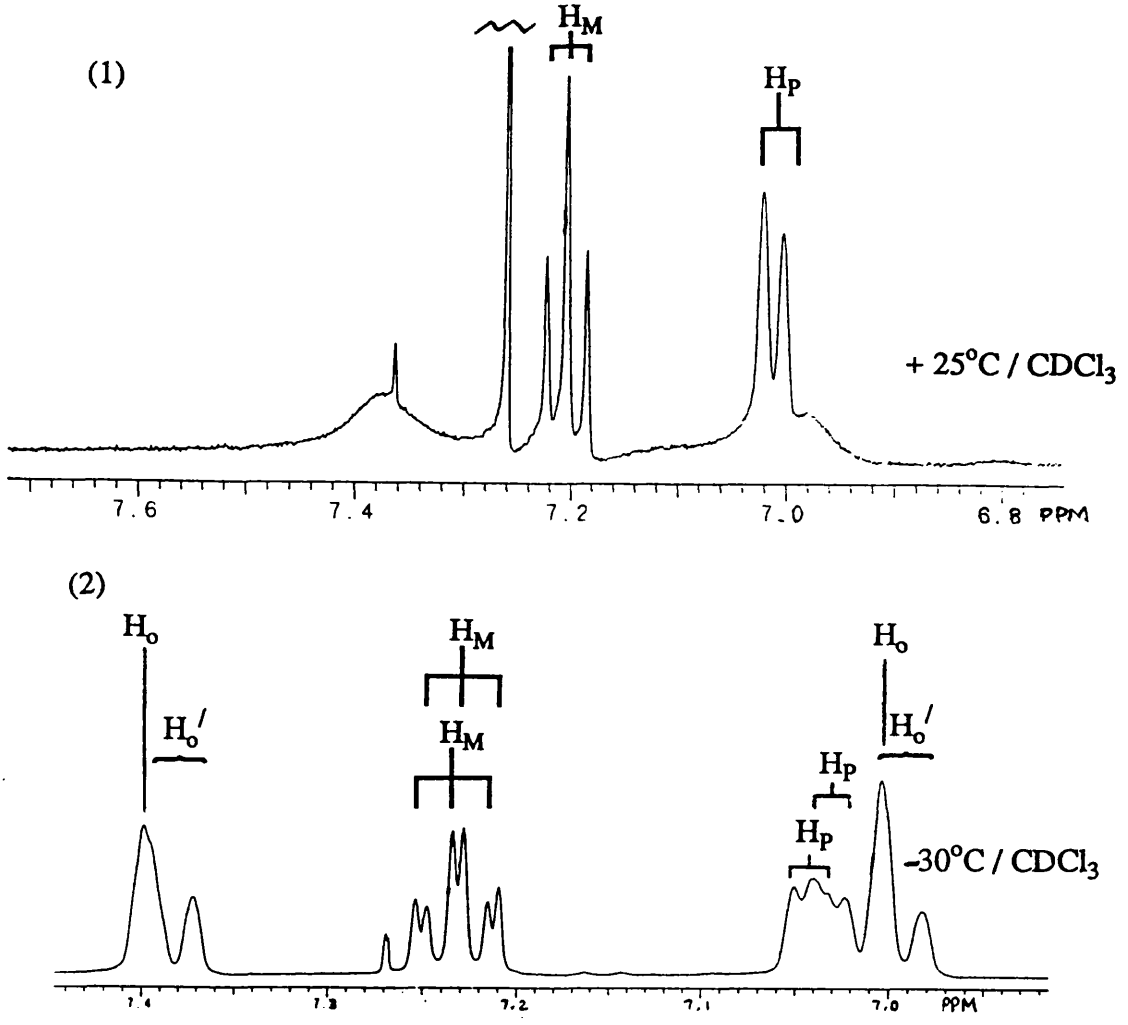

Fig 20: Spectrum 1: aromatic region of **23** at +25°C.
Spectrum 2: aromatic region of **23** at -30°C (different horizontal scale to spectrum 1).

(vi) Low temperature NMR on 1(e)-(3-^{t}Buphenyl)-2(e),6(e)-dimethylcyclohexan-1-ol, **24**

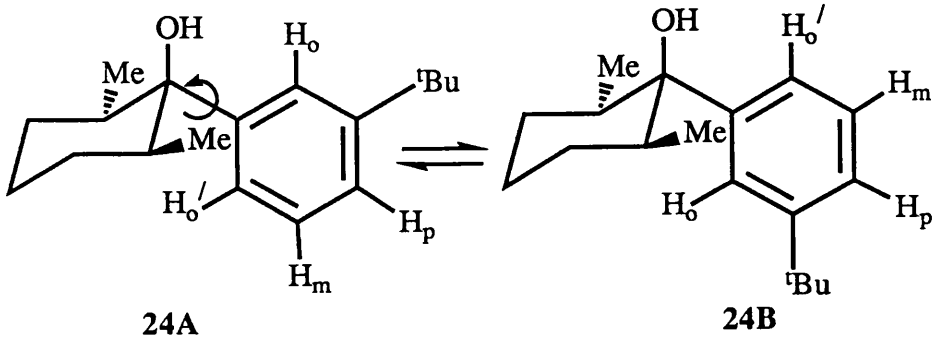

Fig. 21: Rotational equilibrium in 1(e)-(3-^{t}Buphenyl)-2(e),6(e)-dimethylcyclohexan-1-ol, **24**.

Compound **24** exhibited similar low temperature DNMR phenomena to that described for **23** as expected in a very similar temperature range since the meta substituent should not affect the rotational barrier. Inspection of the low temperature limit spectrum of **24** (fig. 22) reveals that the major H_o singlet (7.61 ppm) lies downfield from the minor H_o singlet (7.18 ppm). Examination of conformers **24A** and **24B** (fig. 21) reveals that H_o in **24B** lies closer to the bulk of the cyclohexyl ring than in **24A**. Hence the major singlet is assigned to the more compact conformer **24B**, as predicted by the MMP2 calculations.

Integration of the two H_o singlets at -40°C yields an equilibrium constant of 1.39 for the **24A** $\rightleftharpoons$ **24B** equilibrium.

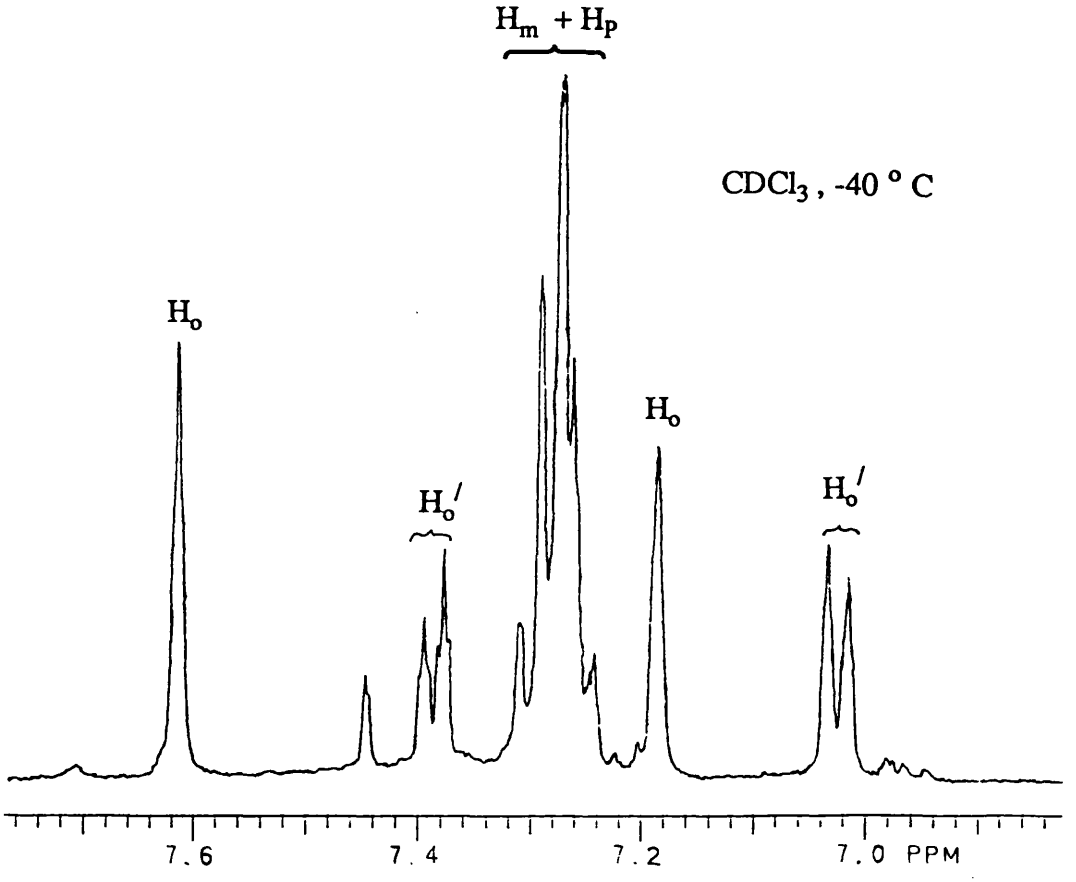

Fig. 22: Low temperature limit spectrum of **24** (^{1}HNMR) at -40°C($CDCl_3$).

(vii) Low Temperature NMR on 1(e)-(3-methylphenyl)-2(e),6(e)-dimethylcyclohexane, **25**

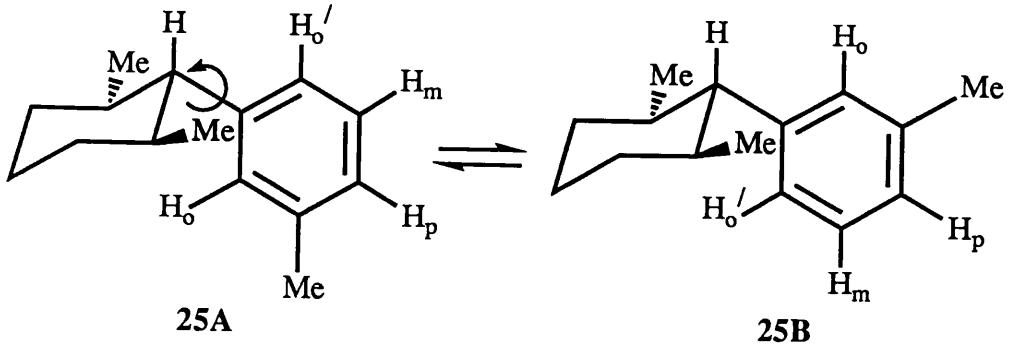

Fig. 23: Rotational equilibrium in 1(e)-(3-methylphenyl)-2(e),6(e)-dimethylcyclohexane, **25**.

The room temperature ^{1}H-NMR spectrum of **25** at +20°C shows exchange broadened aromatic signals (fig. 24, spectrum 1). On cooling to -40°C, 1-(3-methylphenyl) group rotation becomes slow on the NMR timescale, and spectrum 2 (fig. 24) is obtained, which shows a doubling of NMR signals.

Integration of the two H_m triplets at 7.22 and 7.12 ppm yields an equilibrium constant of 1.00 for the **25A** $\rightleftharpoons$ **25B** equilibrium.

A barrier to 1-(3-methylphenyl) group rotation was obtained by observing the decoalescence of the benzylic meta-methyl singlet at 2.33 ppm. At -25°C, this signal decoalesces to two singlets ($\Delta\nu$=4.4Hz), whence a free energy of activation of 13.35 kcalmol^{-1} is calculated *via* the Eyring equation.

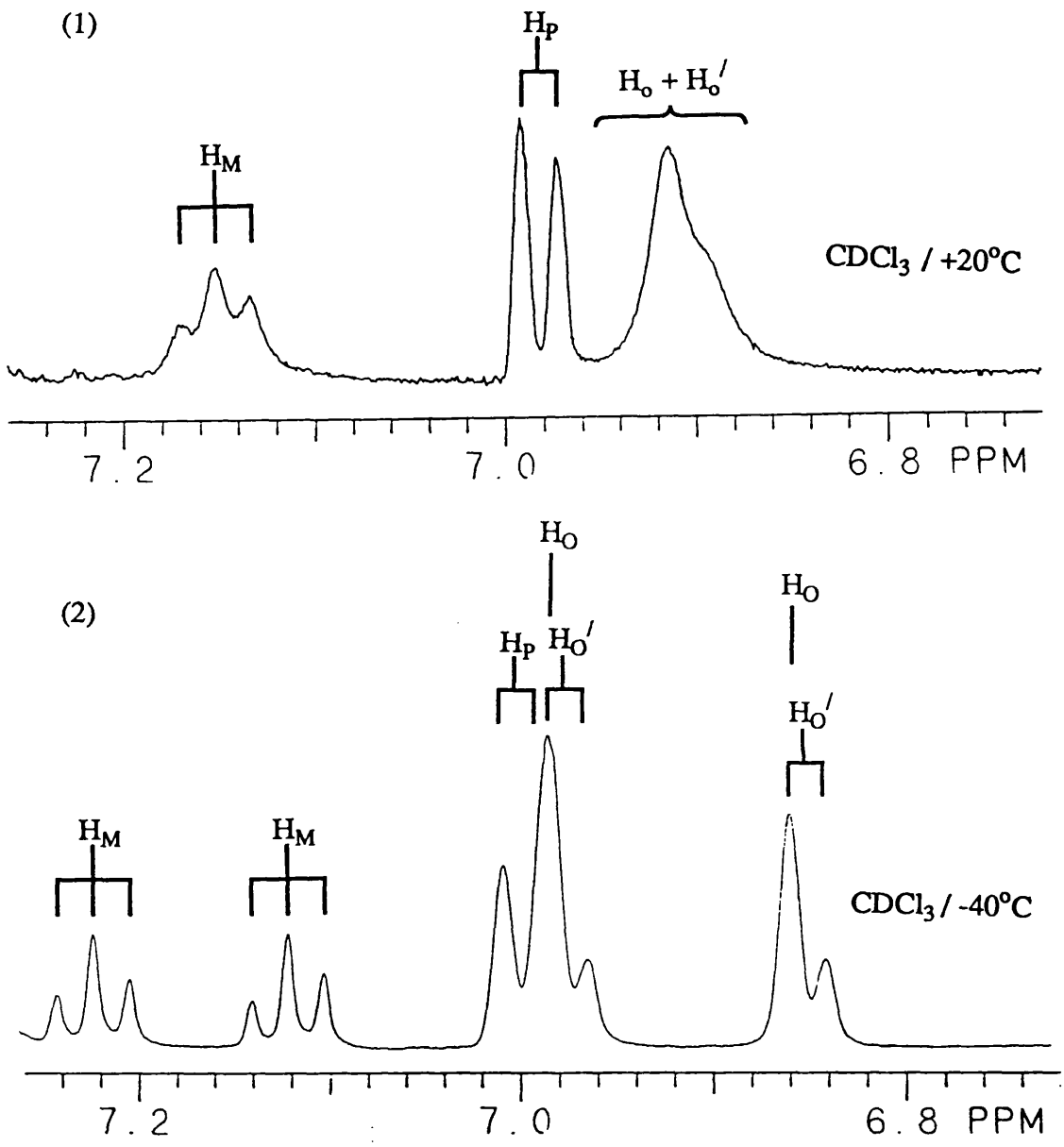

Fig. 24: Spectrum 1: aromatic region of **25** at +20°C ($CDCl_3$).
Spectrum 2: aromatic region of **25** at -40°C ($CDCl_3$).

(viii) Low Temperature NMR on
1(e)-(3-^{t}Buphenyl)-2(e),6(e)-dimethylcyclohexane, **26.**

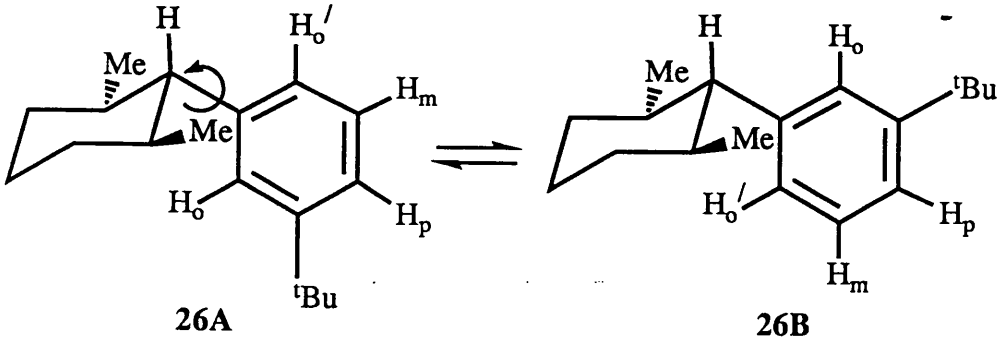

Fig. 25: Rotational equilibrium present in 1(e)-(3-^{t}Buphenyl)-2(e),6(e)-dimethylcyclohexane, **26.**

This compound exhibited analogous low temperature DNMR phenomena to that described for **25.** At -50°C, a low temperature limit spectrum was obtained (fig. 26):

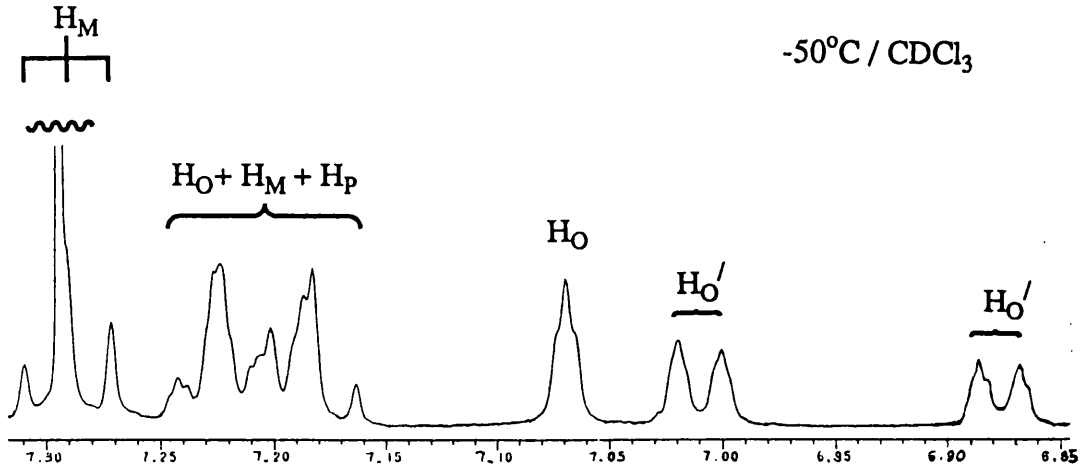

Fig. 26: Aromatic region of **26** at -50°C ($CDCl_3$).

Integration of the two H_o' doublets at 7.01 and 6.88 ppm yields an equilibrium constant of 1.30 for the **26A** $\rightleftharpoons$ **26B** equilibrium.

(d) **Discussion of Results**

For hydrocarbon **25**, conformers **25A** and **25B** are found to be present in solution in equal amounts. For the **26A** ⇌ **26B** equilibrium, the less compact isomer **26B** is found to predominate in solution (K=1.30). This result is in opposition to the prediction of MMP2 calculations, that the more compact conformers **25A** and **26A** are the more populous due to greater van der Waals' attractive stabilisation.

R	K(exptl.)
Me	1.00 ($CDCl_3$, - 40° C)
^{t}Bu	1.30 ($CDCl_3$, -50°C)

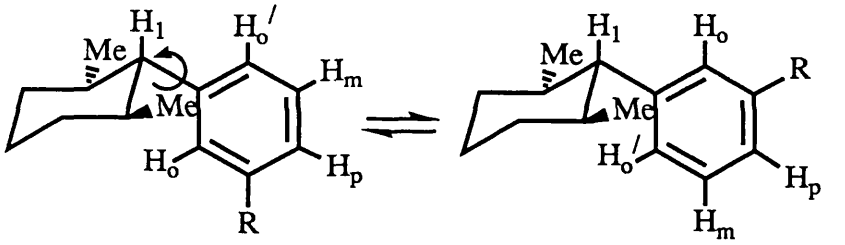

25A (R=Me) **25B** (R=Me)
26A (R=^{t}Bu) **26B** (R=^{t}Bu)

Fig. 27: Summary of results for **25** and **26**.

One possible explanation of these results focuses on the operation of buttressing effects.

It is possible that in **25A** and **26A**, the repulsive interaction of H_o with the cyclohexyl ring is not the same as that of H_o', since H_o is buttressed by the meta alkyl substituent, and thus interacts more strongly. There is no repulsion between H_o or H_o' and H_1 of the cyclohexane ring (fig. 28). This destabilising buttressing interaction is absent in **25B** and **26B** where R is now

remote from the cyclohexyl ring. For **26A** (R=^{t}Bu) this buttressing effect may outweigh any stabilising attractive interactions between the ^{t}Bu group and cyclohexyl ring, resulting in conformer **26A** becoming destabilised relative to **26B**.

For conformer **25A** (R=Me) the buttressing effect may be of similar magnitude to any attractive interactions between the benzylic meta-methyl and the cyclohexyl ring. Hence these two opposing effects cancel, resulting in **25A** and **25B** being of similar stability and hence more or less equally populated.

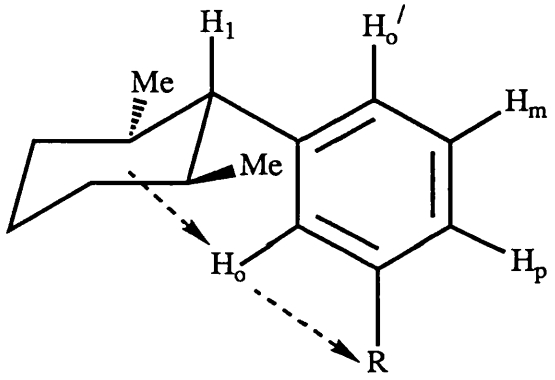

25A (R=Me) ; **26A** (R=^{t}Bu)

Fig 28: H_o is butressed by R in conformers **25A** and **26A**.

For alcohols **23** and **24**, the more compact conformers **23B** and **24B** are found to predominate in solution, as predicted by MMP2 calculations.

R	K(exptl.)
Me	1.09 ($CDCl_3$, - 30° C)
^{t}Bu	1.39 ($CDCl_3$, -40 ° C)

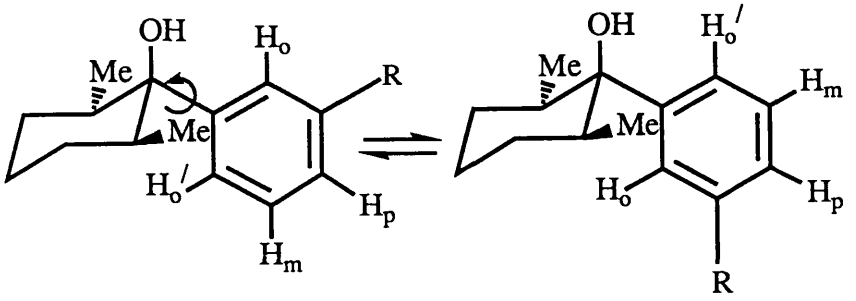

23A (R=Me)
24A (R=^{t}Bu)

23B (R=Me)
24B (R=^{t}Bu)

Fig. 29: Summary of results for alcohols **23** and **24**.

Buttressing effects are undoubtedly involved once again, but in these compounds, H_o has buttressed destabilising interactions in *both* conformations, with the cyclohexyl ring or the *syn*-periplanar OH group (fig. 29). If these cancel out to the same extent, the attactive steric interaction of the meta-alkyl substituent in conformation **B** may dominate the equilibrium and thus determine which conformation is preferred.

Conformation **24B**(R=^{t}Bu) might be expected to have greater van der Waals' attractive stabilisation between the ^{t}Bu-group and the ring as compared to the analogous situation in **23B**(R=Me) where a methyl group is attracting the ring. Hence the greater magnitude of the **24A** $\rightleftharpoons$ **24B** equilibrium constant (1.39) as compared to that for the **23A** $\rightleftharpoons$ **23B** equilibrium (1.09) is explained .

Buttressing effects are certainly not unprecendented in the chemical literature. For example, Adams[40] and his co-workers measured the rates of racemisation of a series of optically active biphenyls derived from 2-nitro-6-carboxy-2′-methoxybiphenyl, **31**, substituted in the 3′, 4′, or 5′ - positions with a single substituent.

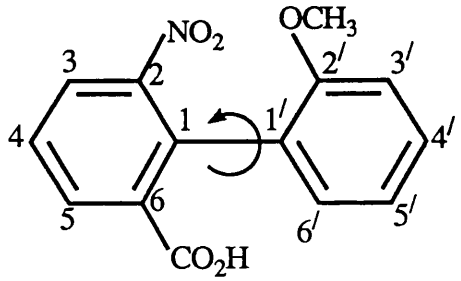

31

The pertinent data for substitution in the 3′ and 5′ - positions is contained in Table 7.

Substituent	$t_{1/2}$(3′)	$t_{1/2}$(5′)
H	9.4	9.4
OCH_3	98.1	10.8
CH_3	332	11.5
Cl	711	31.0
Br	827	32.0
NO_2	1905	35.0

Table 7 : Half-life ($t_{1/2}$, minutes) for racemisation of biphenyls (+25°C)[40].

The data show that substitution in the 3′-position exerts a large retarding effect on the rate. The methoxy group in the 2′-position is buttressed by substituents in the 3′-position thereby increasing the activation energy for bond rotation about the phenyl-phenyl bond. A smaller retarding

effect is seen when the 5′-position becomes substituted. Here the buttressing interactions are reduced by virtue of the smaller steric requirements of H_6' as compared to a methoxy group.

A more recent example of the incursion of buttressing effects appears to occur in the substituted ethane system **32.**

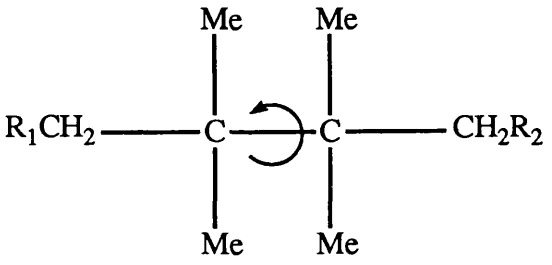

32

The barrier to rotation about the central carbon-carbon bond is heightened as the steric bulk of the remote substituents R_1 and R_2 is increased. This effect is rationalised in terms of a compression effect operating in an eclipsed transition state.[41]

Final comment

It would appear that for the hydrocarbons **25** and **26**, the more compact conformers **25A** and **26A** are destabilised by buttressing interactions. These buttressing interactions in **25A** and **26A** oppose any stabilisation arising from van der Waals' attraction between the meta alkyl group and the cyclohexyl ring.

For the alcohols **23** and **24**, buttressing effects may be operating in *both* conformations **A** and **B**. If these cancel out, attractive steric interactions

between the meta alkyl substituent and the cyclohexyl ring may well determine the preferred conformation.

Molecular mechanics calculations correctly predict the more stable conformer for alcohols **23** and **24** and confirm that it has greater van der Waals' stabilisation energy. The calculations fail to predict the more stable conformer for hydrocarbons **25** and **26**, nor do the calculations appear to model the postulated buttressing effects.

(e) **Experimental**

(i) Preparation of 1(e)-(3-methylphenyl)-2(e),6(e)-dimethylcyclohexan-1-ol, **23**

Hammered lithium shot (0.512g, 0.0731 mol) was placed in a 100 ml, 3-necked round bottom flask, under nitrogen, fitted with reflux condenser and pressure equalising dropping funnel. To this was added bromotoluene (5g, 0.0292 mol) in 20cm^3 of sodium-dried ether and the reaction vessel was heated to +80°C (oil bath temperature) for one hour, topping up with more ether when required. At the end of this time, the brown reaction mixture was cooled in an ice/water slurry and 2,6-dimethylcyclohexanone (3.685g, 0.0292 mol, Aldrich) in 10cm^3 of ether was added slowly over a 10 minute period *via* the dropping funnel to leave a pale yellow reaction mixture. The flask was refluxed for 2 hours 40 minutes at +80°C, and then allowed to stand at room temperature overnight. At the end of this time, excess lithium was filtered off and the reaction mixture quenched by addition to 50cm^3 of vigorously stirred saturated ammonium chloride soln. (a.q.). The aqueous layer was washed with 2 x 30 cm^3 of ether and the combined organic layers washed with 2x40 cm^3 water, dried over magnesium sulphate and rotary evaporated

to yield 6.181g of yellow liquid. NMR showed this to consist of the desired alcohol contaminated with unreacted ketone and bromotoluene. For the purposes of characterisation, a pure sample of the alcohol, **23**, was isolated as a colourless oil *via* preparative TLC, eluting with dichloromethane. The remainder of the alcohol in the reaction mixture was isolated by distilling off the unreacted ketone and bromotoluene to yield 1.70g of crude alcohol, **23**, which was used in the next step of the reaction sequence.

NMR, **23**

^{1}H-NMR ($CDCl_3$, ppm, 400 MHz, 20°C): 0.57(d, 6H, Me,J=6.9Hz); 1.35-1.80(m, 8H, cyclohexyl); 2.35(s, 3H, benzylic meta-methyl); 7.01(d, 1H, H_p, J=7.5Hz); 7.20(t, 1H, H_m, J=7.6Hz); note that the two H_o protons are already decoalesced and are exchange broadened humps at 6.98 and 7.36 ppm).

^{13}C-NMR ($CDCl_3$, ppm, 100MHz, 20°C): 15.74 (cyclohexylmethyl); 21.79 (benzylic meta-methyl); 25.97, 30.38 (methylene); 41.63 (methine); 78.18 (COH); note that the aromatic ^{13}C-resonances are exchange-broadened humps obscured by noise and are not reported.

Accurate Mass Spectrum **23**, m/e: 218, 161, 119, 91, 69, 55, 41

calculated: 218.1671 g mol^{-1}

found : 218.1661 g mol^{-1}

(ii) Preparation of 1(e)-(3-methylphenyl)-2(e),6(e)-dimethylcyclohexane, **25** and 1(a)-(3-methylphenyl)-2(e),6(e)-dimethylcyclohexane, **29**.

1(e)-(3-methylphenyl)-2(e),6(e)-dimethylcyclohexan-1(a)-ol, **23**, (800mg) in 35cm^3 of ethanol and 800mg of 10% Palladium on charcoal was hydrogenolysed in a Berghoff pressure vessel under hydrogen at a pressure of 50 bar and a temperature of +80°C for a total of 11 days. At the end of this time, the catalyst was filtered off through a pad of celite and the solvent rotary evaporated to leave a clear oil. This oil was passed through a short column of flash silica eluting with pet. spirit (30-40°C) to yield 216mg of a colourless oil. NMR showed this oil to be composed of a complex mixture of products. The desired hydrocarbons **25** and **29** were obtained reasonably pure as colourless oils *via* preparative GLC (10ft x 3/8" O.D. carbowax 20M on 80-100 mesh chromoborb W; 150°C; N_2=25psi; t_{ret} **25** = 41 mins, t_{ret} **29** = 52 mins).

NMR data **25**

^{1}H-NMR ($CDCl_3$, ppm, 400MHz, 25°C): 0.61 (d, 6H, cyclohexyl-methyl, J = 6.2 HZ); 1.20-1.80(m, 8H, cyclohexyl); 2.33 (s, 3H, benzylic meta-methyl); 6.91 (exchange broadened doublet, 1H, H_o'); 6.92(exchange broadened singlet, 1H, H_o); 6.98(d, 1H, H_p, J = 7.3Hz); 7.15 (t, 1H, H_m, J = 7.3Hz).

^{13}C-NMR ($CDCl_3$, ppm, 100MHz, 25°C): 21.10 (cyclohexylmethyl); 26.29, 35.85 (CH_2); 38.19(2,6-cyclohexylmethine); 59.71 (benzylmethine); 126.37, 145.30 (aromatic); all other signals too exchange broadened to be seen.

Accurate Mass Spectrum **25**:

calculated = 202.1722 g mol^{-1}

found = 202.1739 g mol^{-1}

NMR data **29**

^{1}H-NMR ($CDCl_3$, ppm, 400MHz, +20°C): 0.66 (d, 6H, cyclohexyl-methyl, J = 7.0Hz); 1.4-2.0 (m, 8H, cyclohexyl); 2.34 (s, 3H, benzylic meta-methyl); 2.74 (t, 1H, benzylic methine, J = 5.2Hz); 7.02(pseudo-doublet, 1H, H_p, J = 7.0Hz); 7.06 (s, 1H, H_o); 7.09 (d, 1H, H_o', J = 7.9Hz); 7.14 (t, 1H, H_m, J = 7.6Hz).

^{13}C-NMR ($CDCl_3$, ppm, 100MHz, +20°C): 20.70 (cyclohexyl-methyl); 21.71 (benzylic meta-methyl); 26.31, 29.31 (CH_2); 36.36 (2,6-cyclohexyl methine); 52.78 (benzylic methine); 126.44, 127.26, 128.05, 132.16. 136.76, 141.57 (aromatic).

Accurate Mass Spectrum **29**:

calculated: 202.1722 g mol^{-1}

found : 202.1702 g mol^{-1}

NMR data **24**

^{1}H-NMR ($CDCl_3$, ppm, 400MHz, +20°C): 0.58 (d, 6H, cyclohexyl-methyl, J = 6.8Hz); 1.33 (s, 9H, ^{t}Bu); 1.4-1.8 (m, 8H, cyclohexyl); 7.2-7.3 (m, 2H, H_m and H_p); H_o' appeared as two broad, decoalesced humps at 7.0 and 7.4 ppm; H_o appeared as two broad, decoalesced humps at 7.2 and 7.6 ppm.

^{13}C-NMR ($CDCl_3$, ppm, 100MHz, 20°C): 15.77 (cyclohexyl methyl); 26.00, 30.42 (CH_2); 31.51 (^{t}Bu-Me); 34.80 (^{t}Buquat); 41.66 (cyclohexyl methine); 78.41 (COH); aromatic signals are exchange broadened humps obscured by noise and are therefore not reported.

Accurate Mass Spectrum **24**:

calculated: 260.2140 g mol^{-1}

found : 260.2156 g mol^{-1}

NMR data **26**

^{1}H-NMR ($CDCl_3$, ppm, 400MHz, 20°C):0.60 (d, 6H, cyclohexyl-methyl, J = 6.2Hz); 1.31 (s, 9H, ^{t}Bu-Me); 1.0-1.9 (m, 8H, cyclohexyl); 6.9 (broad hump, 1H, H_o'); 7.10 (s, 1H, H_o); 7.15-7.20 (m, 2H, H_m and H_p).

^{13}C-NMR ($CDCl_3$, ppm, 100MHz, 20°C): 21.05 (cyclohexyl methyl); 26.31, 35.91 (CH_2); 31.47 (^{t}Bu-Me); 38.22 (2,6-cyclohexyl-methine); 59.98 (benzylic-methine); all other signals too exchange broadened to be seen and hence are not reported.

Accurate Mass Spectrum **26**:

calculated: 244.2191 g mol^{-1}

found : 244.2208 g mol^{-1}

NMR data **30**

^{1}H-NMR ($CDCl_3$, ppm, 400MHz, 25°C): 0.64 (d, 6H, cyclohexyl-methyl, J = 6.8Hz); 1.31 (s, 9H, ^{t}Bu-Me); 1.4-2.0 (m, 8H, cyclohexyl);

2.77 (t, 1H, benzylic-methine, J = 5.0Hz); 7.07 (pseudo-doublet, 1H, H_o', J = 7.4Hz); 7.16 (t,1H, H_m, J = 7.5Hz); 7.21 (d of t, 1H, H_p, ^3J = 7.8Hz, ^4J = 1.6Hz); 7.27 (pseudo-singlet, ^1H, H_o).

^{13}C-NMR ($CDCl_3$, ppm, 100MHz, 25°C): 20.67(cyclohexyl-methyl); 26.34, 29.44 (CH_2), 31.46 (^{t}Bu-Me); 34.40 (^{t}Bu-quat); 36.35 (2,6-cyclohexyl methine); 52.91 (benzylic methine); 122.31, 126.88, 128.13, 128.42, 141.06, 150.00 (aromatic).

Accurate Mass Spectrum **30**:

calculated:		244.2191 g mol^{-1}
found	:	244.2170 g mol^{-1}

Chapter 4

Attractive Steric Interactions in Meta-alkyl Substituted Benzenes

(a) Introduction

(b) Molecular Mechanics Calculations

(c) Low Temperature NMR on Meta-alkylbenzenes. Assignment of Signals in Low Temperature Limit NMR Spectra.

(d) Discussion of Results

(e) Experimental

(a) **Introduction**

The principle interaction between a 1-methylneopentyl group and a benzene ring is likely to be between the sterically bulky tert-butyl group and the phenyl ring[42]. Molecular mechanics calculations carried out in the course of this work predict a ground state with the tert-butyl group at approximately right angles to the plane of the ring and there will be a barrier to rotation to move the tert-butyl group from one side of the plane to the other (see fig. 30).

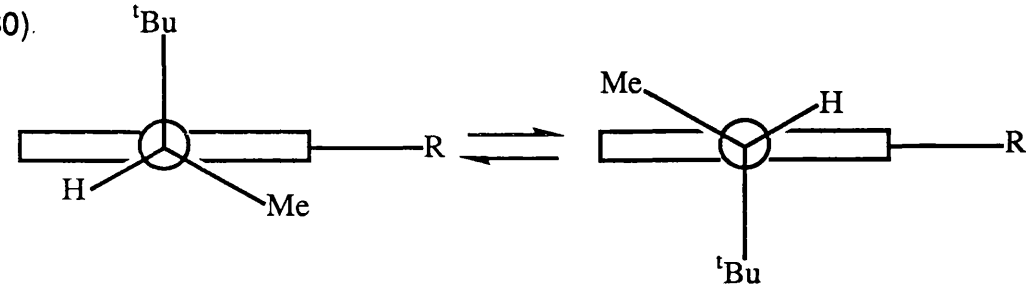

A B

Fig. 30: Edge-on view of a meta-substituted benzene ring showing the two possible ground states for a 1-methylneopentyl group. (R = meta alkyl group).

Meta-alkyl substituents on a benzene ring are too distant from one another for there to be any steric repulsion between them. Consideration of the ground state structures in fig. 30 reveals that conformer **A** has the 1-methyl group of the neopentyl group positioned closer to the alkyl group R than in conformer **B**. The interaction of the ^{t}Bu group with R is expected to be the same in both conformers **A** and **B.** Conformer **A** might therefore be expected to have greater van der Waals' attractive forces between the 1-methyl group of the neopentyl group and the alkyl group R and therefore be more stable. To investigate these points a DNMR and MMP2 study was undertaken of the meta-alkylbenzenes **33**, **34** and **35** shown in fig. 31.

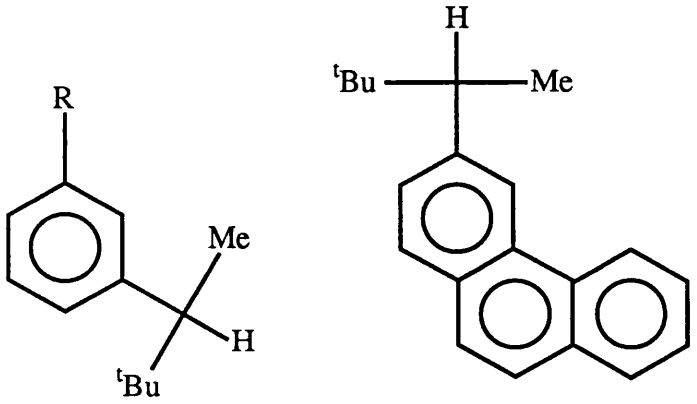

33 (R=Me)
34 (R=^{t}Bu)

35

33 : 3-methyl-1-(1-methylneopentyl)benzene
34 : 3-tert-butyl-1-(1-methylneopentyl)benzene
35 : 3-(1-methylneopentyl)phenanthrene

Fig. 31: Meta alkyl benzenes structures.

It was envisaged that the **A** ⇌ **B** equilibrium described in fig. 30 can be "frozen-out" by low temperature NMR spectroscopy and the equilibrium constant measured by electronic integration of the appropriate NMR signals. An assignment of signals in the low temperature limit NMR spectrum to the respective rotomers **A** and **B** was undertaken using NOE difference spectroscopy experiments and these are described in section (c) of this chapter.

(b) Molecular Mechanics Calculations

Compounds	33B	33A	34B	34A	35B	35A
Total steric energy	4.6398	4.6184	9.2709	9.1239	-6.5080	-6.5956
Compression[a]	1.2373	1.2375	2.0014	1.9992	1.6017	1.5854
Bond angle bending	1.9113	1.9016	2.8933	2.8985	2.4913	2.5083
Stretch-bend	0.2441	0.2438	0.3515	0.3527	0.2672	0.2684
van der Waals' 1,4-energy	8.1974	8.2095	10.7467	10.7480	13.7686	13.7457
van der Waals' longer-range energy[b]	-2.0833	-2.1091	-2.1878	-2.3624	-2.0135	-2.0966
Torsional strain	-4.8962	-4.8934	-4.5622	-4.5401	-22.6233	-22.6068
Dipolar	0.0285	0.0285	0.0279	0.0279	0.0000	0.0000
ΔE^c	0.0214		0.1470		0.0876	

Table 8: MMP2 calculations on the **A** ⇌ **B** equilibrium for compounds **33**, **34**, and **35**. Energies in kcalmol^{-1}.

Notes

[a] Strain energy from lengthening or shortening of bonds.

[b] The negative sign indicates stabilisation rather than strain.

[c] Energy difference between conformers **A** and **B**. Conformer **A** is the more stable in each case.

MMP2 calculations were performed on compounds **33**, **34**, and **35** (Table 8) and in each case predict the more compact conformer **A** (fig. 30) to be the more stable. For compound **33**, the steric energy difference between conformers **A** and **B** is calculated to be quite small (0.0214 kcalmol^{-1}) and the calculations show differences in several terms as contributing to the overall stability of conformer **A**. As regards compounds **34** and **35**, where the steric energy difference between conformers **A** and **B** is calculated to be somewhat larger, the calculations clearly show that the van der Waals' attraction term makes a major contribution to the greater stability of conformer **A** over that of conformer **B**.

(c) **Low Temperature NMR on meta-alkylbenzenes. Assignment of Signals in Low Temperature Limit NMR Spectra**

Compound	Equilibrium constants
33	1.0(CD_2Cl_2, -110°C)
34	1.87(CD_2Cl_2, -110°C)
35	1.27(10%CD_2Cl_2, 45%CHF_2Cl, 45%CF_2Cl_2 V/V, -140°C)

Table 9: Equilibrium constants for **A** ⇌ **B** equilibrium (fig. 30) as measured by integration of low temperature limit NMR signals.

Table 9 lists the equilibrium constants for the meta-alkyl benzenes **33**, **34**, and **35** as measured from their low temperature limit NMR spectra for the **A** ⇌ **B** equilibrium (fig. 30). Assignment of signals to conformers was *via* an NOE difference spectroscopy experiment performed on **35**. On the basis of this experiment it was concluded that conformer **B** (fig. 30) is more populous for all three meta-alkylbenzenes studied. A description of the three meta-alkyl benzenes' low temperature NMR behaviour and attempts at signal assignment using NOE difference spectroscopy follows.

(1) 3-tert-butyl,1-(1-methylneopentyl)benzene, **34**

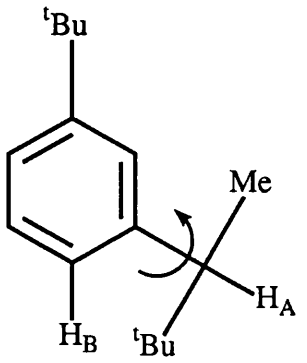

34

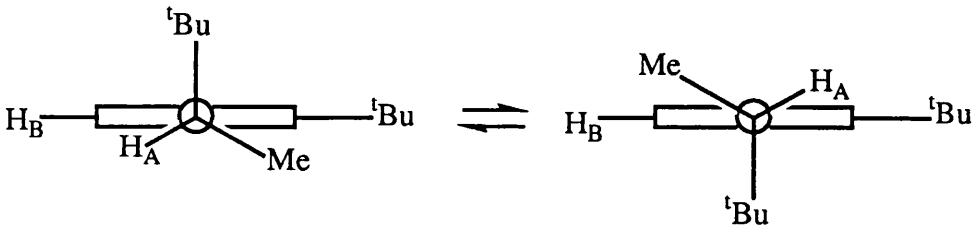

34A **34B**

Fig. 32: 3-tert-butyl-1-(1-methylneopentyl)benzene **34**; **34A** and **34B** represent edge-on views of the phenyl ring.

^{1}H-NMR showed there to be fast exchange for all signals at + 20°C in CD_2Cl_2. The aromatic region of this spectrum is complex due to overlapping of signals. However, the phenyl proton H_B, ortho to the 1-methylneopentyl group, (see fig. 32), is well separated from other aromatic signals and appears as a doublet of triplets (^3J = 6.6Hz, ^4J = 1.8Hz) centred at 6.97 ppm. As the temperature is lowered, this signal broadens and decoalesces (-90°C) until at -110°C this multiplet has split to two unequally intense doublets (^3J = 6.7Hz), separated by a chemical shift difference of 36Hz (see fig.33), whence a free energy of activation of 8.95 kcalmol^{-1} (-90°C) is calculated via the Eyring equation, in good agreement with the

barrier for Ph-CH(Me)^{t}Bu.[43]

Integration of these two non-equivalent doublets yields an equilibrium constant K = 1.87 (CD_2Cl_2, -110°C) for the **34A** ⇌ **34B** equilibrium (fig. 32).

A problem that immediately arises is the question of assignment of signals to rotamers, namely, is the more populous conformer **34A** or **34B** as depicted in fig. 32?

An attempt to address this question was made using NOE difference spectroscopy. The Benzyl proton H_A of **34** appears as a quartet at 2.55ppm. Pre-irradiation of proton H_A in the low temperature limit spectrum should result in an NOE to the doublet H_B in conformer **34A** only, by virtue of H_A's and H_B's relative proximity. Conformer **34B** should show no NOE to the H_B doublet. It should be noted that when performing NOE difference experiments on exchanging systems such as the **34A** ⇌ **34B** equilibrium, it is necessary to ensure that the temperature is low enough to prevent any NOEs built up in one conformer are not transferred by exchange to the other conformer. With a barrier to 1-methylneopentyl group rotation in **34** of 8.95 kcalmol^{-1}, it may be calculated via the Eyring equation that at -140°C, the average lifetime of conformers **34A** and **34B** is approximately 170 seconds, certainly long enough to prevent any transfer of NOEs. Attempts to reach a probe temperature of -140°C failed using a solvent system comprised of 10% CD_2Cl_2 (lock) +90% CF_2Cl_2,V/V. At -125°C, the solvent system began to freeze out. It was not possible to use CHF_2Cl, a freon with better low temperature performance, because its ^1H triplet obscured the samples' peaks. Hence attempts at signal assignment using NOE difference spectroscopy failed for **34**. However, an assignment of signals in 3-(1-methylneopentyl)phenanthrene, **35**, using NOE difference spectroscopy was

successful and a description of this experiment is outlined in the following section.

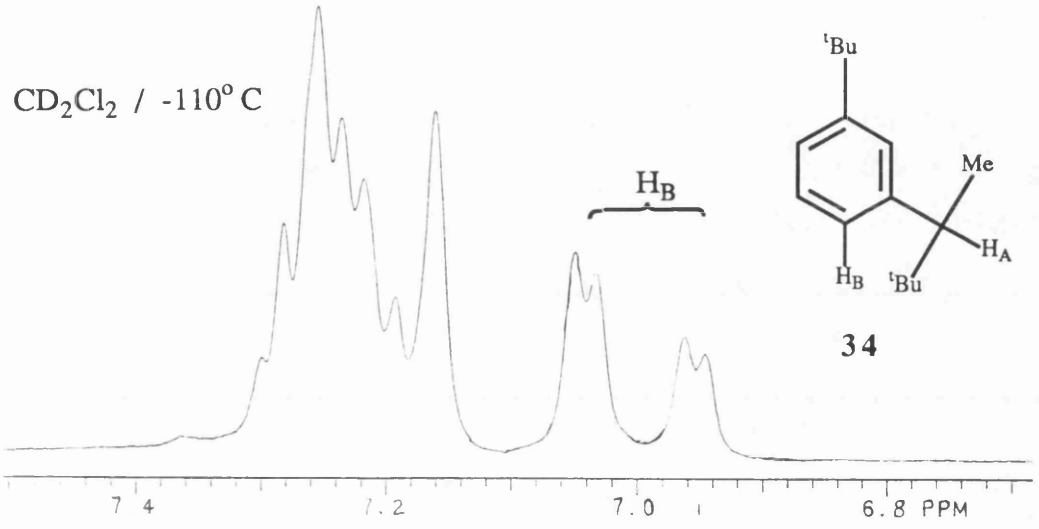

Fig. 33: ^{1}H-NMR (aromatic region) of 3-tert-butyl-1-(1-methylneopentyl)benzene, **34**, in CD_2Cl_2 (-110°C).

(ii) 3-(1-methylneopentyl)phenanthrene, **35**

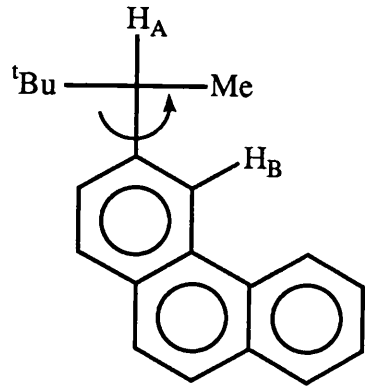

35

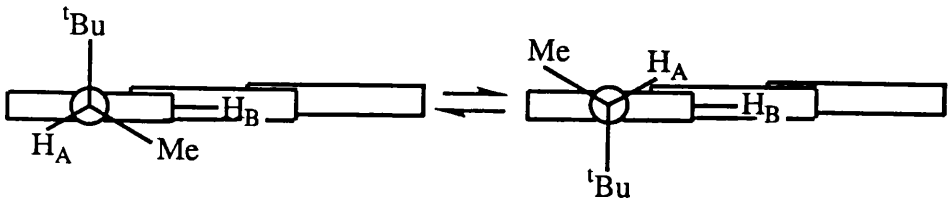

35A **35B**

Figure 34: 3-(1-methylneopentyl)phenanathrene **35**; **35A** and **35B** represent edge-on views of the phenanthrene ring system.

Room temperature NOE

The aromatic proton signals for compound **35** are spread out over a 1.3 ppm chemical shift range (spectrum 2, fig. 35) The isolated proton H_B is assigned to the singlet at 8.5 ppm. Pre-irradiation of proton H_A (a quartet at 2.85 ppm) leads to a positive NOE for H_B's signal (see spectrum 1, fig. 35).

NOE at -140°C

At -140°C H_B's signal has split to two unequally intense singlets in the

ratio 1.27:1 (spectrum 4, fig. 35). Pre-irradiation of proton H_A results in a negative NOE enhancement at the major H_B singlet only (spectrum 3, fig. 35). No NOE is seen at the minor H_B singlet. The fact that the NOE is negative at -140°C is presumably a result of the increased solvent viscosity at low temperatures - large slowly tumbling molecules show negative NOEs even at ambient temperature, so it is reasonable to postulate that a molecule of intermediate size may show a negative NOE in a viscous solution. It may be concluded therefore that **35B**, the less compact conformer is the more populous. This result is in opposition to that predicted by consideration of van der Waals' attractive forces alone, which would predict conformer **35A** to be the more populous.

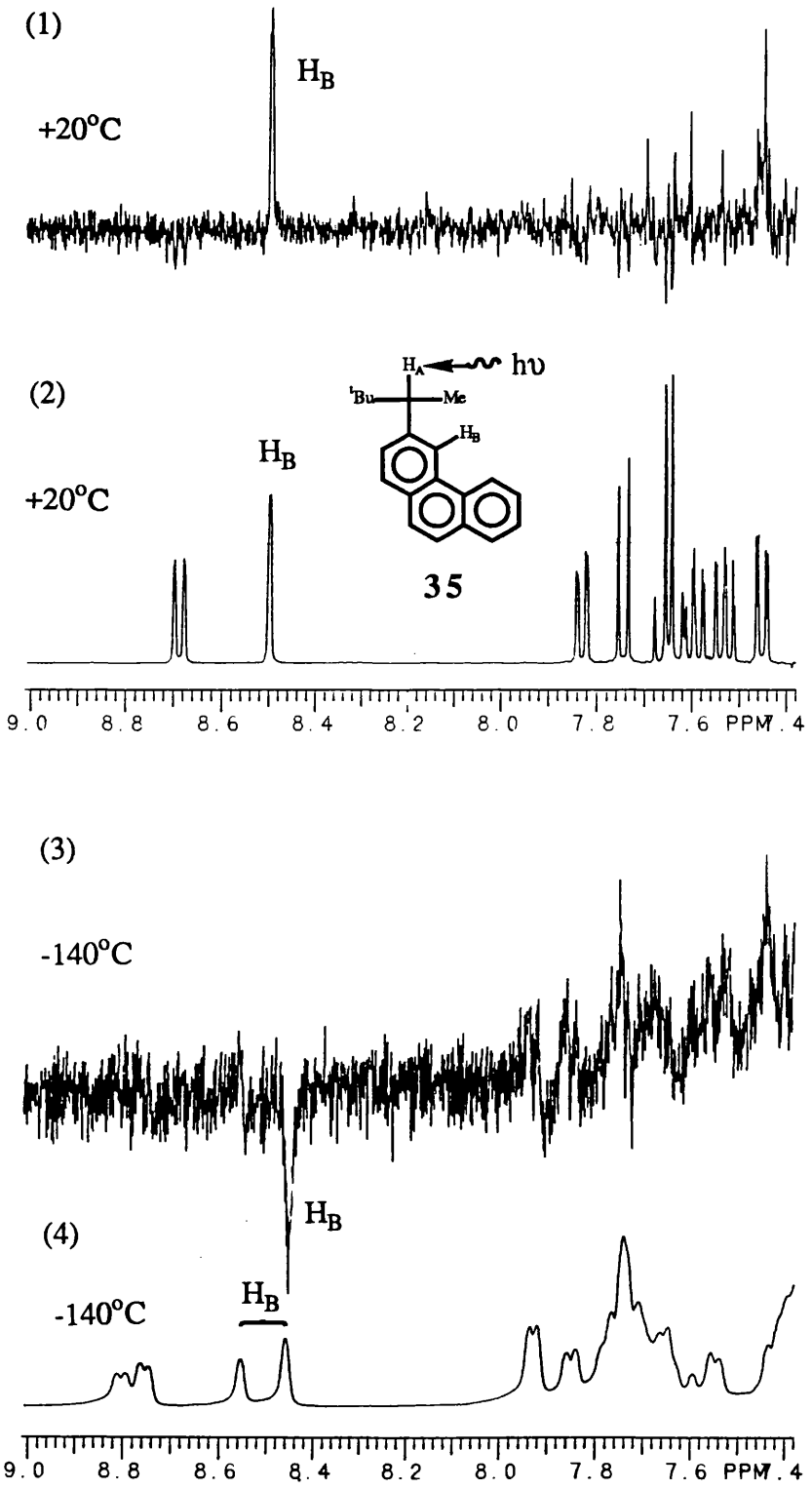

Figure 35: NOE difference spetroscopy experiments at +20°C and -140°C in 45% CHF_2Cl + 45% CF_2Cl_2 + 10% CD_2Cl_2, V/V.

Spectrum 2: ^{1}H-NMR aromatic region of **35** at +20°C.
Spectrum 1: ^{1}H-NMR NOE difference spectrum on pre-irradiation of H_A at +20°C.
Spectrum 4: ^{1}H-NMR aromatic region of **35** at-140°C.
Spectrum 3: ^{1}H-NMR NOE difference spectrum on pre-irradiation of H_A at -140°C.

(iii) 3-methyl-1-(1-methylneopentyl)benzene, **33**.

Low temperature NMR work was performed on compound **33** and yielded an equilibrium constant of 1.0 in perdeuterodichloromethane solution at -110°C.

(d) **Discussion of Results**

For the three meta-alkyl benzenes studied, **33**, **34**, and **35**, the equilibrium constants associated with 1-methylneopentyl group rotation have been measured using NMR spectroscopy and are listed in table 9. An unequivocal assignment of signals via NOE difference spectroscopy has been possible for meta-benzene **35**, namely that the more stable conformer is **B**, the less compact conformer (see fig. 34).

On the basis of the similarity in structures of meta-benzenes **33**, **34**, and **35** it is not unreasonable to conclude that conformer **B** (fig. 36) is the more stable for all three meta-benzenes. This result is clearly in opposition to that predicted by MMP2 calculations which show the more congested isomer **A** to be the more stable by virtue of its greater van der Waals' attractive stabilisation.

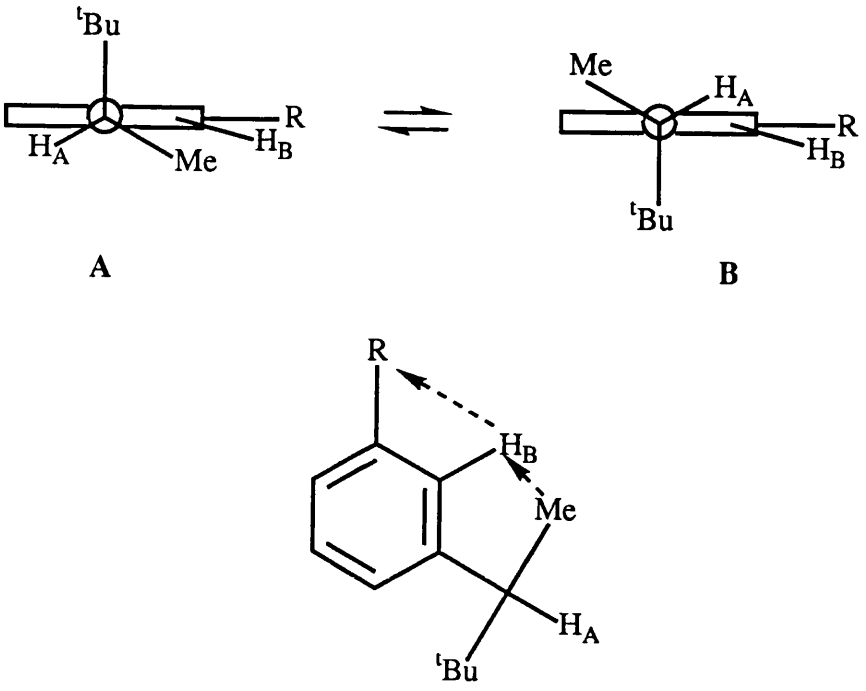

Figure 36: Buttressing effects in meta-alkylbenzenes: Conformer **A** is destabilised due to buttressing of H_B by R

One possible explanation of these results is that the proton H_B (fig. 36) is buttressed by the alkyl group R in conformer **A** by virtue of its proximity to the 1-methyl group of the adjacent neopentyl group. This buttressing interaction is reduced somewhat in conformer **B** where the methyl group is now more distant from the proton H_B. It would thus appear that these buttressing effects overwhelm any greater stabilisation in conformer **A** over that of **B** arising from van der Waals' attractive forces, and thus conformer **A** is destablised relative to conformer **B**.

Final Conclusions

The conformational equilibrium associated with the meta-alkylbenzenes **33**, **34**, and **35** is shown to favour the less compact conformer **B** (fig. 36).

Molecular mechanics calculations fail to reproduce this preference, predicting the more compact conformer **A** to be the more stable, due in part to its greater van der Waals' stabilisation energy. The operation of buttressing effects is invoked as an explanation of the experimentally observed conformational preference.

(e) Experimental

Meta-alkyl substituted benzenes **33**, **34**, and **35** were synthesised via the synthetic scheme outlined in scheme 4.

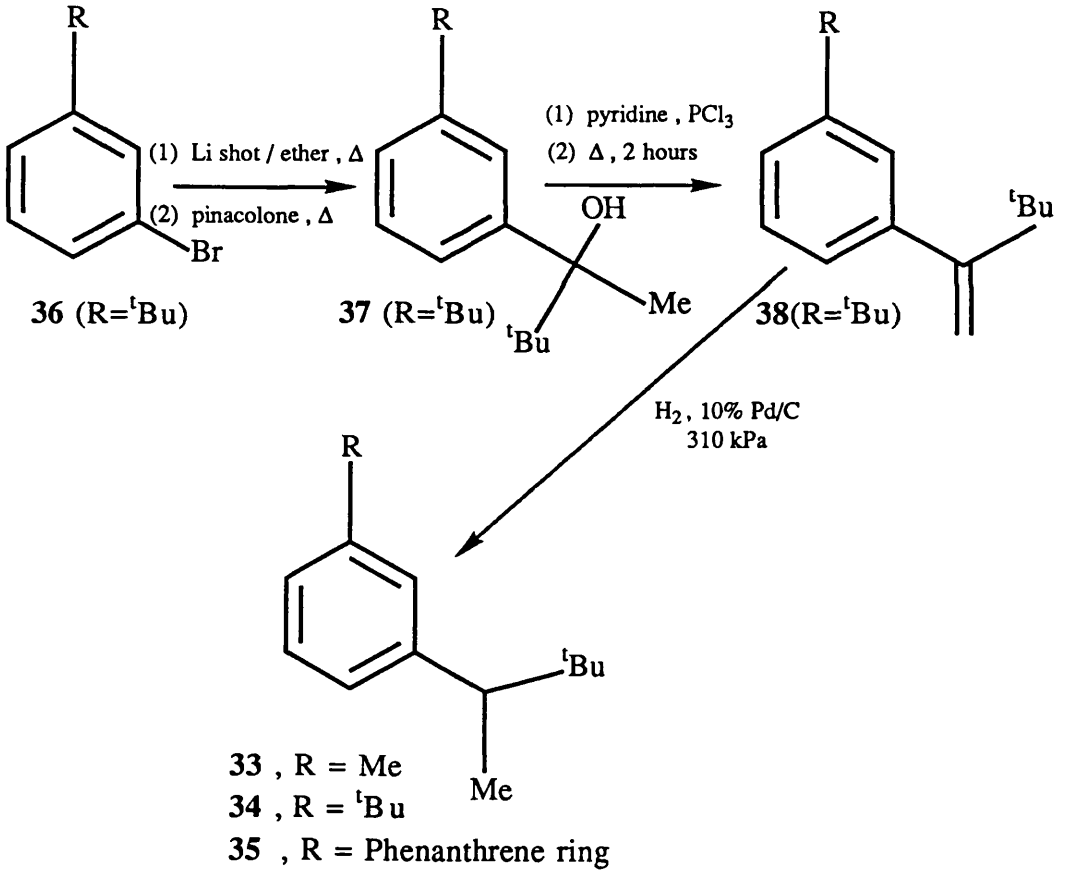

Scheme 4: Synthesis of meta-alkyl benzenes **33**, **34** and **35**.

Compounds **33** and **35** were synthesised in these laboratories by John Hjertling and Frederick Daniels.[44]

3-tert-butylbromobenzene,[45] **36**, was synthesised from 3-tert-butylphenol using the method of Schaefer and Higgins.[46]

The experimental proceedure for the synthesis of 3-tert-butyl-1-(1-methylneopentyl) benzene, **34**, is described below.

(i) Methyl, tert-butyl,(3-tert-butylphenyl)carbinol, **37**

In a three-necked, 50 ml round bottomed flask under nitrogen, fitted with condenser and dropping funnel, was magnetically stirred 3-tert-butylbromobenzene **36** (1.60g, 0.0075 mol), in sodium-dried ether (15cm^3). Lithium shot (0.5g, 0.071 mol) which had been hammered and activated by washing with methanol, was then added to the flask and the reaction vessel heated at an oil bath temperature of +80°C for a period of two hours. At the end of this time, the cloudy yellow reaction mixture was cooled in an ice bath and pinacolone (0.75g, 0.0075 mol) in 2 cm^3 of ether was slowly added via the dropping funnel. The reaction mixture was then heated at an oil bath temp. of +80°C for 90 minutes and allowed to cool. The lithium shot was filtered off and the reaction mixture quenched with saturated ammonium chloride solution (10 cm^3). The organic phase was washed with water, dried over magnesium sulphate and rotary evaporated to leave 1.416g of yellow liquid. This material was then subjected to column chromatography (silica gel) eluting first with neat pet. spirit (30-40°C) to remove unreacted 3-tert-butylbromobenzene and then with neat ether to remove the desired carbinol. Rotary evaporation of the ether fraction yielded 0.741g of **8** contaminated with approximately 5% unreacted pinacolone. This material was used without further purification in the next reaction step.

NMR data, **37**

^{1}H-NMR: (400 MHz, ppm, $CDCl_3$): 0.93 (9H, singlet, ^{t}Bu); 1.34 (9H, singlet, ^{t}Bu); 1.61 (1H, singlet, OH); 1.63 (3H, singlet, Me); 7.22-7.53 (4H, complex second order multiplets, aromatic).

^{13}C-NMR: (100 MHz, ppm, $CDCl_3$); 25.81 (^{t}BuMe); 31.40 (Me); 31.45 (^{t}BuMe); 34.71 (^{t}Bu quat); 37.97 (^{t}Buquat);78.75 (C-OH), 123.08, 124.27, 124.35, 126.66. 145.73, 149.68 (aromatic).

Accurate Mass Spectrum **37**

calculated: 234.1984 $gmol^{-1}$

found : 234.1971 $gmol^{-1}$

(ii) 1-tert-butyl,1-(3-tert-butylphenyl)ethene, **38**

In a three-necked, 50 ml round bottomed flask, fitted with a reflux condenser and under nitrogen, was stirred **37** (0.741g) in dry pyridine (14 cm^3). The flask was cooled in an ice bath and phosphorus oxytrichloride (1.59g, 0.010 mol) was added dropwise. The flask was refluxed at an oil bath temperature of +140°C for nine hours and then cooled in an ice bath before cautiously quenching with water (7 cm^3). The reaction mixture was then extracted with 3 x 20 cm^3 pet. spirit (30-40°C) and the combined organic phases washed with 3 x 20 cm^3 water, dried over magnesium sulphate and rotary evaporated to yield a yellow liquid. This material was passed through a short column of flash silica using neat pet. spirit (30-40°C) as eluant to yield 0.317g of a colourless liquid. NMR showed this to be **38**, in greater than 98% purity.

NMR, **38**

^{1}H-NMR: (400 MHz, ppm, $CDCl_3$): 1.11 (9H, singlet, ^{t}Bu); 1.32 (9H, singlet, ^{t}Bu); 4.97 (2H, AB quartet: ν_A = 2066.0Hz, ν_B = 1910.2Hz, J = 1.8Hz, olefinic); 6.94 (1H, doublet of triplets: ^{3}J = 7.3HZ, ^{4}J = 1.6HZ); 7.14 (1H, H_o, triplet, ^{4}J = 1.7Hz); 7.20 (1H, H_m doublet of doublets: ^{3}J = 7.9Hz); 7.27 (1H, doublet of triplets: ^{3}J = 7.9Hz ^{4}J = 1.2Hz)

^{13}C - NMR: (100 MHz, ppm, $CDCl_3$); 29.65, 31.38 (^{t}BuMe); 34.52 36.08 (^{t}Bu-quat); 111.16 (olefinic); 122.98, 126.09, 126.16, 126.80, 142.97, 149.89(aromatic), 160.24 (benzylic-olefinic).

Accurate Mass Spectrum **38**

calculated = 216.1878 gmol^{-1}

found = 216.1896 gmol^{-1}

(iii) 3-tert-butyl-1-(1-methylneopentyl)benzene **34**

1-tert-butyl,1-(3-tert-butylphenyl)ethene, **38**, (317 mg), in ethanol (17 cm^3) was hydrogenated in a Cook hydrogenation apparatus using 10% palladium on carbon (100 mg) at a pressure of 310 kPa for 19 hours. At the end of this time, the reaction mixture was filtered through a short column of celite to leave 232 mg of a colourless liquid. NMR showed this to be pure **34**.

NMR **34**

^{1}H-NMR: (400 MHz, ppm, $CDCl_3$); 0.86 (9H, singlet, ^{t}Bu); 1.26 (3H, doublet: J = 7.3Hz, Me); 1.31 (9H, singlet, ^{t}Bu); 2.55 (1H, quartet: J = 7.2Hz, benzylic); 6.68 (1H, doublet of triplets:

^3J = 6.6Hz, ^4J = 1.8Hz, aromatic); 7.15-7.23 (3H, complex multiplet, aromatic).

^{13}**C-NMR**: (100 MHz, ppm, $CDCl_3$); 15.76 (Me); 27.83, 31.40 (^{t}Bu); 33.65, 34.49 (^{t}Bu quat); 50.09 (benzylic); 122.46, 125.89, 126.52, 126.95, 144.65, 149.90 (aromatic).

Accurate Mass spectrum **34** m/e: 218, 203, 175, 161, 147, 131, 117, 105, 91, 77, 57, 41, 29.

calculated = 218.2035 $gmol^{-1}$

found = 218.2019 $gmol^{-1}$

Chapter 5

Van der Waals' Attraction in 2-methylalkyl-4,4-dimethyl-1,3-dioxanes

(a) Introduction

(b) Results

(c) Discussion of Results

(d) Preferred Conformation in

2-(methyl-(2-propyl))-4,4-dimethyl-1,3-dioxane

(e) Experimental

(a) **Introduction**

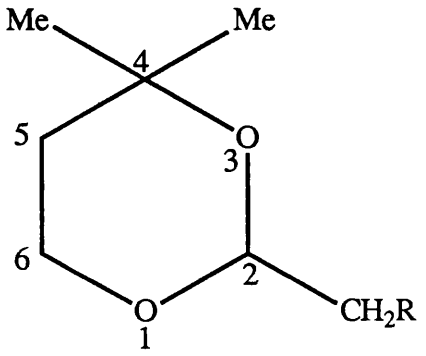

R	Compound
iPr	**39**
1-Ad	**40**
Ph	**41**

The preferred conformation of a 1,3-dioxane ring is a chair[47], and alkyl substituents in a 2- position on the ring occupy the equatorial position,[48,49,50] as in cyclohexane. A primary alkyl group, $-CH_2R$, on a 4,4-dimethylsubstituted-1,3-dioxane ring is expected to undergo the equilibrium outlined in fig. 37.

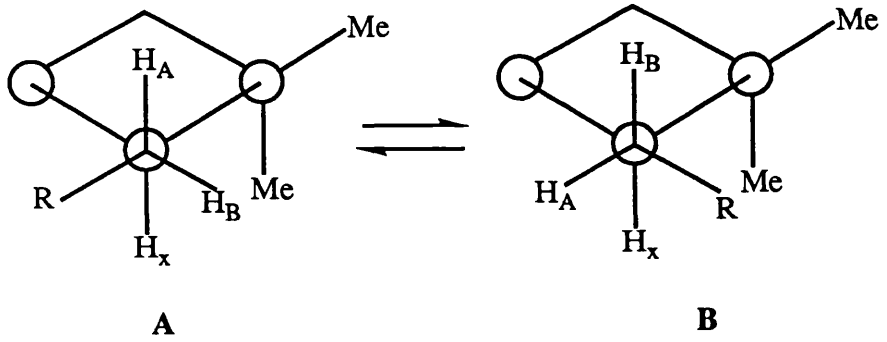

Figure 37: 2-methylalkyl group rotational equilibrium in 2-methylalkyl-4,4-dimethyl-1,3-dioxane.

A third possible conformation where R lies anti-periplanar to H_x is not expected to be appreciably populated at room temperature and is therefore neglected in this analysis.

In the more compact conformer **B**, it is expected that the alkyl group R will be attracting the 4,4-dimethyl groups, whereas in conformation **A** where the R group is now more distant from the geminal dimethyl groups,

this van der Waals' interaction is expected to be negligable.

Hence conformer **B** is envisaged to be the more stable and therefore the more populous by virtue of its greater van der Waals' stabilisation energy.

Rotation about the RCH_AH_B-CH_x bond has too low a barrier to rotation for the population of the two conformers **A** and **B** to be measured directly by low temperature NMR integration of signals. However, the $H_AH_BH_X$ protons form an ABX spin system.[51] If states **A** and **B** are equally populated then $^3J_{AX} = {}^3J_{BX}$. Any deviation from a 1:1 population of conformers **A** and **B** will be reflected in non-equal coupling constants $^3J_{AX}$ and $^3J_{BX}$, both of which can be measured from the ^{1}H-NMR spectrum of the dioxane.

(b) **Results**

	$^3J_{AX}$	$^3J_{BX}$
39 (R = ipr)[a]	5.50 Hz	5.50 Hz
40 (R = 1-Ad)[b]	4.88	4.80
41 (R = Ph)[b]	3.74	6.70

Table 10: Coupling constants J_{AX}, J_{BX} for dioxanes **39**, **40**, **41**.
[a] measured in neat $CDCl_3$; [b] measured in 2:1 C_6H_6 /$CDCl_2$, V/V.

The coupling constants $^3J_{AX}$ and $^3J_{BX}$ were found to be the same (within experimental error) in dioxanes **39** (R = ipr) and **40** (R = 1-Ad), (Table 10), indicating that conformers **A** and **B** (fig. 37) are equally populated for these two dioxanes. However for dioxane **41** (R = Ph), $^3J_{AX}$ and $^3J_{BX}$ were found to have two appreciably different values, namely 3.74 and 6.70 Hz, indicating a significant population difference between rotamers **A** and **B** (fig. 38).

It was not possible to measure $^3J_{AX}$ and $^3J_{BX}$ for dioxane **41** in $CDCl_3$ as solvent since the H_A, H_B resonances in this dioxane are isochronous in this solvent. This results in the H_A, H_B portion of the ABX spectrum appearing as a doublet and the H_x-part appearing as a triplet, despite the non-equivalence of $^3J_{AX}$ and $^3J_{BX}$. However, in the presence of benzene as solvent, the accidental chemical shift equivalence of H_A and H_B is removed, enabling $^3J_{AX}$ and $^3J_{BX}$ to be measured.

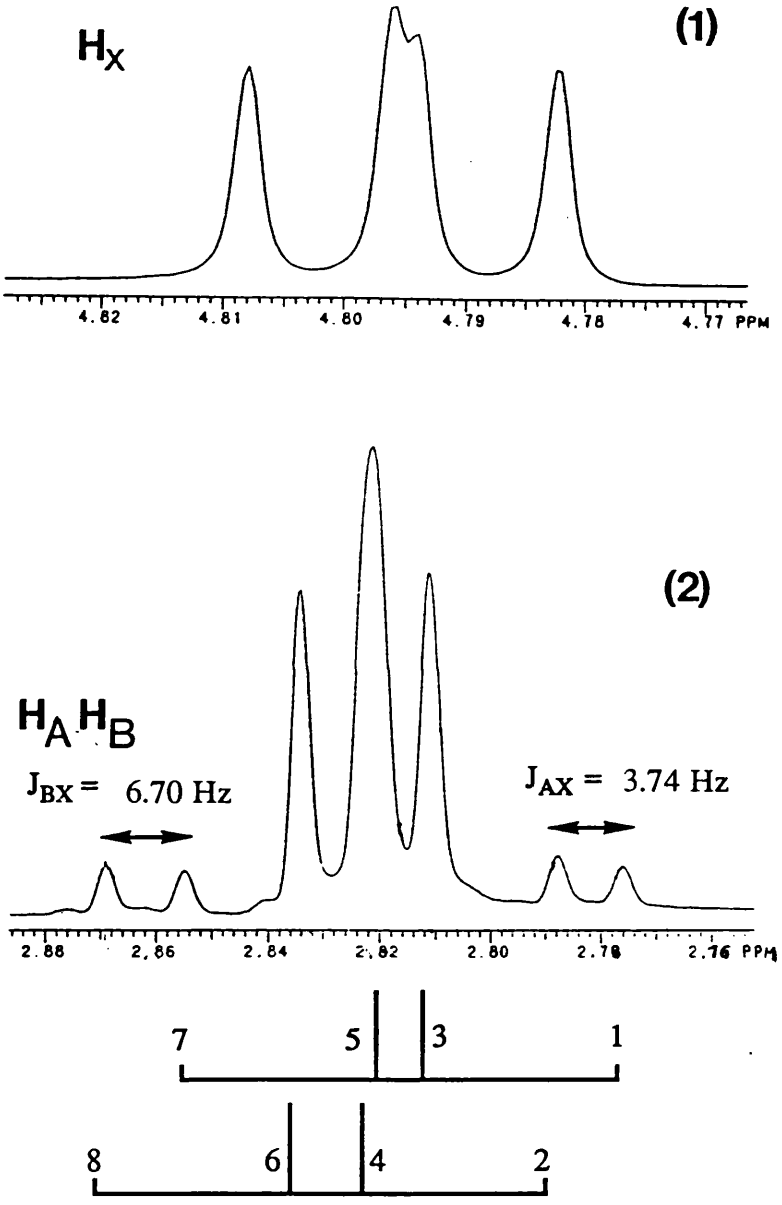

Figure 38: ^{1}H-NMR spectrum of 2-methylphenyl-4,4-dimethyl-1,3-dixoane **41** in 2/1 v/v C_6H_6/CD_2Cl_2 showing the ABX - spin system for protons $H_AH_BH_X$. Spectrum (1) shows H_X; Spectrum (2) H_AH_B; 1,3,5,7 and 2,4,6,8 denote the two AB quartets making up the A,B- portion of the ABX-spin system.

(c) **Discussion of results**

An explanation of the above results, namely the equivalence of $^3J_{AX}$ and $^3J_{BX}$ in dioxanes **39**(R = ipr) and **40** (R = 1-Ad) and the non-equivalence of $^3J_{AX}$ and $^3J_{BX}$ in **41** (R = Ph), may be found in a consideration of buttressing interactions. The following discussion presupposes that the more compact conformer **B** (fig. 37), rather than conformer **A**, is the more populous for dioxane **41**, since during the course of this work no experiment could be devised which would unequivocally assign H_A and H_B in the ^{1}H-NMR spectrum of **41**.

The ipr and 1-Ad alkyl groups (R) in dioxanes **39** and **40** will have a destabilising gauche interaction with the nearest oxygen atom neighbours in both conformations **A** and **B** (fig. 37), since R and O are 1,2 vicinal substituents on a carbon-carbon single bond. However, this destablising gauche interaction is greater in **B** than **A** since in **B** the oxygen atom is buttressed by the 4,4-gem-dimethyl groups whilst in **A** this buttressing interaction is absent. Hence conformer **B** is destablised relative to **A**. If these buttressing interactions in **B** are of similar magnitude to any van der Waals attraction stabilisation in **B** then the net result is that conformers **A** and **B** are of equal energy and hence equally populated.

As regards the phenyl dioxane **41**, a phenyl group is sterically less demanding than an ipr or 1-Ad group since a phenyl group may be considered to be a "flat board" in terms of its steric requirements. Hence any buttressing interactions are minimised in **B** and van der Waals' attraction (or more strictly speaking, CH/π interaction[18]) dominates, resulting in conformer **B** being more stable and therefore more populous.

(d) Preferred Conformation in 2-(methyl-(2-propyl))-4,4-dimethyl-1,3-dioxane, **39**

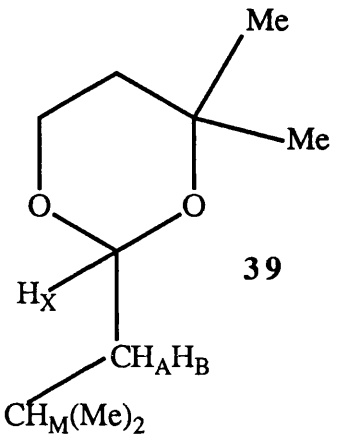

39

The conformation about the iprCH_AH_B-CH_X bond in dioxane **39** shows equivalent $^3J_{AX}$ and $^3J_{BX}$ values, indicating two equally populated gauche conformations about this bond. However, spin decoupling in $CDCl_3$ soln. at the H_X triplet (4.79 ppm) reduces H_A and H_B to two AB-quartets (due to coupling to H_M), from which $^3J_{AM}$ and $^3J_{BM}$ are determined to be 7.00 and 7.36 Hz, indicating a preferred conformation about the CH_AH_B-$CH_M(Me)_2$ bond.

It may be that the methyl groups of the ipr-group in **39** are orientated so as to maximise van der Waals' attraction between them and the 4,4-gem dimethyl groups of the dioxane ring. Certainly this would explain the non-equivalent values of $^3J_{AM}$ and $^3J_{BM}$. However, without any further experimental evidence to support this interpretation, this point must remain open to question.

(e) **Experimental**

Dioxanes **39**[52], **40**, **41** were prepared via the method of Chan[53] and his co-workers by refluxing 3-methylbutan-1,3-diol **42** with the appropriate aldehyde in the presence of chlorotrimethylsilane as catalyst and dichloromethane as solvent (scheme 5). Isovaleraldehyde and phenylacetaldehyde are commercially available whilst 1-adamantlyacetaldehyde,[54] **44**, was prepared by oxidation of 2-(1-adamantyl)-ethanol with pyridinium chlorochromate.

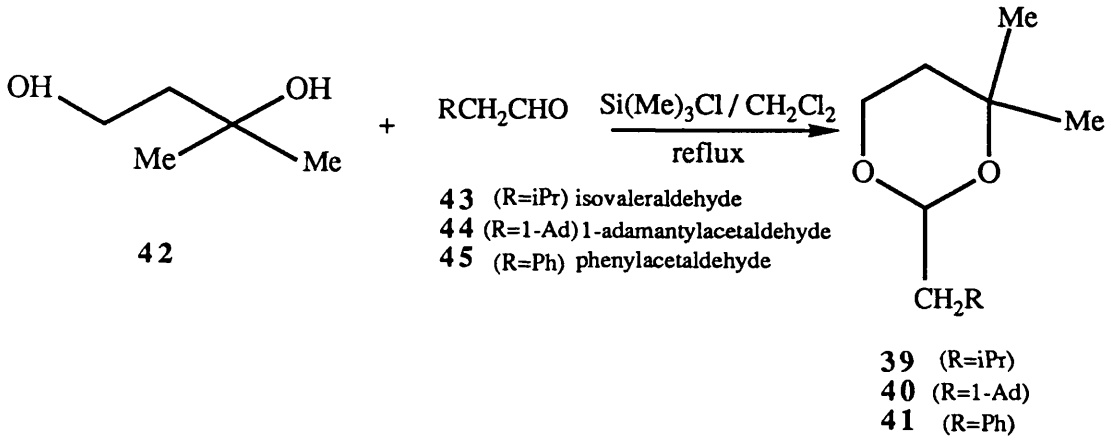

Scheme 5: Preparation of 2-methylalkyl-4,4-dimethyl-1,3-dioxanes **39**, **40**, **41**.

(i) Preparation of 1-adamantylacetaldehyde, **44**

To a magnetically stirred solution of pyridinium chlorochromate (1.498g, 0.00695mol) in dichloromethane (9 cm^3) was added 2-(1-adamantyl)ethanol (0.835g, 0.00463 mol) in dichloromethane (7 cm^3) in one aliquot. The reaction mixture rapidly changed in colour from orange to brown and was stirred at room temperature for 3 hours. At the end of this time the reaction mixture was diluted with 80 cm^3 of ether and the liquid decanted off. The black gum remaining in the reaction vessel was washed with more ether and the combined ethereal solutions were filtered through a short column of

florosil and rotary evaporated to yield 0.703g of the desired 1-adamantylacetaldehyde **44** as a pale yellow liquid in high purity. The spectral characteristics of this product were identical to those reported in the literature[54] for this compound.

(ii) Preparation of 2-(methyl-(1-adamantyl))-4,4-dimethyl-1,3-dioxane **40**

1-adamantylacetaldehyde (0.703g, 3.94 mmol) and 3-methylbutan-1,3-diol (0.902g, 8.67 mmol) in dry dichloromethane (19 cm^3) were magnetically stirred in a two-necked round bottomed flask under nitrogen fitted with reflux condenser and anti-bumping granules. Chlorotrimethylsilane (1.89g, 17.3 mmol) was then added to the reaction mixture in one aliquot and the reaction mixture refluxed for 2 hours 45 minutes. At the end of this time the reaction mixture was allowed to cool to room temperature and was then quenched with aqueous sodium bicarbonate (40 cm^3). The aqueous layer was washed with ether (2 x 30 cm^3) and the combined organic layers washed with brine (2 x 30 cm^3), dried over magnesium sulphate and rotary evaporated to leave 0.924g of a yellow oil. This material was subjected to flash column chromatography (dichloromethane eluant) to yield 0.538g of the desired dioxane **40** in high purity, as a very pale yellow oil.

NMR, **40**

^{1}H-NMR: (2:1 V/V C_6H_6/CD_2Cl_2, ppm, 400 MHz); 0.96-1.01 ($C\underline{H}_{eq}$-$C(Me)_2$, m, 1H); 1.15 (Me_{eq}, s, 3H); 1.16 (Me_{ax}, s, 3H); 1.40-1.49 ($C\underline{H}_2$-Ad, AB-portion of ABX-spin system, 2H); 1.56-1.67 (Ad, m, 12H); 1.65-1.74 ($C\underline{H}_{ax}$-$C(Me)_2$, m, 1H); 1.88-1.93 (Ad, broad s,

3H); 3.62-3.78 (CH_2-0-, m, 2H); 4.86 (C<u>H</u>CH_2Ad, t, J = 4.82Hz, 1H).

^{13}C-NMR: ($CDCl_3$, ppm, 100 MHz): 21.57, 31.85 (Me); 28.68 (Ad-methine); 31.24 (Ad_{quat}); 37.09, 42.90 (Ad-methylene); 35.74 (<u>C</u>$H_2C(Me)_2$); 49.64 (Ad-<u>C</u>H_2); 62.89 (<u>C</u>H_2-0-); 71.06 (<u>C</u>$(Me)_2$); 93.14 (<u>C</u>HCH_2Ad).

Accurate Mass Spectrum **40**:

calculated = 264.2089 $gmol^{-1}$

found = 264.2089 $gmol^{-1}$

NMR **39**

^{1}H-NMR: ($CDCl_3$, ppm, 400MHz); 0.90 ($CH(\underline{Me})_2$, d, J = 6.6Hz, 3H); 0.91 ($CH(\underline{Me})_2$, d, J = 6.6 Hz, 3H); 1.25, 1.30 (O-$C(\underline{Me})_2$, s, 6H); 1.28-1.32 ($C\underline{H}_{eq}$-$C(Me)_2$, m, 1H); 1.40-1.50 ($C\underline{H}_2CH(Me)_2$, AB-portion of ABMX spin system, 2H); 1.80 ($C\underline{H}(Me)_2$, nonette, 1H); 1.82-1.91 ($C\underline{H}_{ax}$-$C(Me)_2$, m, 1H); 3.82-3.97 ($C\underline{H}_2$-0-, m, 2H); 4.79 (C<u>H</u>CH_2ipr, t, J = 5.50Hz).

^{13}C-NMR: ($CDCl_3$, ppm, 100MHz); 21.58, 31.81 (-O-$C(\underline{Me})_2$); 22.75, 22.82 ($CH(\underline{Me})_2$); 23.91 (<u>C</u>$H(Me)_2$), 35.96 (<u>C</u>$H_2C(Me)_2$); 44.22 (<u>C</u>H_2ipr); 63.16 (<u>C</u>H_2-0-); 71.20 (<u>C</u>$(Me)_2$); 94.55 (<u>C</u>HCH_2ipr).

NMR **41**

^{1}H-NMR: (2:1 V/V C_6H_6/CD_2Cl_2, ppm, 400MHz): 0.89-0.91 ($C\underline{H}_{eq}C(Me)_2$, m, 1H); 1.01 ($Me_{ax}$, s, 3H); 1.10 ($Me_{eq}$, s, 3H); 1.60-1.70 ($C\underline{H}_{ax}C(Me)_2$, m, 1H); 2.76-2.86 ($C\underline{H}_2$Ph, AB-portion of ABX-spin system, 2H); 3.45-3.70 (CH_2-0-, m, 2H); 4.78-4.81 (C<u>H</u>CH_2Ph, m, 1H); 6.90-7.40 (Ph, m, 5H)

^{13}C-NMR: ($CDCl_3$, ppm, 100MHz): 21.60, 31.71 (Me); 35.78 ($\underline{C}H_2$-$C(Me)_2$; 42.23 ($\underline{C}H_2Ph$) 63.12 ($\underline{C}H_2$-0-); 71.59 ($\underline{C}(Me)_2$); 96.14 ($\underline{C}HCH_2Ph$); 126.29, 128.12, 129.61, 136.99 (aromatic).

Accurate Mass Spectrum **41**:

calculated = 206.1307 $gmol^{-1}$

found = 206.1315 $gmol^{-1}$

Chapter 6

General Experimental Considerations

(a) General

(b) NMR

(i) General

(ii) Conditions for NOE Difference Spectroscopy

(iii) Conditions for Saturation Transfer Measurements

(iv) Conditions for NMR Integration of Signals

(a) **General**

Column chromatography separations were performed using flash silica (Woelm, 40-63μm).

Melting points were determined using a Buchi oil bath melting point apparatus.

GLC separations were carried out on a Varian 712 preparative GLC machine.

Molecular mechanics calculations used the MMP2 (82) force field.[4]

The hydrogenolysis reactions of alcohols **23** and **24** in chapter (3) were carried out in a Berghoff pressure vessel.

n-Butyllithium (in hexanes) and *tert*-butyllithium (in n-pentane) were obtained commercially from the Aldrich Chemical Co. Ltd and were titrated with 2,5-dimethoxybenzyl alcohol according to literature methods.[55]

(b) **NMR**

(i) General

All NMR spectra, unless indicated otherwise, were recorded on a Varian VXR-400 spectrometer, operating at 400 MHz for ^{1}H and 100MHz for ^{13}C.

NMR solutions were approximately 0.1M in solute.

A 5mm, switchable, variable temperature probe was used for both ^{13}C and ^{1}H-NMR spectra, the spectra being recorded in the pulse fourier transform mode.

Temperature calibration of NMR samples in a V.T. run was effected using a chemical shift thermometer. Low temperature and room temperature samples were calibrated using an NMR tube containing neat methanol and 0.01% by volume HCL (aq).[56] High temperature ^{1}H-NMR spectra required the

use of an NMR-tube containing neat ethylene glycol.[57]

Tetramethylsilane was used as a reference compound in all cases, and chemical shift values given in this work are measured on the δ-scale in ppm.

(ii) Conditions for NOE Difference Spectroscopy

NOE difference spectroscopy experiments were carried out on undegassed samples. A typical difference experiment was performed in the following manner: a total of 64 on-resonance, 64 off-resonance transients were recorded, a block size of 8 being used with interleaving of the off-resonance and on-resonance spectra. A pre-irradiation time of approximately 6 seconds was used with the decoupler being gated off during a 3.5 second aquisition period.

(iii) Conditions for Saturation Transfer Measurements

The saturation transfer measurement of the valence isomerisation rate in dimethylcyclooctatetraene, **7**, was carried out by making use of Sanders' expression[26] for a two spin, first order, equilibrium exchange process:

$$X \rightleftharpoons Y \qquad ; \qquad k_X = \frac{[Y]}{[X]} R_Y \left\{ \frac{Y_o - Y_X}{Y_X} \right\}$$

where k_X = rate constant for interconversion of X to Y

$\frac{[Y]}{[X]}$ = equilibrium constant

R_Y = spin-lattice relaxation rate constant for spin Y

Y_o = intensity of Y resonance in absence of irradiation at X

Y_X = intensity of Y resonance in presence of saturation at X

Selective irradiation of the isolated olenific proton signal in the 1,4-

dimethylCOT bond-shift isomer **7A** (signal D, fig.6) results in saturation transfer to the corresponding signal in the 1,6-isomer **7B** (signal C, fig.6).

To determine k_x, the rate of valence isomerisation for the 1,4-isomer, signal D (fig.6) was pre-irradiated in a series of experiments using an array of increasing pre-irradiation times, D_1, ranging from 0.5 S to 7.0 S, the decoupler being gated off during the resultant aquisition time. The D_1 which gave a limiting reduction in the intensity of signal C (fig.6) was the experiment used to determine Y_x.

The equilibrium constant for the X $\rightleftharpoons$ Y equilibrium was determined via planimetric integration of the X and Y signals.

R_Y, the spin-lattice relaxation constant for spin Y, was determined via a standard T_1-spin-inversion recovery pulse sequence,[58] the exponential magnetisation recovery curve being fitted directly using the VXR-400 computer software.

(iv) Conditions for NMR Integration of signals

To minimise the errors associated with the NMR integration of a signal, the following precautions were taken:

(1) A digital resolution of at least 10 data points/Hz or greater was used.

(2) The spectra were essentially noise free, particular care being taken to ensure the spectrum was well phased and possessed a flat baseline.

(3) The spectra were derived from unweighted FIDS since resolution enhancement functions have the effect of suppressing the intensity of broader lines relative to sharper lines.

(4) Planimetry rather than electronic integration of a signal was

used for determining signal intensity.

(5) NMR data were collected under conditions that allowed uniform recovery of all signals that were to be integrated. In practice this meant that a relaxation delay of 30 seconds was inserted between pulses, and, a pulse width somewhat less than $\pi/2$ was used, to ensure complete recovery of all the signals to be integrated.

(6) Since the integrations were performed on signals arising from a conformational exchange equilibrium, it was necessary to ensure that the exchange process had reached equilibrium for a particular sample at a given temperature. In practice this meant that the sample was allowed to equilibrate at a particular temperature for at least 5 x half-life for the exchange process to ensure that equilibrium had been reached. The $(^tBu)_2COT$ equilibrium described in chapter (2) illustrates this point: the rate of bond shift in this sample is reported[14] as 22.6 $kcalmol^{-1}$. Hence 5 x $t_{½}$ is calculated via the Eyring equation to be approximately 11 hours at +20°C.

(7) References

References

1. J.E. Lennard Jones, Proc. R. Soc. London, Ser. A, **106**, 463, (1924).
2. Figure adapted from Atkins, "Physical Chemistry", 3rd Edition, Oxford University Press.
3. For a review of molecular mechanics upto 1982 See U. Berkert and N.L. Allinger, "Molecular Mechanics", American Chemical Society, Washington D.C., (1982).
4. N.L. Allinger, J. Amer. Chem. Soc., **99**, 8127, (1977).
5. T.L. Hill, J. Chem. Phys., **16**, 399, (1948).
6. N.L. Allinger, M.A. Miller, F.A. van Catledge and J.A. Hirsch, J. Amer. Chem. Soc., **89**, 4345, (1967).
7. (a) J-H. Lii and N.L. Allinger, J. Amer. Chem. Soc., **111**, 8576, (1989). (b) N.L. Allinger, Y.H. Yuh and J-H. Lii, J. Amer. Chem. Soc., 8551, **111**, (1989).
8. J.F. Liebman and A. Greenberg, Chem. Rev., **76**, 311, (1976).
9. M.E. Squillacote and J.M. Neth, Mag. Res. Chem., **25**, 53, (1987) and references cited therein.
10. B. van der Graaf, J.M.A. Baas and B.M. Wepster, Rec. Trav. Chim. Pays-Bas, **97**, 268, (1978).
11. R.E. Carter, B. Nilsson and K. Olsson, J. Amer. Chem. Soc., **97**, 6155, (1975).
12. R.E. Carter and P. Stilbs, J. Amer. Chem. Soc., **98**, 7515, (1976).
13. U. Berg and I. Pettersson, J. Org. Chem., **52**, 5177, (1987).
14. M.H. Lyttle, A. Streitwieser Jnr. and R.Q. Klutz, J. Amer. Chem. Soc., **104**, 4592, (1982).

15. L.A. Paquette, G.J. Hefferon, R. Samodral and Y. Hanzawa, J. Org. Chem., **48**, 1262, (1983).

16. N.L. Allinger, M. Frierson and F.A. Van Catledge, J. Amer. Chem. Soc., **104**, 4592, (1982).

17. C. Tosi, J. Compt. Chem., **5**, 248, (1984).

18. M. Nishio and M. Hirota, Tetrahedron, **45**, 7201, (1989).

19. Stryer, "Biochemistry", 3rd Edition, W.H. Freeman and Company, New York.

20. Cantor and Schimmel, "Biophysical Chemistry Part III", (1980), W.H. Freeman and Company, San Francisco.

21. "Molecular Foundations of Drug-Receptor Interaction", P.M. Dean, Cambridge University Press, (1987) and references cited therein.

22. R.J. Abraham and P. Loftus "Proton and Carbon-13 NMR Spectroscopy", John Wiley and Sons, (1983), p.166.

23. A.A. Frost and R.G. Pearson, "Kinetics and Mechanism", John Wiley and Sons, New York (1961).

24. H.S. Gutowsky and C.S. Holm, J. Chem. Phys., **25**, 1228, (1956).

25. Z.V. Todres, G.Ts. Ovsepyan, V.I. Bakhmutov and A. Yu, Russ. Jour. Org. Chem., **25**, 67, (1989).

26. J.K.M. Sanders and B.K. Hunter, "Modern NMR Spectroscopy, A Guide for Chemists", Oxford University Press, (1988), p.225.

27. L.A. Paquette, T.-Z. Wang, J. Luo, C.E. Cottrell, A.E. Clough and L.B. Anderson, J. Amer. Chem. Soc., **112**, 239, (1990) and references cited therein.

28. M.H. Lyttle, Ph.D. thesis, University of California, Berkeley, (1983).

29. J.T. Miller, C.W. Deckock and M.A. Brault, J. Org. Chem., **44**, No. 20,

3508, (1979).

30. M.J. Miller, M.H. Lyttle and A. Streitwieser Jnr., J. Org. Chem., **46**, No. 10, 1977, (1981).

31. A.C. Cope and W.R. Moore, J. Amer. Chem. Soc., **77**, 4939, (1955).

32. L.A. Paquette, S.V. Ley, R.H. Meisinger, R.K. Russel, and M. Oku J. Amer. Chem. Soc., **96**, 5806, (1974).

33. L.A. Paquette, U. Jacobsson and S.V. Ley; J. Amer. Chem. Soc., **98**, 152, (1976).

34. E. Leete and R.M. Riddle, Tetrahedron Lett., **52**, 5163, (1978).

35. E.W. Garbisch Jnr., J. Org. Chem., **27**, 3363, (1962).

36. B. Nilsson and T. Drakenberg, Org. Mag. Resn., **6**, 155, (1974).

37. N.L. Allinger and M.T. Tribble, Tetrahedron Lett., **35**, 3259, (1971).

38. M.E. Squillacote and J.M. Neth, J. Amer. Chem. Soc., **109**, 198, (1987).

39. C.A. Demay, A.J. Dekok, J. Lugtenbury and C. Romers, Recl. Trav. Chim., **91**, 383, (1972).

40. Newman, "Steric Effects in Organic Chemistry", Wiley, (1956), p.552-553.

41. J.E. Anderson and H. Pearson, J. Amer. Chem. Soc., **97**, 764, (1975).

42. (a) U. Berg, T. Liljefors, C. Roussel and J. Sanström, Acc. Chem. Res., **18**, 80, (1985).

(b) J.E. Anderson and D.J.D. Barkel, J. Chem. Soc. Perkin Trans. II, 1053, (1984).

(c) J.E. Anderson, H.A. Pearson and D.I. Rawson, Chem. Comm., 95, (1973).

(d) J.E. Anderson and D.J.D. Barkel, J. Chem. Soc. Perkin Trans.

II, 199, (1988).

43. J.E. Anderson, unpublished results.

44. J.E. Anderson, F. Daniels and J. Hjertling, unpublished results.

45. E.K. Fields, J. Org. Chem., **43**, No. 25, 4705, (1978).

46. J.P. Shaefer and J. Higgins, J. Org. Chem., **32**, 1607, (1967).

47. M. Hanack, "Conformation Theory", P.380, Academic Press, London (1965).

48. E. Eccleston and E. Wyn-Jones, J. Chem. Soc. (B), **12**, 2469, (1971).

49. E.L. Eliel and S.M.C. Knoeber, J. Amer. Chem. Soc., **90**, 3445, (1968).

50. V.I.P. Jones and J.A. Ladd, J. Chem. Soc. (B), 567, (1971).

51. R.J. Abraham and P. Loftus, "Proton and Carbon-13 NMR Spectroscopy", John Wiley and Sons, (1983), pp. 72-80.

52. Y.B. Yasmin, N.A. Nikiforova, R.S. Musavirov, E.A. Kantor, R.A. Karakhanov and D.L. Rakhmankulov, Tezisy Dokl. - Vses. Konf. "Stereokhim. Konform. Anal. Org. Neftekhim Sint.", 3rd (1976), 50 Russ.

53. T.H. Chan, M.A. Brook and T. Chaly, Synthesis, No.3, 203, (1983).

54. J.R. Luly, J.F. Dellaria, J.J. Plattner, J.L. Soderquist and N. Yi, J. Org. Chem., **52** (8), 1487, (1987).

55. M.R. Winkle, J.M. Lansinger and R.C. Ronald, J. Chem. Soc. Chem. Commun., 87, (1980).

56. Van Geet, Anal. Chem., **42**, 679, (1970).

57. Van Geet, Anal. Chem., **40**, 2227, (1968).

58. R.J. Abraham and P. Loftus, "Proton and Carbon-13 NMR Spectroscopy", John Wiley and Sons, (1983), pp. 122-125.

Molecular Structures Determined by Intramolecular Attractive Steric Interactions. Dynamic NMR and Molecular Mechanics Investigation of 1,6-Dimethylcyclo-octatetraene

J. Edgar Anderson * and Peter A. Kirsch
Chemistry Department, University College, Gower Street, London, WC1E 6BT

1,6-Dimethylcyclo-octatetraene equilibrates with 1,4-dimethylcyclo-octatetraene by a bond-shift process which is slow on the NMR timescale at ambient temperature. The greater stability of the former valence isomer (ΔG_0 = 0.081 kcal mol^{-1}† at 20 °C in perdeuteriobenzene solution) is attributed to attractive steric interaction between methyl groups. NMR spectra of the equilibrium mixture are considered in detail with a view to characterising other 1,6 ⇌ 1,4-disubstituted cyclo-octatetraene equilibria. Diagnostically useful differences in spectra are demonstrated, while some apparently clear differences are due to second-order effects. Molecular mechanics calculations agree with experimental results as to the preferred valence isomer and confirm that it has greater methyl–methyl attractive steric interactions. There are three slightly different conformations present in similar relative amounts for each valence isomer due to methyl rotation, and NMR results do not disagree with this suggestion.

Attractive steric interactions within molecules are much more common than repulsive ones yet have received much less attention in the history of conformational analysis.[1] In all but the smallest molecules, most pairs of atoms will be separated by more than the sum of their van der Waals radii, *i.e.* beyond repulsion, but the contribution to the enthalpy of the molecule of the few atoms interacting repulsively will usually be greater, often much greater, than the stabilisation from attractive steric interactions. The maximum value of any single pairwise attraction is likely to be about 0.05 kcal mol^{-1}.

The most elusive aspect of attractive steric interactions is the stabilisation produced by the interaction of two saturated hydrocarbon fragments too distant to repel each other. In the limiting case where both fragments are non-polar there remains a weak induced dipole/induced dipole interaction (weak, as carbon–carbon and carbon–hydrogen bonds in saturated fragments are not very polarisable). Practically, however, this will be enhanced by the weak polarity of the first fragment (weak, as there are no large differences in atom electronegativity) interacting with the weak polarity or polarisability of the second.

In view of the dominating omnipresence of repulsive interactions, one tactic for studying attractive steric interactions is to devise and study molecules for which there are two similar structures in both of which the repulsive steric interactions are the same, but which have different attractive interactions.[1]

It has recently been shown that 1,6-disubstituted cyclo-octatetraenes (**1**) equilibrate with the 1,4-isomers (**2**) by a bond-shift process slow enough on the NMR timescale to allow direct measurement of the populations of the two states.[2,3] The cyclo-octatetraene conformation is tub-shaped and the immediate environment of each group R in both forms is the same, the only difference appearing to be whether the groups R are near to each other as in the 1,6-isomer (**3**), or further away as in the 1,4-isomer (**4**). For the di-t-butylcompounds,[2] the 1,6-isomer (**3a**) with the t-butyl groups close together in space is more stable than the 1,4-isomer (**4a**), the ratio of populations being 2.08 at 25 °C in deuteriochloroform solution, representing a free energy difference of 0.43 kcal mol^{-1} in favour of (**3a**).

Molecular mechanics calculations[4,5] satisfactorily reproduce the (**3a**), (**4a**) energy difference as do *ab initio* calculations, as long as the latter[5] are carried out without approximations

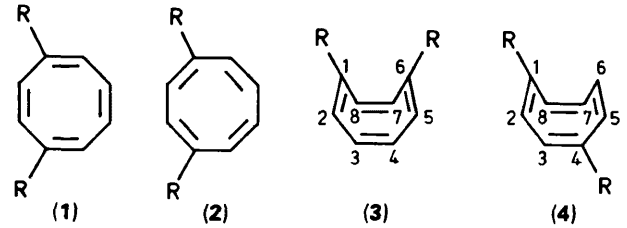

(**1**) (**2**) (**3**) (**4**)

a; R = $C(CH_3)_3$
b; R = CH_3
c; R = CD_3

which preclude electron correlation between pairs of atoms, *i.e.* attractive steric interactions. Calculations have also been carried out[4,5] on corresponding dimethylcyclo-octatetraenes (**1b**) and (**2b**) and suggest that in this case as well, the 1,6-isomer should be slightly more stable than the 1,4-isomer by 0.02 kcal mol^{-1}. This pair of compounds has been prepared previously, presumably as a mixture[6] but the equilibrium has not been studied.

We feel that the subject of attractive steric interactions deserves greater investigation not only for itself but also as an intramolecular model for lipophilic interaction, and that the (**1**) ⇌ (**2**) equilibrium is a good basis for a systematic study. In simpler examples than the di-t-butyl set, coupling between the substituent and the ring protons should give detailed information on the interaction between groups and the differences between group conformations.

This has been shown to be the case, and we want now to give a detailed account of the (**1b**) ⇌ (**2b**) equilibrium, showing the extent of the information that is available from careful NMR work, supported by molecular mechanics calculations.

Results

NMR Spectra.—The (**3b**) ⇌ (**4b**) equilibrium mixture was synthesized by the method of Paquette and co-workers[6] exploit-

† 1 cal = 4.184 J.

Table 1. ^{1}H Chemical shifts[a] and relaxation times[b] (T_1/s) at 20° and −32° for (**3b**) ⇌ (**4b**).

	Methyl group			H_2, H_3			H_7, H_8		
	Shift	T_1[c]	T_1[d]	Shift	T_1[c]	T_1[d]	Shift	T_1[c]	T_1[d]
(**3b**) 1,6-isomer	1.609	2.59	1.33	5.15, 5.73	4.73	2.61	5.63	4.54	2.51
(**4b**) 1,4-isomer	1.626	2.53	1.27	5.54	4.48	2.45	5.67, 5.70	4.54	2.58

[a] C_6D_6 solution. [b] $CDCl_3$ solution. [c] At 20 °C. [d] At −32 °C.

Table 2. ^{13}C Chemical shifts and relaxation times (T_1/s) for $CDCl_3$ solution of (**3b**) ⇌ (**4b**).

	Methyl group		Methine carbons						C-carbon	
	Shift	T_1	Shift	T_1	Shift	T_1	Shift	T_1	Shift	T_1
(**3b**) 1,6-isomer	23.76	5.02	126.44	6.22	131.22	6.07	133.24	6.40	140.12	30.27
(**4b**) 1,4-isomer	23.50	5.33	127.09	6.47	130.03	6.25	134.97	5.93	138.94	32.67

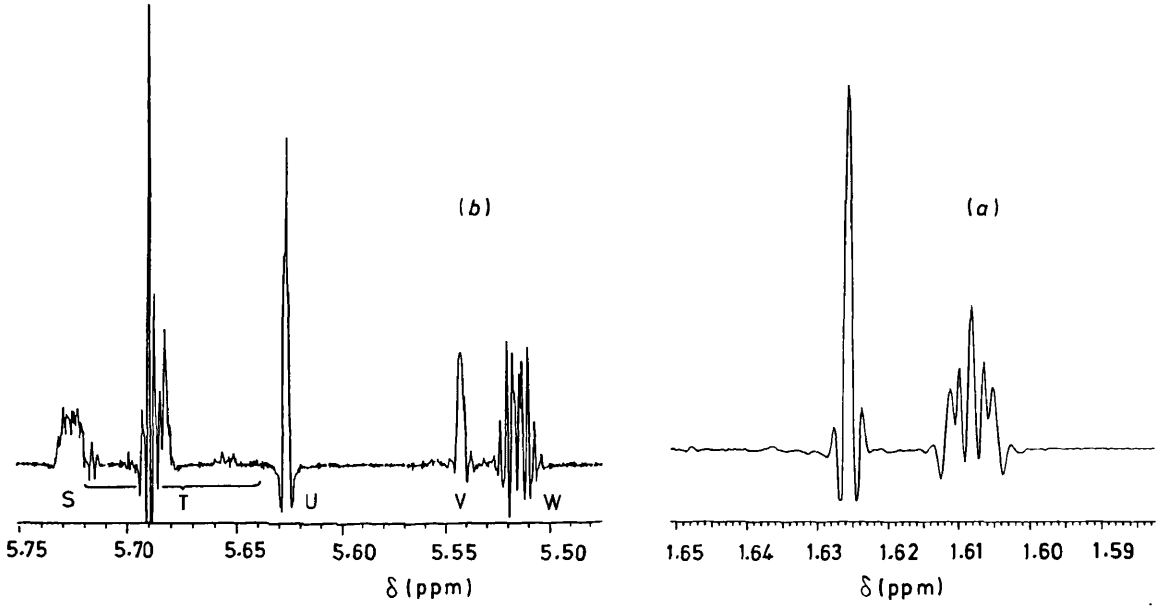

Figure 1. ^{1}H NMR spectra of a perdeuteriobenzene solution of the (**3b**) ⇌ (**4b**) mixture. (*a*) Methyl region; (*b*) alkene region. S,W = H2–H5; U = H7, H8 in (**3b**); V = H2, H3, T = H5–H8 in (**4b**), X,Y = methyl in (**4b**) and (**3b**), respectively.

ing Huisgen's synthesis of cyclo-octatetraene-1,4-sulphone.[7] The 400 MHz proton NMR spectrum for a perdeuteriobenzene solution is shown in Figure 1(*a*) for the methyl protons, and in Figure 1(*b*) for the alkenic protons, and comprises two subspectra in the intensity ratio (**3b**):(**4b**) 1.15:1, determined from various signals by various integration methods, see the Experimental section. From this ratio, the relative enthalpy of the two isomers is 81 cal mol^{-1} at 20 °C, if their entropies are the same. The assignment of peaks is as indicated in the Figure, and is based on the reliable premise that in the 1,4-isomer non-identical adjacent protons [7 and 8 in (**4b**)], will have a coupling constant of about 11 Hz, a vicinal coupling *cis* on a double bond, while in the 1,6-isomer the corresponding coupling constant (between non-identical adjacent protons 2 and 3) will be about 3 Hz, a vicinal coupling along a single bond where the dihedral angle is 45–50° according to molecular mechanics calculations. Table 1 gives details of the spectra.

Two sets of subspectra of different intensity are seen in the ^{13}C NMR spectrum of (**1b**) + (**2b**). Table 2 has details while Figure 2 shows the methyl region of the spectrum without proton decoupling.

NMR spectra are solvent dependent to the extent that some relative chemical shifts change sign, but the position of the (**3b**) ⇌ (**4b**) equilibrium does not seem to change. Similar observations have been described less unequivocally for the (**3a**) ⇌ (**4a**) equilibrium.[6]

On raising the temperature of a DMSO solution, all signals broaden up to about 52 °C at 200 MHz when signals merge. On further heating signals sharpen until a single average spectrum is obtained for the (**3b**) ⇌ (**4b**) mixture, indicating that the bond shift has become rapid on the NMR timescale. All changes are reversed on return to room temperature. At the coalescence temperature the barrier to the interconversion is calculated to be 17.3 kcal mol^{-1}.

Molecular Mechanics Calculations.—Calculations for bond shift-isomers (**1b**) and (**2b**) have been reported elsewhere.[4] We have repeated these in rather more detail with respect to the methyl groups' rotational conformations which are undoubtedly significant but which were not considered in that earlier report.

There are two stable conformations for a methyl group, separated by 60° of rotation, depending on whether a proton is antiperiplanar (**5**) or synperiplanar (**6**) with respect to the double bond, and the former is calculated to be more stable by

Table 3. Molecular mechanics calculations of the three conformations, *anti, anti*; *anti, syn*; and *syn, syn* of (**3b**) and (**3b**), enthalpies in kcal mol^{-1}.

	anti, anti		*anti, syn*		*syn, syn*	
	1,6-isomer (**3b**)	1,4-isomer (**4b**)	1,6-isomer (**3b**)	1,4-isomer (**4b**)	1,6-isomer (**3b**)	1,4-isomer (**4b**)
Methyl-1 dihedral angle[a]	−172.1	−179.6	−172.7	−179.7	−2.0	−4.1
Methyl-4(6) dihedral angle	171.8	−179.6	1.5	−3.5	3.2	−4.1
Total steric energy	10.3742	10.4253	10.6420	10.6798	10.8946	10.9322
Compression[b]	0.1784	0.1800	0.1860	0.1927	0.1950	0.2053
Bond angle bending	2.1514	2.2018	2.2365	2.2584	2.3059	2.3140
Stretch-bend	0.0366	0.0345	0.0388	0.0375	0.0411	0.0403
van der Walls 1,4-energy	4.4016	4.3988	4.2986	4.3067	4.2050	4.2186
van der Waals longer-range energy[c]	−1.7460	−1.7615	−1.5406	−1.5026	−1.3233	−1.2418
Torsional strain	5.3332	5.3561	5.4035	5.3716	5.4518	5.3802
Dipolar	0.0191	0.0155	0.0192	0.0155	0.0192	0.0155
Sum of 16 pairwise methyl atom interactions	−0.0898	−0.0223	−0.0967	−0.0223	−0.1059	−0.0222

[a] Angle in °. For *syn* and *anti* methyl groups dihedral angles reported are for the hydrogen nearly eclipsing the double bond and nearly antiperiplanar to the double bond, respectively. Values are never exactly 0 and 180°, and in every case the sign tells that rotation has taken the hydrogen to a position outside perfectly periplanar rather than inside. [b] Strain energy from lengthening or shortening bonds. [c] The negative sign indicates stabilisation rather than strain.

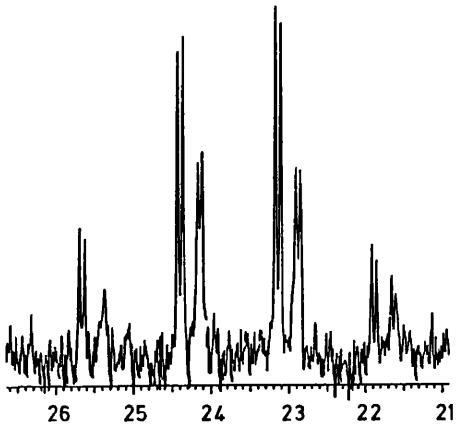

Figure 2. Methyl region of the ^{13}C NMR spectrum of the (**1b**) ⇌ (**2b**) mixture in deuteriobenzene solution at 20 °C.

about 0.26 kcal mol^{-1}. For both dimethylcyclo-octatetraenes there are thus three different conformations, *anti, anti*; *anti, syn*; and *syn, syn*. The calculated enthalpies of these are shown in Table 3, and in each case the 1,6-dimethyl compound is more

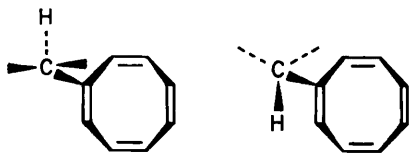

(**5**) (**6**)

stable than the 1,4 compound by 38–51 cal mol^{-1}. The Table shows the various contributions to the total enthalpy of the two isomers and the sum of the sixteen pairwise atomic interactions of the two methyl groups for each conformation.

The difference between bond-shift isomers is thus much smaller than the difference between methyl group conformations within each isomer but the conformational behaviour of the two compounds is parallel within the limits of reproducibility of molecular mechanics minimisation. Each compound should exist as a very similarly composed mixture of all conformations *viz.*, 37% *anti, anti*, 24% each of *anti, syn* and *syn, anti*, and 15% of *syn, syn*. The conformationally weighted enthalpy difference is calculated to be 43 cal mol^{-1} whence the relative amounts of the two valence isomers is calculated to be 1.076:1 in satisfactory agreement with the experimental observation of 1.15:1.

Discussion

The (**3b**) ⇌ (**4b**) *Equilibrium.*—Molecular mechanics calculations predict and NMR observations confirm that (**3b**) is more stable than (**4b**) by 43 and 81 cal mol^{-1} respectively. The molecular mechanics comparison focuses on very small differences between large quantities, where the difference between isomers is much smaller than conformational differences within isomers. The justification for seeing significance in the results is that the experimental one is incontrovertible and in agreement with the calculations. With more highly substituted analogues of (**1**) and (**2**), the effects will be greater, yet discussion of spectra, of conformations, and of energy differences will inevitably be in terms similar to those used now. It is gratifying that calculations and experiment agree as to the sense of the stability and the order of magnitude.

A feature of the calculations which should not be ignored when attaching significance to small enthalpy differences is that of reminimisation discrepancies. Minimum energy co-ordinates when resubmitted to the program as starting co-ordinates may, and in the present case do, lead to slightly different minimum energies which vary randomly if the process is repeated several times. This probably reflects the finite size of the improvement cut-off point and other approximations in the minimisation procedure. In the case of the *anti, anti* conformation of the two isomers the range of minimum energies was found to be 9 cal mol^{-1} over six reminimisations.

Such a reminimisation discrepancy contrasts with our experience in polycyclic compounds such as adamantane derivatives where successive reminimisations lead by minute steps to increasingly stable structures. This may be associated with the greater interdependence of parameters in the polycyclic structure compared with a more open one.

The (**3b**) ⇌ (**4b**) equilibrium as measured by the ratio of peak intensities is not significantly temperature dependent over the range that could be measured, −50 °C to +40 °C. It thus seems that there is a true enthalpy difference favouring the 1,6-isomer, and the entropies of the two isomers are the same within experimental error. The 1,6-isomer might have lower entropy since the methyl groups interact, and might thus restrict each other, but the results do not indicate this.

This contrasts with the observation of Streitwieser and his

Table 4. Barriers to bond-shift in substituted cyclo-octatetraenes.

Substituents	Barrier, G^+, kcal mol^{-1} and (temperature, K)	Reference
None	13.7 (263)	8
1-OCH_3	16.4 (273)	9
1,2-$(CH_3)_2$	21.1 (395)	10
1,2,3-$(CH_3)_3$	26.8 (363)	11
1,2,3,4-$(CH_3)_4$	33.7 (433)	11
1,4- and 1,6-$(Bu^t)_2$	22.6 (298)	2
1,4- and 1,6-$(CH_3)_2$	17.3 (325)	This work

colleagues[2] on the (**3a**) $\rightleftharpoons$ (**4a**) equilibrium which showed a temperature dependence of the equilibrium which led to enthalpy and entropy differences of 0.489 kcal mol^{-1} and 0.92 eu,* respectively. Paquette[3] and his co-workers were not able to confirm this temperature dependence.

The molecular mechanics calculations predict differences in many terms as contributing in different senses to the overall relative stability of (**3b**) compared with (**4b**). This suggests caution in assigning the stability of (**3b**) to attractive steric interactions. However, molecular mechanics reports all the adjustments the molecule makes to lower its total enthalpy including increasing other kinds of strain when this leads to an even greater increase in attractive interactions. We therefore extracted and summed the sixteen pairwise interactions between methyl group atoms in the various conformations of the structures (**3b**) and (**4b**), see Table 3, and these sums, between 67 and 84 cal mol^{-1} always favouring (**3b**), emphasize the importance of these interactions.

Table 4 lists the barriers to bond shift in substituted cyclo-octatetraenes. There is a well-defined trend to higher barriers with increased number, size, and relative proximity of substituents, into which the present result, a barrier of 17.3 kcal mol^{-1} to interconversion of (**3b**) and (**4b**), fits. In a planar or near-to-planar transition state, interaction of substituents along what were originally single bonds must be greatly increased, and this can be expected to be the main source of substituent effects on the barrier.

NMR Spectra.—The calculations do not predict significantly different mixtures of conformations about the methyl to cyclo-octatetraene bond for the two isomers. NMR spectra of the isomers, on the other hand, show different coupling patterns between methyl groups and the rest of the molecule, see Figures 1 and 2, but these do not reflect different methyl-group conformations, but rather differing complexity of coupling pathways.[12]

The signals U and V in Figure 1(*b*) are assigned to the isolated identical alkenic protons at the 7,8-position in (**3b**) and the 2,3-position in (**4b**) respectively. These have weakly resolved splitting of about 0.5 Hz magnitude, shown by double-irradiation experiments to represent coupling with the adjacent methyl group. The *cis*-proton to methyl-proton coupling in propene is 1.27 Hz.[13] In both U and V the splitting is less than the coupling constant since an isolated proton is coupled in a different way, with opposite sign, to each of the methyl groups. Furthermore, the different ways are not the same in (**3b**) and (**4b**), where the identical isolated protons are linked by a double bond and by a single bond, respectively. The differing appearance of the methyl signals in the proton NMR, see Figure 1(*a*), is explained similarly.

Signal T in Figure 1(*b*) is an AA'BB' spectrum for protons 5–8 in (**4b**) where an AB coupling of about 11 Hz can be distinguished. Decoupling the appropriate methyl signal at δ 1.626 (which shows little structure), has only a small effect on T, and the decoupled spectrum can be simulated as an AA'3B' spectrum with J_{AB} 11.1 and $J_{AB'}$ 3.5 Hz. Again the apparent absence of coupling of A and B to the methyl groups reflects the opposite sign of these couplings, the near coincidence of the A and B chemical shifts and the large AB coupling constant.

Signals S and W in Figure 1(*b*) make up the AA'BB' spectrum for protons 2–5 in (**3b**), where A and B have a large relative chemical shift equivalent to 84 Hz at 400 MHz and are weakly coupled, J_{AB} 3.0 Hz. This coupling emerges from decoupling the methyl group at δ 1.627 and spectral simulation, as do couplings of A and B to the methyl group of 1.3 and 0.6 Hz respectively, quite usual values.[13]

We expect that the difference in the AA'BB' spectra due to protons 2–5 in (**3b**) and 5–8 in (**4b**) will be diagnostic of the 1,6- and 1,4-isomers respectively. These are chemically quite different AA'BB' systems so such spectral differences are to be expected.

Turning to the ^{13}C NMR spectrum of the compounds (**3b**) and (**4b**), chemical shifts, although clearly different, deserve only a little comment. The methyl groups in (**3b**) are attracting each other, and may have a different rotational conformation from those in (**4b**). Whether either of these explanations will prove to be a characteristic explanation of the downfield displacement of the methyl and C-1 shift in (**3b**) compared with (**4b**), remains to be seen.

Differences between ^1H–^{13}C coupling constants for (**3b**) and (**4b**) are expected to be more significant. The one bond coupling constant of the methyl carbon is the same within experimental error, 126.7 and 126.4 Hz for (**3b**) and (**4b**), respectively. There is, however, a significant difference in the *cis* vicinal coupling of the methyl carbon to the vinylic proton in the two isomers, 6.8 ± 0.2 Hz in the major isomer (**3b**), and 5.5 ± 0.3 Hz for the minor isomer (**4b**). The question arises again whether this reflects a change in methyl group conformation between isomers, but a consideration of structures (**3**) and (**4**) and spectral simulation show that this need not be so. 3-H in (**4**) is identical with 2-H, so the first-order analysis of the ^{13}C spectrum which can be used for the 1,6 isomer (**3**), is no longer appropriate for (**4**). Rather, the coupling of 3-H with the methyl carbon, reasonably of opposite sign to that of 2-H means that the doublet splitting is the algebraic sum of these two coupling constants. The heights of the two quartets (see Figure 2) are in a ratio different from the signal intensity ratio of 1.51:1, confirming the complex nature of the apparent doublets of the minor isomer. Spectral quality is too low to justify further study of this point.

The question arises as to whether nuclear spin relaxation times are different in the isomers, *i.e.* whether they are affected by the postulated attractive steric interactions. Results are shown in Tables 1 and 2 and show no significant differences. Determination of spin–lattice relaxation times T_1 at room temperature is complicated by the fact that although interconversion of the two isomers is slow on the NMR timescale, it is not slow on the relaxation timescale, that is, the half-life for valence isomerism is comparable to relaxation times. Proton relaxation times T_1 were therefore also determined at − 32 °C, see Table 1, but no significant differences emerged at this temperature either.

We exploited the similarity in rates of valence isomerisation and nuclear spin relaxation at room temperature to carry out a saturation transfer measure of the valence isomerisation rate.[14] Pre-irradiation of a signal from one isomer leads to saturation of the corresponding signal of the other isomer, which appears as a decrease in the intensity of that signal, depending on the pre-irradiation time and the rate constant for valence isomerisation. By this means we measured a

* 1 eu = 4.184 J K^{-1} mol^{-1}.

rate-constant of 0.58 s^{-1} for interconversion of (**3b**) $\rightleftharpoons$ (**4b**) at 20 °C which leads to a free energy of activation for valence isomerisation of 17.48 kcal mol^{-1} at 20 °C, in good agreement with the value of 17.3 kcal mol^{-1} at 52 °C found from the coalescence of the signal.

We also investigated the bond-shift equilibrium for the isomers (**3c**) and (**4c**) with two trideutieriomethyl groups. The appearance of the alkene region was very similar to the parent spectrum with decoupling at the methyl proton signals. The fractional populations of the two isomers were the same as for the protio series within experimental error.

Experimental

The mixture of (**3b**) and (**4b**) was prepared according to the method of Paquette and co-workers.[6] Compounds (**3c**) and (**4c**) were prepared similarly using deuteriated methyl iodide at the alkylation stage.

NMR spectra were recorded using a Varian VXR400 spectrometer operating at 400 MHz for protons and 100.6 MHz for carbon. Relative intensities of signals were determined from ^1H NMR spectra using the spectrometer's electronic signal integrator, and by planimetry of plotted signals. Care was taken to avoid saturation effects. In various solvents, using various signals, at various temperatures, slight variations in the (**3b**):(**4b**) equilibrium constant were measured, none of which were systematic enough to indicate a solvent or temperature effect on the equilibrium. All measured equilibrium constants fell within the range $(1.23 \pm 0.11):1$ whence a free energy difference of 121 ± 56 cal mol^{-1} at 20 °C can be calculated. Molecular-mechanics calculations were carried out using Allinger's MMP282 program.[15]

Acknowledgements

Financial support from the Science and Engineering Research Council and Smith, Kline, and French is gratefully acknowledged. We are grateful to a referee for prompting us towards a better appreciation of the contribution of second-order coupling effects[12] to the differences between the spectra of isomers.

References

1 For a recent review see U. Berg and I. Pettersson, *J. Org. Chem.*, 1987, **52**, 5177.
2 M. H. Lyttle, A. Streitwieser, Jr., and R. Q. Klutz, *J. Am. Chem. Soc.*, 1981, **103**, 3232.
3 L. A. Paquette, G. J. Hefferon, R. Samodral, and Y. Hanzawa, *J. Org. Chem.*, 1983, **48**, 1262.
4 N. L. Allinger, M. Frierson, and F. A. Van-Catledge, *J. Am. Chem. Soc.*, 1982, **104**, 4592.
5 C. Tosi, *J. Comput. Chem.*, 1984, **5**, 248.
6 L. A. Paquette, S. V. Ley, R. H. Meisinger, R. K. Russell, and M. Oku, *J. Am. Chem. Soc.*, 1974, **96**, 5806.
7 J. Gasteiger and R. Huisgen, *J. Am. Chem. Soc.*, 1972, **94**, 6541.
8 F. A. L. Anet, *J. Am. Chem. Soc.*, 1962, **84**, 671.
9 J. F. M. Oth, R. Mereny, T. Martini, and G. Schroeder, *Tetrahedron Lett.*, 1966, 3087.
10 L. A. Paquette, *Pure Appl. Chem.*, 1982, **54**, 987.
11 J. M. Gardlik, L. A. Paquette, and R. Gleiter, *J. Am. Chem. Soc.*, 1979, **101**, 1617.
12 R. J. Abraham, 'The Analysis of High Resolution NMR Spectra,' Elsevier, Amsterdam, 1971.
13 (*a*) A. A. Bothner-By and C. Naar-Colin, *J. Am. Chem. Soc.*, 1961, **83**, 231; (*b*) F. H. A. Rummens, C. Simon, C. Coupry, and N. Lumbroso-Bader, *Org. Magn. Reson.*, 1980, **13**, 33; (*c*) F. H. A. Rummens and L. Kaslander, *Can. J. Spectrosc.*, 1972, **17**, 99; (*d*) F. H. A. Rummens, J. S. Lomas, B. Tiffon, C. Coupry, and N. Lumbroso-Bader, *Org. Magn. Reson.*, 1982, **19**, 35.
14 R. A. Hoffman and S. Forsen, *Prog. Nucl. Magn. Reson. Spectrosc.*, 1966, **1**, 89.
15 N. L. Allinger and H. L. Flanagan, *J. Comput. Chem.*, 1983, **4**, 399.

Paper 9/04090K
Received 25*th September* 1989
Accepted 12*th January* 1990